URBMAT:

An Urban Canyon Sampling Format

for Nocturnal Long Wave Radiation

Regime Modelling

by

Philip M. Wakefield

A THESIS SUBMITTED IN PARTIAL FULFILLMENT

OF THE REQUIREMENTS FOR THE DEGREE OF

MASTER OF ARTS

in the Department

of

Geography

ACCEPTED
FACULTY OF GRADUATE STUDIES

[redacted]
DEAN

DATE Sept 8, 1987

We accept this thesis as conforming
to the required standard

[redacted]

Stanton E. Tuller

[redacted]

Colin J. B. Wood

[redacted]

George A. Beer

[redacted]

Denton E. Hewgill

UNIVERSITY OF VICTORIA

June 1987

ABSTRACT

The study of long wave radiation regimes within urban canyons is an area of urban climatology requiring more intensive and extensive investigation. Long wave irradiances that create these regimes are the principal sources and sinks of energy for energy budgets in the urban canyon at night under clear, calm and dry conditions. It is desirable to model urban nocturnal long wave radiation regimes to save time and costs incurred in direct measurement as well as lend insight and understanding into the theoretical controls of the irradiances. This research focuses on URBMAT which addresses the three preconditions deemed necessary for the development of "good" models. These preconditions include the clear and concise identification of those variables, properties and factors that may be relevant to modelling; a thorough knowledge of those instruments available for measuring specific variables; and the development of standardized methods for sampling the relevant variables in urban canyon, vegetative and building air-volumes.

The principal dependent variables that should be modelled are radiant surface temperatures and radiant sky temperatures. These temperatures can be employed in the Stefan-Boltzmann Law to yield a value for long wave irradiance. The key independent variables suggested by this research are associated with the urban canyon, vegetative and building air-volumes. They are the dry-bulb air temperature and wind speed in each air-volume as well as the wet-bulb air temperature in

the urban canyon air-volume. Net long wave irradiances are recommended as a "test" variable to be used for model validation. The key properties for consideration in model development are the emissivity and thermal conductivity of surface materials. Key factors include aspect, height or depth of vegetative canopies, vegetative canopy cover, thickness of materials, and viewfactors for the sky and urban surfaces.

Radiant temperatures can be measured using a compact and portable infra-red radiometer affixed to a tripod. A guide is provided to assist in setting up the radiometer when surface temperatures on vertical surfaces are to be sampled. When dry-bulb and wet-bulb air temperatures are to be sampled concurrently, an aspirated psychrometer can be used. A thermistor - thermometer can be used when the dry-bulb air temperature is to be sampled alone. Wind speeds should be measured using a hot-wire or hot-film anemometer. The hot-wire anemometer used in this research was very sensitive to movements of air. It was determined that an average between a high and low measurement of wind speed over a 10 second time interval could be used to represent a single wind speed measurement for a specific sampling location. Air temperatures and wind speed are measured in air-volumes at an instrument height ranging between 1.0 and 1.5 metres above the floor of the room or urban canyon.

Vertical and horizontal surface areas can be sampled for radiant surface temperature by either single measurements at the surface's centre or by traversing the surface when the centre is not accessible. Radiant sky temperatures can be measured at 0°, 41°, 60° and 76° from the zenith in the N, E, S and W direc-

tions where the radiometer is placed at the urban canyon centre. Net long wave irradiances can be sampled at the centre of the urban canyon at an instrument height between 1.0 and 1.5 metres using either a net pyrradiometer or a net pyrgeometer.

Air temperatures and wind speeds in air-volumes can be sampled at the centre of the urban canyon for homogeneous canyon floors and at the centre of a room. Vegetative air-volumes are sampled for air temperature and wind speed halfway between the trunk or ground surface and the outer edge of the canopy. Where the urban canyon floor is heterogeneous, single measurements for air temperature and wind speed taken at the centre of individual surface areas can be averaged using a weighting factor based on the surfaces' areas.

In addition, this research introduces the concept of surface elements, configurations and components. Formulae for deriving sampling intervals are developed based on areal dimensions and the desired accuracy of results. Further, a view-factor model is introduced that may enhance the development and use of subsequent models.

Examiners:

[redacted]

Stanton E. Tuller

[redacted]

Colin J. B. Wood

[redacted]

George A. Beer

[redacted]

Denton E. Hewgill

Table of Contents

List of Tables

List of Figures

List of Symbols

ROMAN CAPITAL LETTERS

A	area of spot
C	urban canyon centre
EVF	urban surface viewfactor
HI	height of instrument
K^*	net solar irradiance
K_H	eddy diffusivity of dry air
K_W	eddy diffusivity of water vapour
L^*	net long wave irradiance
L^+	incoming long wave irradiance
L^-	outgoing long wave irradiance
L^+_e	incoming long wave irradiance from urban surfaces
L^+_o	incoming long wave irradiance from the open sky
L_r	received long wave irradiance
L_v	latent heat of vaporization
N	total number of intervals
P	total atmospheric pressure
Q^*	net radiation flux density
Q_E	evaporative heat flux density
Q_G	conductive heat flux density
Q_H	convective heat flux density
SVF	sky viewfactor
T	surface temperature
T_a	air temperature of canyon air-volume
T_{ac}	air temperature of canopy air-volume
T_{ai}	air temperature of building air-volume
T_i	interior temperature (substrata)volume
T_k	surface temperature of black body cavity
T_o	radiant sky temperature
T_r	apparent radiant temperature
T_{si}	inside surface temperature
T_w	wet-bulb air temperature
U	thermal conductance
X,Y,Z	dimensions of surface areas and urban canyons

ROMAN SMALL LETTERS

a	spot height
c	vegetative canopy cover
c_p	specific heat of dry air at constant pressure
d	distance from vertical surface to instrument
e	vapour pressure
e_a	vapour pressure in air-volume
e_s	vapour pressure at surface
$e^*_{(Tw)}$	saturation vapour pressure at T_v
g	horizontal distance from instrument to spot centre
h	height or depth of vegetation

h_c convection coefficient in canyon air-volume
h_{cc} convection coefficient in canopy air-volume
h_{ci} convection coefficient in interior air-volume
h_e evaporative coefficient in canyon air-volume
k thermal conductivity
n_x number of intervals along the X dimension
n_y number of intervals along the Y dimension
p zero plane displacement
q specific humidity
q_a specific humidity in air-volume
q_s specific humidity at surface
s standard deviation of sample
u wind speed in canyon air-volume
u_c wind speed in canopy air-volume
u_i wind speed in interior air-volume
v von Karman's constant
w spot width
z thickness of materials; variable sampling distance
z_o roughness length
$z_{\alpha/2}$ z-score for confidence interval

GREEK CAPITAL LETTERS

E desired accuracy of temperature measurement
$\sum$ summation

GREEK SMALL LETTERS

γ angle from vertical or horizontal plane of radiometer to centre of instrument viewfactor
ε surface emissivity
ε_b emissivity of black body cavity
ε_o emissivity of the open sky
λ wavelength
ρ_a density of dry air at T_a
σ Stefan-Boltzmann constant
ϕ instrument viewfactor

Chapter I

INTRODUCTION TO THE RESEARCH

Since most of the world's population now live and work in urban areas, it has become imperative that our knowledge of urban climates be expanded. The changes in surface materials and vertical structure; the modification of atmospheric composition; and the direct emission of heat are factors that distinquish urban environments from rural environments. These factors may lead to significant differences between the climates of urban areas and those for surrounding rural areas. Wind velocities may reach gale force as air is channeled down streets while vortexes are created behind buildings. Direct radiation from the sun may fall upon taller buildings throughout the day while certain streets and alleys have not seen a direct beam of sunlight for more than one hundred years. Water that would be held in vegetation and soils in the surrounding countryside now runs down storm drains and sewers in the city creating a desert at the surface. There is no doubt that urban environments create their own unique climates.

Urban climatology is the science that seeks to describe and explain the nature of urban climates, why they differ from place to place, and how these climates relate to other elements of the environment including human activities (Critchfield, 1974). The study of urban climates is expanding and diversifying into a variety of areas. An important but little studied area is that of urban long wave radiation regimes.

The focus of this research is URBMAT which I developed as an acronym for "An Urban Canyon Sampling Format for Nocturnal Long Wave Radiation Regime Modelling". This thesis is intended to be a preliminary step in the development of models for urban long wave radiation regimes and addresses the three preconditions that help to ensure "good" models.

Chapter 1 will explain long wave radiation through to the concept of urban long wave radiation regimes followed by why, where and when these regimes are important. Next, the advantages of modelling as well as the three preconditions needed for good models will be discussed. A justification for URBMAT will be offered based on a literature review. Finally, URBMAT will be discussed in more detail as it relates to the context of this thesis.

A. Urban Long Wave Radiation Regimes

All bodies whose temperatures are above absolute zero emit radiation. Radiation is the transfer of energy by the rapid oscillation of electromagnetic fields where these oscillations may be considered as travelling waves characterized by their wavelength, λ . For most atmospheric and climatic applications, the wavelengths of principal concern are those in the approximate range 0.1 to 100 micrometers (10^{-6} meters) which represents a small portion of the electromagnetic spectrum. Atmospheric scientists and climatologists have designated radiation in the range 0.15 to 3.0 micrometers to be solar, or short wave, radiation and that in the range 3.0 to 100 micrometers to be terrestrial, or long wave, radiation (Oke, 1978). Long wave radiation is the focus of this thesis.

Radiation that is emitted from or incident upon a non-dimensional point is measured in terms of its flux where the S.I. units are Joules of energy per second (also known as Watts). However, urban environments are composed of surfaces and objects where radiation is measured in terms of irradiance (or flux density). Since all objects have surfaces, this research will focus on irradiances at surfaces. The S.I. units for irradiance are Watts per square metre (Wm^{-2}).

The long wave irradiance emitted from a surface may be accurately estimated using the Stefan-Boltzmann Law :

$$L\uparrow = \varepsilon \sigma (T + 273.2)^4 \qquad \text{Eq. 1.1}$$

where

$L\uparrow$ is the outgoing long wave irradiance emitted from the surface (Wm^{-2}),

T is the actual surface temperature (°C),

ε is the surface emissivity (decimal), and

σ is the Stefan-Boltzmann constant (5.67×10^{-8} Wm^{-2} K^{-4}).

This law suggests that a body or surface emits long wave radiation as a function of its emissivity and its temperature. Surface emissivity is the ratio of the total irradiance emitted or absorbed by a surface at wavelengths characteristic of long wave radiation and at a specific surface temperature to that of a black body (ε = 1.0) under the same conditions (Oke, 1978).

A surface has a net long wave irradiance (L^*) identified by :

$$L^* = L^+ - L^- \qquad \text{Eq. 1.2}$$

where the difference between all incoming long wave irradiances, L^+, and all outgoing long wave irradiances, L , yields a net long wave irradiance, L^*. Figure 1.1 illustrates these irradiances at an urban surface.

At an urban surface, incoming long wave irradiances, L^+, are those that are emitted from the atmosphere and urban surfaces which lie within the field-of-view of the surface, regardless of the surface's orientation (i.e. horizontal, vertical or sloped). Outgoing long wave irradiances, L^-, are those that are emitted and reflected directly from the surface itself. Thus, the net long wave irradiance, L^*, for the surface is the difference between all long wave irradiances striking the surface and those long wave irradiances that are emitted or reflected from the surface (Fig. 1.1).

An urban long wave radiation regime is created when net long wave irradiances occur over any surface in the urban environment. This regime assumes that all

Figure 1.1: Net long wave irradiances at a surface

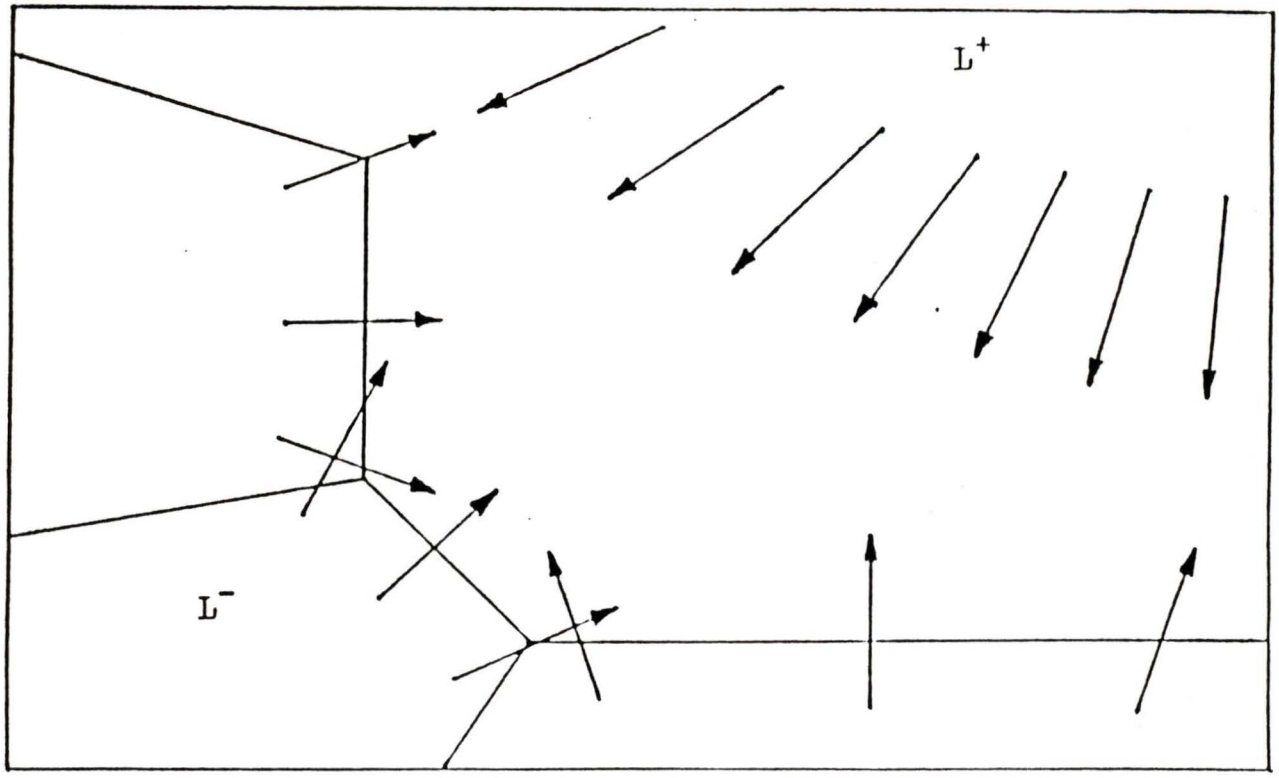

Figure 1.2: The urban long wave radiation regime

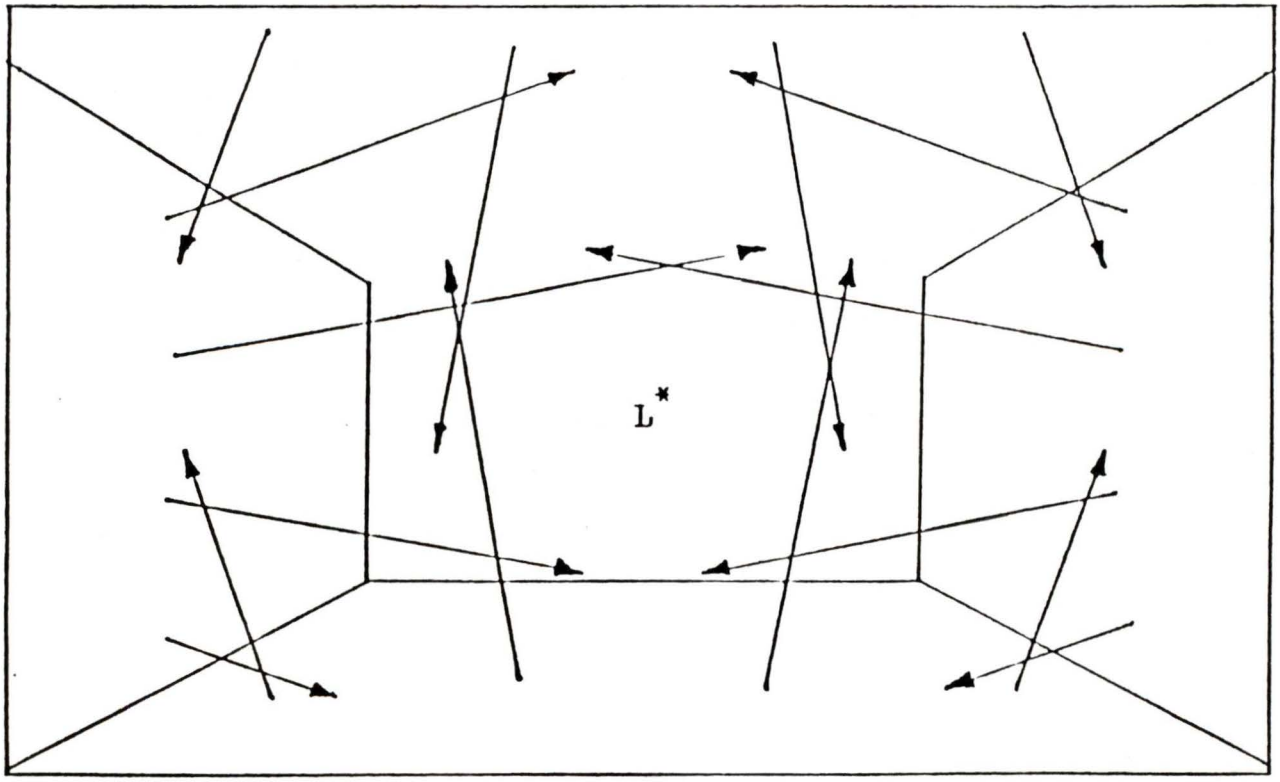

stationary surfaces and urban skies within and composing the immediate urban environment emit long wave irradiances at a constant rate over a specific period of time. Visually, this regime might appear as a multitude of intersecting rays within this environment (Figure 1.2). A net long wave irradiance occurs when an object or surface is placed within these intersecting rays.

Based upon the assumptions outlined for an urban long wave radiation regime, in the time it takes to roll a ball across a street, the long wave radiation regime will not change. However, the net long wave irradiance (L^*) at the ball's surface does change. As the ball rolls, its surface sees different portions of long wave irradiances emitted from buildings, trees, the sky above, and other emitters of long wave irradiances in the ball's changing field-of-view. The incoming long wave irradiance is changing. Similarly, the outgoing long wave irradiance may also change as friction between the ball and the street effects a change in the ball's surface temperature, although this change may be very small.

The change in the net long wave irradiance over the ball's surface with location during its travels across the street underlies the importance and difficulty of determining the urban long wave radiation regime. Since different locations in the urban environment will give different relative exposures to incoming long wave irradiances, the net long wave irradiance will change with location. Of course most climatologists are not concerned with balls rolling across streets. However, if the ball were a man then the urban long wave radiation regime takes on a new significance. While an urban surface will receive long wave irradiances from a hemispherical area lying above it, a three dimensional object, such as a man, will receive these irradiances from all urban emitters, or a spherical area.

The net long wave irradiance at the surface of any organism, whether it is a man, animal, plant or building, can indicate if the organism is under stress from long wave radiation overloading or underloading. Overloading may occur with extreme positive L while underloading may occur with extreme negative L^*. Note that buildings can be considered organisms since they have internal metabolisms maintained by heating or cooling systems. When an organism is under stress, internal metabolism is expected to help compensate and maintain a constant functional temperature within the organism.

Since most organisms occupying the urban environment are below the rooftops, urban long wave radiation regimes in urban street canyons are most significant. Urban street canyons, or urban canyons, are convenient and manageable working units for climatic studies of urban environments.

Boundaries of the urban canyon are relatively easy to define. Urban canyons have all the elements of a simple rectangular box. The floor of the box is the ground - often a street or other paved surface. The sides are two or more building walls with the remaining sides being trees or the atmosphere lying below the rooftops. The lid of the box is a portion of the atmosphere lying above the rooftops, often referred to as the open sky. These features of the urban canyon are generally considered to be stationary and are the prime contributors to the urban long wave radiation regime of the canyon. Contained within this box is the canyon air-volume, or urban canopy layer, which changes over time. Figure 1.3 illustrates a simple urban canyon.

Figure 1.3: A simple urban canyon

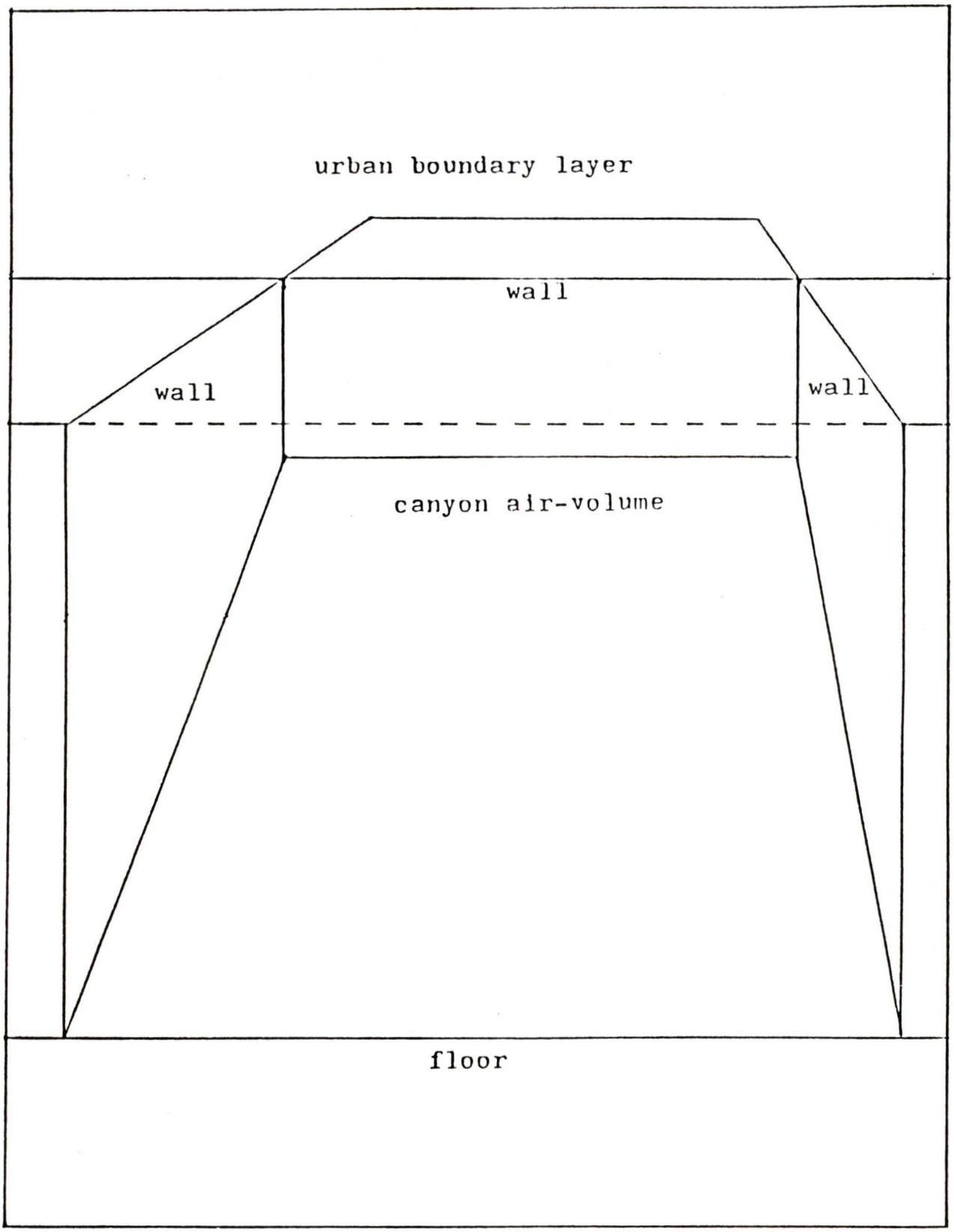

The urban long wave radiation regime of an urban canyon gains special importance when certain conditions are met. At night, there are no direct effects on the urban environment or organisms from solar radiation. The principal sources of radiation are those that emit long wave radiation. When the skies over the urban canyon are clear, long wave irradiance from the atmosphere can be significantly lower than those irradiances from urban surfaces. A clear nocturnal sky can act as a "radiation sink" to long wave irradiances. Calm wind conditions, less than 0.3 metres per second (List, 1966), minimize forms of energy exchange such as convective heat flux density (sensible heat exchange) and evaporative heat flux density (latent heat exchange). Long wave irradiances become principal sources of energy at night, and under calm conditions these irradiances can dominate the heating or cooling of a surface. Dry surfaces eliminate the process of evaporative cooling with the exception of some plants. Again, evaporative heat flux densities are minimized where only condensation can contribute to the heating of a surface. Thus, the urban long wave radiation regime of an urban canyon is most significant under clear, calm nocturnal conditions when non-vegetative surfaces are dry.

B. Modelling Urban Long Wave Radiation Regimes

Although it is possible to measure the urban long wave radiation regime at a plane or surface, it is also desirable to model this regime. For an existing urban environment, modelling can save time and costs involved in direct measurement. Models can also lend insight and understanding into the theoretical controls of urban long wave irradiances. Of equal importance, models can be used to simulate urban long wave radiation regimes resulting from modifications to urban environments.

A model is only valuable when it is a "good" model. A "good" model should be practical in that it has real world applications using easily or readily obtainable data. It should also be valid and reliable. A valid and reliable model consistently yields good estimates of the dependant variable it is intended to model. URBMAT focusses on the procedures that will lead to the development of "good" models. These procedures are not only central to this research, but in principle are deemed critical to model development in general.

There are three procedures that help to ensure that models of the urban long wave radiation regime will be "good". The first procedure involves the clear and concise identification of the variables, properties and factors that may be relevant to these models. Here, variables are model parameters that vary with climatic and environmental conditions. In terms of this research, a list of variables might include air temperatures, wind speeds and vapour pressures. Properties are parameters that vary in value as a function of the variables. For example , the density of an air-volume is a property that varies with the temperature

of that air-volume. Increasing the temperature of an air-volume from 5°C to 30°C leads to a decrease in the air-volume's density from 1.269 to 1.164 kg m^{-3}. Factors are parameters that are climatically and environmentally constant for a specific session of data collection. A list of factors might include viewfactors, depths of vegetative canopies, and thicknesses of surface materials. The second procedure is selecting the proper instrumentation based on a thorough knowledge of those instruments available for measuring specific variables including their accuracies, calibrations and practical considerations for their use. The final procedure involves the development of standardized methods for sampling the relevant variables. These sampling methodologies should take into account time and cost limitations related to the data collection process.

C. Justification for URBMAT

The necessity for URBMAT arose from a thorough review of the literature and research related to urban long wave radiation modelling. Searching through the literature, it became apparent that urban long wave radiation regimes are indeed little studied. The research pertaining explicitly to urban nocturnal long wave radiation regimes under clear, calm and dry conditions is minimal.

Research relating to urban long wave irradiances falls into three basic groups:

1. those that measure net long wave irradiance in an urban canyon air-volume,
2. those that model the energy budget of an urban surface to obtain an equilibrium surface temperature, and
3. those that measure or model incoming long wave irradiance from the sky.

These three groups were investigated for their theoretical and actual relevancy to this particular thesis and research.

The most comprehensive studies of net long wave irradiance in urban canyons at night were conducted by Nunez and Oke (1976, 1977). These studies greatly increased the understanding of nocturnal urban canyon climates and concluded that L^* must be considered in any study of energy balances in the urban canyon. Unfortunately, no models developed out of this study. A later study by Oke (1981) utilized a scale model for comparison with field observations of L^*. During the course of their studies, Oke and Nunez provided good descriptions of the site, instrumentation and sampling methodologies.

Solving for an equilibrium surface temperature (in the energy conservation law) is the focus of much of the urban canyon climatic studies at U.C.L.A. The solution of the equilibrium surface temperature in urban environments began with work by Myrup (1969) and Outcalt (1972) leading to the intensive computer modelling by Terjung and Louie (1974), Terjung and O'Rourke (1980 a, b, c) and O'Rourke and Terjung (1981) at U.C.L.A. Nunez and Oke (1980) also investigated equilibrium surface temperature.

The basic equation of energy transfer climatology is the energy conservation law for a surface (Outcalt, 1972):

$$Q^* \pm Q_E \pm Q_H \pm Q_G = 0 \qquad \text{Eq. 1.3}$$

where

Q^* is the net radiation flux density,

Q_E is the evaporative heat flux density,

Q_H is the convective heat flux density, and

Q_G is the conductive heat flux density.

Each of these terms incorporates a surface temperature variable. By sampling or assuming values for all other variables, a solution for surface temperature can be derived. This solution is the equilibrium surface temperature. These models then imply that the equilibrium surface temperature can be utilized in the Stefan-Boltzmann Law to yield a value for the outgoing long wave irradiance from a surface. However, there is no proof that the equilibrium surface temperature and the actual surface temperature are equivalent in urban environments.

There is also a radiant surface temperature which is the temperature at which the surface would emit long wave radiation if it were a perfect black body (ε = 1.0). Actual and radiant surface temperatures are often considered equal because the emissivity of most surface materials is close to 1.0. There are advantages to this generalization. The knowledge of surface emissivities for all materials is not easily obtainable. Further, the radiant surface temperature is easily measured with remote sensing devices (i.e. infra-red thermometers) whereas the measurement of actual surface temperatures requires contact with the surface. This research will treat radiant and surface temperatures as being equivalent.

The U.C.L.A. models simply create simulations of equilibrium surface temperatures that lack feedback between the surface and air-volume (Terjung and Louie, 1974). There is also a lack of validation for these models which is evident by such quotes as "It is believed that energy budget features of real cities cannot vary drastically from those simulated and described in this report" (Terjung and O'Rourke, 1980 b). Surely this lack of validation questions the usefulness of the U.C.L.A. models.

Models of incoming long wave irradiances from the sky are the most numerous in climatic study. These include models by Brunt (1932), Swinbank (1963), Idso and Jackson (1969), Monteith (1973), Unsworth and Monteith (1975) and Unsworth (1975). All these models utilize air temperature as an independent or input, variable. Brunt (1932) also utilizes vapour pressure. These models were developed for applications in rural environments under clear skies. However, these models may not be applicable to modelling incoming long wave irradiances from the open sky into the urban canyon.

Most of these models tend to overestimate incoming sky long wave irradiances at night in urban areas (Oke and Maxwell, 1975). This overestimation occurs despite the fact that urban areas receive increased incoming sky long wave irradiances compared to surrounding rural areas due in part to the higher concentrations of pollutants and particulates that are characteristic of many urban atmospheres (Aida & Yaji, 1979; Oke & Fuggle, 1972).

Some of the overestimation can be explained through the air temperature variable used in most of these models. The major problem with using air temperature in these models is the difference in vertical air temperature profiles between urban and rural areas. The incoming long wave irradiance from the sky originates from a deep layer of the atmosphere. The constants employed in the models are based on particular air temperature profiles that statistically correlate the surface air temperature with the temperature of the atmospheric layer. Only when the air temperature profile at a specific location mirrors those under which the models were developed can these models be used with any confidence. When the air temperature decreases more rapidly from the surface to the atmospheric layer than the models' profiles suggest, then overestimation occurs.

Several factors may alter air temperature profiles in urban environments. Urban surfaces are usually warmer than rural surfaces. An exchange of heat energy between the surface and adjacent air mass will occur resulting in an increase in urban air temperature (Bärring et al., 1985). Further, the reduced sky viewfactors of urban canyons delays the surface cooling during clear, calm nights while obstructing objects (e.g. buildings, trees, etc.) radiate more incoming long wave

radiation than corresponding areas of the open sky (Bärring et al., 1985). Thus, a reduced sky viewfactor tends to increase low level urban air temperatures.

All models require data for either their creation, use or validation. Unfortunately, the collection of data is not always clearly documented in the literature. Data collection techniques require details of the instruments used including when, where and how to use them; exactly what it is they measure; and how accurately they measure it. The variables to be measured require detailed sampling methodologies to guide model users in future data collection. Often, a misplaced instrument or a misguided researcher will collect data that is totally irrelevant for one model, but usable in another.

Incoming and outgoing long wave irradiances, and radiant temperatures can be amongst the more poorly sampled variables in urban areas. Much of the problem lies with the instrumentation. Most of the inexpensive instruments used to measure incoming long wave irradiances are multi-directional and sense an entire hemisphere which is fine for a horizontal surface but awkward for a three dimensional object. Jacobs (1984) details the development and use of a more expensive infra-red scanning radiometer that is programmed to take 59 measurements of long wave irradiances from the sky in 3 minutes. However, Jacobs does not discuss the applicability of this instrument in the confines of an urban canyon. Minnis and Harrison (1984) describe a methodology for sampling radiant sky temperatures for use in the Stefan-Boltzmann Law that employs an infra-red thermometer. They also do not discuss the applicability of their method to nocturnal urban canyons.

Measuring outgoing surface long wave irradiances and radiant surface temperatures is rarely discussed in detail. Directional infra-red thermometers permit most radiant surface temperatures to be measured. Unfortunately, the literature never seems to get beyond a "point-and-shoot" sampling methodology (e.g. Monteith, 1961). Direct measurements of outgoing long wave irradiances from surfaces require large and readily accessible surface areas. Airborne techniques for measuring radiant surface temperatures are very good for horizontal urban surfaces but do not sense vertical urban surfaces (Bärring et al., 1985).

The instruments, their principals and their accuracies are generally poorly documented in the literature. Even instruction manuals rarely go beyond specifications and "care-and-maintenance". Calibration techniques are seldom covered as an integral part of the research design. Occasionally, a text that covers instrumentation, principals, accuracies, calibrations, and practical considerations for use becomes available (Dobson et al., 1980). However, each research design should include details of the instruments used in order to replicate the data collection process.

Although site descriptions are generally provided, exact instrument stations are often neglected. With few exceptions (Oke, 1978), there is no mention of instrument heights for such common variables as air temperature or justification for sampling this variable at a specific location within the urban canyon.

Occasionally, an outstanding research design appears in the literature. Novak and Black (1985) have detailed such a design. Even though the study focusses upon a net radiation model over bare soils, their attention to detail is commendable. They have done an outstanding job of researching and outlining the theory, justifying variables used in the model, detailing the instruments used, and describing a sampling methodology. Because of this detail, there may be future applications of their model to urban environments.

D. URBMAT

URBMAT is a preliminary step in model development that covers the three preconditions deemed necessary for "good" urban nocturnal long wave radiation regime models. No new models will be developed in this research.

URBMAT is based on the hypothesis that standardized methodologies can be developed for sampling variables relevant to modelling urban nocturnal long wave radiation regimes assuming the following preconditions are met:

1. conditions at night are clear and calm,
2. non-vegetative surfaces are dry,
3. variables are accurately identified, and
4. appropriate instruments are evaluated.

To this end, Chapter 2 will identify the relevant variables, properties and factors associated with urban nocturnal long wave radiation regime modelling focusing particularly on dependent and independent variables since they require instrumentation and sampling. Chapter 3 will provide a detailed analysis of instrument groups designed for measuring specific variables. Chapter 4 will introduce a standardized format of sampling methodologies for each variable in the urban canyon based upon methods developed in the field. Chapter 5 will briefly review URBMAT as well as discuss prospects for future research and improvements to URBMAT.

E. Chapter Summary

In this chapter, urban nocturnal long wave radiation regimes were introduced as a viable but little studied area in urban climatology. In particular, modelling these regimes under clear, calm and dry conditions could prove valuable to the understanding of urban/organism interactions. As a preliminary step toward modelling urban nocturnal long wave radiation regimes, URBMAT was introduced. URBMAT is designed to cover the three preconditions deemed essential to the development of "good" urban nocturnal long wave radiation regime models.

During the course of the literature review that justified the need for URBMAT, several terms and concepts were introduced that need clarification. These include net radiation, convective heat flux density, evaporative heat flux density, and conductive heat flux density. How these terms and concepts relate to urban nocturnal long wave radiation regimes will be discussed in more detail in Chapter 2 as the relevant variables, properties and factors for modelling the regimes are analyzed.

It is important to note that throughout this research radiant surface temperature and actual surface temperature will be treated as one and the same term. For simplicity, the term "surface temperature" will be used to refer to either and both.

Chapter II

VARIABLES, PROPERTIES AND FACTORS FOR MODEL DEVELOPMENT

Perhaps the worst sin in model development is to consciously overlook a variable, property or factor that may be relevant to a model. It may not always be possible to identify every relevancy, but through careful analysis of related research, literature and other models the chances of committing this sin can be greatly reduced. Aside from identifying relevant properties and factors, identification of both dependent and independent variables is of particular importance since these parameters require instrumentation and sampling methodologies. Here; a dependent, or output, variable is the variable that a model is attempting to estimate or simulate. An independent, or input, variable is a variable used in a model to help arrive at a value for the dependent variable.

Chapter 2 will identify those dependent and independent variables deemed relevant to urban nocturnal long wave irradiances and regimes in the urban canyon. Relevant properties and factors will also be identified. The identification will focus on irradiances at surfaces for model development. To assist in focussing research and model development, the concept of elements, configurations and components will be introduced. In addition, the dimensions of each relevant variable will be detailed to aid the development of sampling methodologies for URBMAT.

A. Relevant Variables, Properties and Factors

Analyzing related theoretical and empirical models is perhaps the easiest method of identifying the variables, properties and factors that may be relevant to modelling urban nocturnal long wave radiation regimes. Some of these models may take the form of equations that are commonly accepted and used in climatology and other fields (e.g. mechanical engineering). Other models may be statistically based and use constants or parameters, some of which are unique to a specific set of environmental conditions. Regardless of their origins or developments, their very existence reflects a certain degree of inherent fact that makes them a good source for identifying relevant variables, properties and factors. It is these models, or equations, that will be used here to identify the relevant dependent and independent variables as well as those properties and factors associated with each type of variable.

1. The Dependent Variables

Identification of relevant dependent variables, properties and factors begins with the analysis of terms in the net long wave irradiance equation (Eq. 1.2).

The outgoing long wave irradiance, $L^{\uparrow}$, from a surface may be calculated using the Stefan-Boltzmann Law (Eq. 1.1). In Chapter 1, emitted surface irradiances were identified as being critical to the urban long wave radiation regime. Therefore, $L^{\uparrow}$ constitutes a relevant dependent variable. However, through Eq. 1.1 a combination of surface temperature, T, and surface emissivity,

ε, will also yield a value for L^{-}. Since some values for ε can often be obtained from tables (e.g. Table A2, Appendix B) and σ is the Stefan-Boltzmann constant, T is the only truly unknown variable in Eq. 1.1. This implies that T can be used in place of L as a dependent variable for modelling since direct measurement is the only method of obtaining a value for T at present.

The incoming long wave irradiance, $L^{\cdot}$, to a surface appears more complex:

$$L^{+} = \sigma \sum_{j=1}^{m} EVF_{j}\varepsilon_{j} (T_{j} + 273.2)^{4} + (SVF * L^{+}_{o}) \quad \text{Eq. 2.1}$$

where

T_j is the surface temperature for a specific emitting surface, j (°C),

$L^{\cdot}_{0}$ is incoming long wave irradiance from the open sky to the subject surface (Wm^{-2}),

ε_j is the surface emissivity for surface, j,

m is the total number of urban surfaces emitting long wave irradiances to the subject surface,

EVF_j is the proportion of radiation leaving surface, j, that is intercepted by the subject surface, and

SVF is the proportion of radiation leaving the open sky that is intercepted by the subject surface such that $\sum EVF_j + SVF = 1.0$

Here, the subject surface is simply that surface currently under investigation for L^{*}.

EVF and SVF are often referred to as viewfactors. Several viewfactor models have been developed including those by Bärring et al. (1985), Burt et al. (1982), Fanger (1970), Johnson & Watson (1984a and b), and Nunez & Oke

(1980). One such viewfactor model was developed in the course of this research, (Appendix C) which closely resembles the viewfactor models of Steyn (1980) and Johnson & Watson (1984a). In its present state of development, this model illustrates basic viewfactor calculations for urban canyon surfaces as seen by the centre of a specific urban canyon surface. This viewfactor model (Appendix C) requires height and width measurements of urban surfaces as well as relative distance measurements to the centre of the subject surface. These measurements are then used to calculate angles in both radians and degrees for use in determining the size of a "window" on a hemispherical surface. Unlike the models by Steyn (1980) and Johnson & Watson (1984a), the model in Appendix C does not take into account the cosine relationship between the intensity of the radiation emitted from a surface and the intensity of this radiation as it is received by a subject surface. A future project will further develop and computerize this model.

It is important to note that the surfaces referred to in Eq. 2.1 also function to emit long wave radiation according to the Stefan-Boltzmann Law. Aside from the viewfactors, each surface has a surface temperature and surface emissivity. Therefore, these surfaces must have an outgoing long wave irradiance, $L^{\uparrow}$. The viewfactor for each surface serves only to identify the relative proportion of these outgoing irradiances directed to the other surfaces. Thus, by modelling either $L^{\uparrow}$ or T for all urban surfaces, a significant portion of L^{*} and the urban long wave radiation regime can be solved. This implies that Eq. 2.1 is not as complex as it appears.

Incoming long wave irradiances from the open sky, $L^{\downarrow}_{0}$, also functions according to the Stefan-Boltzmann Law:

$$L^{\downarrow}_{0} = \sigma (T_0 + 273.2)^4 \qquad \text{Eq.2.2}$$

where

T_0 is the average radiant sky temperature (°C).

It is important to consider an average for T_0 because the radiant sky temperature at a zenith angle = 0° (directly overhead of a horizontal surface) is generally the coldest part of the sky. Usually, T_0 increases as the zenith angle approaches the horizon (90°). Being the coldest part of the sky merely indicates that the least amount of long wave irradiance is emitted from the zenith (0°). The sky is not a perfect emitter of long wave radiation (ε does not equal 1.0). Using the radiant sky temperature (T_o) takes into account , in part, this inequity such that the emissivity of the open sky may be considered equal to 1.0 (Oke, 1978). Therefore, $L^{\downarrow}_{o}$ and T_o may both be used as dependent variables.

Outgoing long wave irradiances from urban surfaces (L) and incoming long wave irradiances from the open sky($L^{\downarrow}_{0}$) can be used to construct the urban long wave radiation regime for an urban canyon at night. The relevant dependent variables include either $L^{\uparrow}$ or T for all urban surfaces, and $L^{\downarrow}_{0}$ or T_0 for open skies over urban areas. Surface emissivities are relevant properties while viewfactors are relevant factors. The net long wave irradiance, L^{*}, is also a viable dependent variable. However, L^{*} is probably best left as a test variable for further validation of any models developed in subsequent research. L^{*} can be measured at a plane above or adjacent to a surface using a net pyrradiometer or net pyrgeometer.

2. The Independent Variables for L and T

Relevant independent variables, properties and factors for L and T may be identified through the energy conservation law (Eq. 1.3). It has been suggested that a complete understanding of the causal processes which produce urban climates must be based upon an evaluation of the energy conservation law, or more specifically on the radiation and energy budgets as they apply to urban environments (Tuller, 1981). These budgets are identified as:

$$\underbrace{Q^{*} \pm}_{\text{Radiation Budget}} \underbrace{Q_{H} \pm \; Q_{E} \pm \; Q_{G}}_{\text{Energy Budget}} = 0 \qquad \text{Eq. 2.3.}$$

Net radiation flux density (Q^{*}) at a surface is defined as the difference between the sum of the radiant energy inputs to the surface and the sum of its radiant energy losses (Arnfield, 1975) such that:

$$Q^{*} = K^{*} \pm L^{*} \qquad \text{Eq. 2.4}$$

where K^{*} is the net solar irradiance (Wm^{-2}).

The net radiation term of the radiation budget is a term of fundamental climatological importance since it is the sole energy source for the convective (Q_H), evaporative (Q_E), and conductive (Q_G) heat flux densities. Thus, where Q^{*} indicates the balance of energy inputs and outputs, the energy budget indicates how this energy is channeled or dispersed to and from a surface in the form of heat energy.

Daytime in the urban canyon is usually dominated by solar irradiances resulting in a positive Q at most surfaces. At night, the direct influences of solar irradiances are removed and long wave irradiances become the sole source, or sink, of energy for surface net radiation. Net long wave irradiance, L*, can represent either an energy gain or loss at a surface. The sign of L* depends on whether the surface is absorbing more long wave radiation from the surrounding environment than it is emitting to its surroundings. Therefore, nighttime sees the energy conservation law as:

$$L^* \pm Q_H \pm Q_E \pm Q_G = 0 \qquad \text{Eq. 2.5}$$

where the net radiation, Q*, equals the net long wave irradiance, L*.

The outgoing long wave irradiance (L↑) can be isolated using Eq. 1.2 and Eq. 2.5:

$$L^{\uparrow} = L^{\downarrow} \pm Q_H \pm Q_E \pm Q_G \qquad \text{Eq. 2.6}$$

where all the terms on the right may provide relevant variables, properties and factors for modelling L↑ or T. Note that these terms can only serve to identify variables, properties and factors that control fluctuations in T, and ultimately L↑. The incoming long wave irradiance can be measured, but it has no method of solution since it is dependent upon models not yet developed. However, it is possible to speculate on those parameters controlling L↓ which may relate to L* and T. The energy budget terms (Q_H, Q_E and Q_G) each utilize an actual surface temperature variable which is related to but not equal to the radiant surface temperature (Chapter 1). These energy budget terms indicate how and when heat energy is exchanged at a surface, and the possible effects on T.

This subsection will evaluate L^{+}, Q_H, Q_E and Q_G solely in terms of relevant variables, properties and factors that control T, and thus control L . The reader should be aware of the complexities involved in the relationships to be outlined in this subsection, especially those relating to the energy budget terms. The equations describing the terms of the energy budget merely estimate the heat energy exchange at a surface. The heat energy exchanges themselves are difficult to varify. Further clarification of these terms may be obtained from Oke(1978) and Rogers and Mayhew(1980).

a) Incoming Long Wave Irradiances, L^{+}

As mentioned previously, the L^{+} term is itself subject to model development. However, research by Bärring et al. (1985) indicates that there are relationships between the sky viewfactor, SVF, and each of T and the urban canyon air temperature, T_a . These relationships are inverse such that an increase in SVF affects a decrease in T and T_a . Results of a field study (Appendix A) verified this relationship between SVF and T_a (Data Sheet 1). Since the open sky can act as a radiation sink relative to urban surfaces, it seems quite logical that this relationship would hold true at night in an urban canyon. Thus, a direct relationship between environmental viewfactors, EVF, and T_a and T would hold true. This implies that the urban canyon air temperature (T_a) may be used as an independent variable in the modelling of T and L . The relationship noted by Bärring et al.(1985) strongly suggests that the SVF be noted for modelling purposes.

b) Convective Heat Flux Density, Q_H

Convective heat flux density, Q_H, involves the exchange of sensible heat between a surface and the air-volume adjacent to that surface. A careful evaluation of the Q_H term reveals that the air temperature (T_a) and wind speed (u) are independent variables that may be relevant to modelling surface temperature. In addition, the height or depth of vegetative cover (h) should be considered for modelling the surface temperatures for vegetative surfaces.

The Q_H equation (Table 2.1) indicates the importance of the differential between the surface temperature, T, and the air temperature, T_a. When T exceeds T_a, energy is released from the surface to the air-volume. Energy is released from the air-volume to the surface when T_a is greater than T. It is apparent that a relationship exists between T_a and T through Q_H thus making T_a a logical independent variable.

The convection coefficient, h_c (Table 2.1), dictates the rate of exchange of sensible heat between the surface and adjacent air-volume. The specific heat of air at constant pressure, c_p, is considered a constant equal to 1010 $Jkg^{-1}°C^{-1}$ (Oke, 1978). The density of air, $\rho(kgm^{3})$, is both a function of T_a measured at a sampling distance, z (m), from or above the surface and air pressure. ρ varies inversely with T_a and some typical values are given in Table A4 (Appendix B). The eddy diffusivity of air, $K_H(m^2s^{-1})$, reflects the ability of eddies in the adjacent air-volume to transfer sensible heat energy between the surface and air-volume. Evaluating the relative importance of the variables, properties and fac-

Table 2.1: Convective Heat Flux Density

1) convective heat flux density equation:

$$Q_H = h_c(T - T_a)$$

2) convective coefficient:

$$h_c = \frac{\rho c_p K_H}{z}$$

3) variables:

a)	T	surface temperature (°C)
b)	T_a	air temperature (°C)

4) properties:

a)	ρ	density of air at T_a
b)	c_p	specific heat of air at constant pressure
c)	K_H	eddy diffusivity for air

5) factors:

a)	z	sampling distance from surface of variables (e.g. T_a)

tors in the convection coefficient is a complex process revealing several conflicting and contradicting relationships. Analysis of the eddy diffusivity in particular illustrates several of these relationships.

The eddy diffusivity of air may be calculated from (Rogers and Mayhew, 1980):

$$K_H = \frac{v^2 \, u \, (z - p)}{\ln \frac{(z - p)}{z_0}} \qquad \text{Eq. 2.7}$$

where

u is the wind speed (m s^{-1}) at

z, the sampling distance (m),

p is the zero plane displacement (m)

z_0 is the roughness length (m), and

v is von Karman's constant (0.405).

The roughness length, z_0, and zero plane displacement, p, of a surface are a function of the height of the surface material, h, such that a crop, h=1.5 m, would have a higher p and z_0 than a concrete surface, h=0.001 m. Some typical values for p and z_0 are given in Table A3 (Appendix B). The roughness length is a measure of the aerodynamic roughness of a surface while the zero plane displacement is the level at which the surface exerts the bulk of its dragging forces such that p is less than h (Oke, 1978). With the exception of vegetative surfaces such as lawns, most urban surfaces can be considered relatively smooth. The zero plane displacement for vegetative surfaces can be calculated using (Szeicz et al.,1969):

$$\log p = 0.9793 \log h - 0.1536 \qquad \text{Eq. 2.8}$$

while the roughness length can be calculated using (Tanner & Pelton,1960):

$$\log z_0 = 0.997 \log h - 0.883 \qquad \text{Eq. 2.9.}$$

In urban areas, the critical independent variable in the determination of K_H is the wind speed, u. Working within the calm range for u ($u < 0.3$ m s^{-1}), assume $z_0 = 0.001$ m (p = 0) and z = 1.5 m. Raising u from 0.10 to 0.11 m s^{-1} (10 %) affects a raise in K_H from 3.36×10^{-3} to 3.70×10^{-3} $m^2 s^{-1}$. With u = 0.10 m s^{-1}

and z = 1.5 m, z_0 (and h) would have to double in order to affect an equivalent increase in K_H . The sampling distance, z, holds little significance. The field study indicates that the independent variables, T_a and u, should be averaged over the floor of the urban canyon at a constant instrument height, HI, between 1.0 and 1.5 m (Data Sheets 2 to 5, Appendix A).

The importance of u, through K_H, is also reflected in the convection coefficient, h_c . The density of air, ρ, is the only other property in h_c subject to variability due to variations in T_a and air pressure. Based on the values for u and K_H previously mentioned and ρ = 1.246 kgm^{-3} at T_a = 10°C, h_c increases from 2.82 Wm^{-2}°C^{-1} (u = 0.10 m s^{-1}) to 3.10 Wm^{-2}°C^{-1} (u = 0.11 m s^{-1}). In order to affect a similar increase in h_c with z = 1.5 m and K_H = 3.36 x 10^{-3} m^{2}s^{-1}, ρ would have to be 1.370 kgm^{-3} which represents a drop in T_a of approximately 25°C ($T_a \simeq -15$°C).

In summary, the two most important independent variables from Q_H are T_a and u. The height of the surface material, h, is significant to z_0 and p only for the few vegetative surfaces found in urban canyons. An average h for horizontal vegetative surfaces is usually easy to determine. For a vertical vegetative surface, the average depth of the canopy from its outside edge to the trunk or stem at the canopy base can be used. Where vegetation is bare of leaves, the trunk or underlying ground becomes the surface of active energy exchange. Vegetative surfaces such as hedgerows may be treated as walls of vegetation where h is based on an average canopy depth. Thus, models for L* or T should initially include T_a and u as well as h for vegetation.

The significance of Q_H and the heat flux densities (evaporative and conductive) to L and T will be discussed separately in a later subsection.

c) Evaporative Heat Flux Density, Q_E

Evaporative heat flux density, Q_E, involves the exchange of latent heat between a surface and the air-volume adjacent to that surface. The careful evaluation of this term reveals that, like Q_H , the air temperature and wind speed in the urban canyon air-volume may again be relevant to modelling surface temperature when the basic assumption of a dry surface is met. Indeed, the equations for Q_E and Q_H take on a marked similarity when this assumption is met. Further, the vegetative factor (h) again appears relevant to modelling surface temperature.

The Q_E equation (Table 2.2) indicates that when there is a positive differential between the specific humidities of the air-volume (q_a) and surface (q_s), evaporation will occur and latent heat will flow from the surface to the air-volume. This presupposes that moisture is available at the surface for evaporation. A negative differential indicates condensation at the surface with a resulting flow of heat to the surface . Some surfaces (e.g. vegetative surfaces) have effective specific humidities which are a function of their temperature and moisture content. However, for the hard impermeable surfaces associated with urban environments, this research assumes that the thin film of air adhering to the surface (laminar boundary layer) takes on the specific humidity the surface might have.

Note that the evaporative coefficient (h_e) introduced in Table 2.2 is actually an evaporative heat flux density coefficient because it includes the latent heat of vaporization (L_v) which brings in a heat flow factor.

Table 2.2: Evaporative Heat Flux Density

1) evaporative heat flux density equation:

$$Q_E = h_e(q_s - q_a)$$

2) evaporative coefficient:

$$h_e = \frac{\rho L_v K_w}{z}$$

3) variables:

a)	q_s	specific humidity at the surface (gkg^{-1})
b)	q_a	specific humidity of the air (gkg^{-1})

4) properties:

a)	ρ	density of air at T_a
b)	L_v	latent heat of vaporization
c)	K_w	eddy diffusivity of water vapor

5) factors:

a)	z	sampling distance from surface of variables (e.g. q_a)

The specific humidity can be approximated using (Oke,1978):

$$q \simeq \frac{0.622\ e}{P} \qquad \text{Eq. 2.10}$$

where

q is the specific humidity of moist air ($g\ kg^{-1}$),

e is the vapour pressure (kPa), and

P is the total atmospheric pressure (kPa).

The specific humidity, q, is defined as the ratio of the mass of water vapour to the mass of moist air in a sample air-volume (Oke, 1978). The total atmospheric pressure, P, varies with time and location but with most locations at or near sea level this changes q by less than one percent. Thus, it is assumed that P will take on the value of the standard atmospheric pressure, P = 101.33 kPa. The vapour pressure, e, is the portion of the total atmospheric pressure due to water vapour content. Vapour pressure can be determined by:

$$e = e_{(Tw)} - \frac{c_p P}{L_v} (T_a - T_w) \qquad \text{Eq. 2.11}$$

where

T_w is the wet-bulb air temperature (°C),

$e^*_{(Tw)}$ is the saturation vapor pressure at T_w (kPa), and

L_v is the latent heat of vaporization at T_a (Jkg^{-1}).

The wet-bulb temperature, T_w, is less than T_a due to evaporative cooling where, in the absence of external energy, it is assumed that all of the energy used to evaporate the water is supplied by cooling a wick over a temprature sensor (Oke, 1978). The saturation vapour pressure, $e_{(Tw)}$, is the maximum amount of water vapour that air can "hold" in the vapor phase at T_w. The latent heat of vaporization, L_v, is the energy required to affect a change between liquid water and water vapour. L_v is inversely proportional to the temperature of the evaporating water or surface.

In order to solve for Q_E, equation 2.11 is substituted in 2.10 for each of q_a and q_s where e_a is the vapor pressure in the canyon air-volume and e_s is the vapor pressure at the surface. The specific humidities calculated from Eq. 2.11 are then

used in the Q_E equation from Table 2.2. The principal independent variables in e_a are T_a and the wet-bulb air temperature of the air-volume, while for e_s at the surface T is used in lieu of T_s . The wet-bulb air temperature at the surface is impossible to obtain directly which is the reason the temperature gradient is measured in the air rather than between the surface and the air. However, this research discovered that the T_w between 2.0 m and 0.1 m over both vertical and horizontal surfaces in an urban canyon did not vary substantially. For this reason, it is assumed that T_w in q_a and q_s are also the same. This implies that $e^*_{(Tw)}$ in e_a and e_s are also the same. Thus, the $T - T_s$ differential becomes important in the $e_s - e_a$ and $q_s - q_a$ differentials. The only other source of variability is in the L_v ,but this variation amounts to only 4 percent in the range of T_a between - 5°C and 40°C(Table 4A, Appendix B). Often, K_H and K_w are considered equal within z = 2.0 m and for most applications this equality holds true although it is seldom accurate (Oke, 1978). Since this section is dealing with variable and property identification, it is assumed that K_H and K_w are equal throughout the urban canyon.

Based upon the previous assumptions and the small variability of L_v, the evaporative heat flux density tends to function like the convective heat flux density. This observation seems probable in light of the basic assumption of dry surface conditions. If a solid urban surface is dry, then $Q_E = 0$, evaporation will not occur and only the convective heat flux density will affect the exchange of heat between the surface and the adjacent air-volume. For unwatered vegetative surfaces, moisture is stored and evaporation will usually be minimal since most plants have mechanisms which will prevent the moisture level within the plant from

reaching a critically low level. However, many urban vegetative surfaces are watered and evaporative heat flux density can be a significant heat exchange process. Condensation, which often occurs when q_a exceeds q_s , returns a minimal amount of heat to a surface since the water vapour required for this process is generally dispersed throughout an air-volume.

This implies that the $T - T_a$ differential is important to the latent heat exchange as well as the sensible heat exchange. Since h_a approximates h_c when K_w approximates K_H, u and h (for vegetation) are significant to Q_E, and along with T_a, may prove relevant to models of L and T.

d) Conductive Heat Flux Density, Q_G

Conductive heat flux density, Q_G, involves the exchange of heat energy between a surface and the strata underlying that surface. There are two equations for Q_G (Table 2.3) : a substrata equation and a sectional equation (Rogers and Mayhew, 1980).

The substrata equation identifies an interior temperature (T_i) within the substrata as possibly being relevant to the surface temperature adjacent to the substrata. The sectional equation identifies an inside surface temperature (T_{si}) as being relevant for modelling surface temperature. Both equations suggest that thermal conductivity (k) and stratum thickness (z) are relevant factors for modelling.

The substrata equation is applied to the flux of energy between a surface and an underlying stratum of material, or strata of materials. The differential

Table 2.3: Conductive Heat Flux Density

1) conductive heat flux density equation (substata):

$$Q_G = U(T - T_i)$$

2) conductive heat flux density equation (sectional):

$$Q_G = U(T - T_{si})$$

3) thermal conductance equation:

$$U = \frac{1}{\sum_{t=1}^{\omega}\left[\frac{z_{it}}{k_{it}}\right]}$$

4) variables:

a)	T	surface temperature (°C)
b)	T_i	interior temperature (°C)
c)	T_{si}	inside surface temperature (°C)

5) properties:

a)	k	thermal conductivity

6) factors:

a)	z	thickness of stratum or layer
b)	r	number of stratum or layers

between the surface temperature, T and an interior temperature, T_i, at a point within the substrata next to T determines the magnitude and direction of Q_G . When T exceeds T_i energy is conducted from the surface toward the substrata. Further, when T_i exceeds T, energy is conducted to the surface. It is apparent that a relationship exists between T and T_i through Q_G thus making T_i a logical independent variable.

The thermal conductance, U, as it relates to the Q_G for substrata is a function of the thermal conductivity, k ($Wm^{-1}°C^{-1}$), for stratum i of thickness z (m). The thermal conductivity of a material, or stratum, describes the materials ability to conduct heat by molecular motion (Oke, 1978). Thermal conductivities for a variety of materials can be found in Table A1 (Appendix B). Like h_c and h_e, U dictates the rate at which heat energy is conducted between the surface and substrata. As k increases so does U and the rate of heat exchange while an increase in z has the reverse effect on U. Both k and z are equally important to U. Note that each stratum of material is treated separately with unique k and z since heat conduction through each stratum is considered as a separate entity. Therefore, the sum of all z_i must equal the depth at which T_i is sampled or estimated.

The sectional equation applies primarily to building shells (e.g. wall sections) that enclose their own air-volume. Here, the differential is between the surface temperature, T, and the inside surface temperature of the wall section, T_{si}, adjacent to T. This differential implies a relationship between T_{si} and T , and suggests that T_{si} is a logical independent variable.

The thermal conductance, U, of the building shell is also a function of k and z. However, the sum of all z_i now equals the overall thickness of the shell. The sectional U controls the rate of energy exchange in a similar manner to the substrata U. Table A1 (Appendix B) includes some common values for k that relate to materials found in wall sections.

To summarize, the interior temperature within substrata (T_i) and the inside surface temperature for a section separating two air-volumes (T_{si}) may both be significant variables. The substrata and wall sections separating T_{si} and T_i from T suggests that the thermal conductivity of each stratum or layer (k) and the thicknesses of these strata (z) may also be relevant to the modelling of surface temperatures.

e) The Significance of Q_H, Q_E and Q_G to L^* and T

A great deal of controversy surrounds the exchange of heat energy between buildings, solids, vegetative surfaces and air-volumes. Terjung and O'Rourke (1980a) identify a steady-state and a transient-state of heat transfer. In a transient-state, heat energy is stored while in a steady-state no storage occurs. They acknowledge the fact that the transient-state is more accurate, but that the differences between the two states were not significant over a daily time period.

This research assumes that heat is transferred in a steady-state. Employing a steady-state implies that for a dry surface above substrata (where Q^* and $Q_E = 0$) $Q_G = Q_H$ where:

$$U(T_i - T) = h_c(T - T_a) \qquad \text{Eq. 2.12}$$

The T variable can be isolated to show the effects of certain variables and properties on T and ultimately L via the Stefan-Boltzmann Law such that:

$$T = \frac{UT_i + h_cT_a}{h_c + U} \qquad \text{Eq. 2.13}$$

There are several significant items associated with Eq. 2.13 First, it indicates the link between T_i and T_a where, assuming $Q^* = 0$ and regardless of the values for U and h_c, if either variable is greater than the other, T will lie somewhere between. It also suggests that if $T_i = T_a$, then T will equal both these variables and heat energy will not flow between any medium (e.g. air, surface or substrata).

A steady-state applied to the dry surface of a building shell operates in a similar manner to a surface over substrata such that:

$$h_{ci}(T_{ai} - T_{si}) = U(T_{si} - T) = h_c(T - T_a) \quad \text{Eq. 2.14}$$

where

T_{ai} is the air temperature of the interior air-volume, and

h_{ci} is the convection coefficient for that air-volume.

The equation for a building shell T is :

$$T = \frac{Uh_{ci}T_{ai} + T_a(Uh_c + h_ch_{ci})}{Uh_{ci} + Uh_c + h_ch_{ci}} \quad \text{Eq. 2.15}$$

First, note that the T_{si} variable factors out of Eq. 2.15. It also indicates that T lies between T_{ai} and T_a . Similarly, heat energy will not flow to any medium when $T_{ai} = T_a$. This equation also introduces h_{ci} where the most important variable would be the wind speed of the interior air-volume, u_i, where it is assumed h_{ci} operates in a similar manner to h_c . Further, T_{ai} may be substituted for T_{si} as a relevant independent variable for modelling T and L when used in association with u_i .

The steady-state can also be applied to a vegetative surface, especially a vegetative canopy with its own interior air-volume within the canopy such that:

$$h_{cc}(T_{ac} - T) = h_c(T - T_a) \quad \text{Eq. 2.16}$$

where

T_{ac} is the air temperature within the canopy, and

h_{cc} is the convection coefficient for the canopy air-volume.

In this case, the outer surface of the canopy is treated as a plane where the surface temperature, T, of the outer vegetative canopy is:

$$T = \frac{h_{cc}T_{ac} + h_cT_a}{h_{cc} + h_c} \quad \text{Eq. 2.17}$$

Now there is a link between T_{ac} and T_a whereby T will lie somewhere between these two variables. Again, when $T_{ac} = T_a$ there will be no energy flowing between any medium. Note that the most important variable associated with h_{cc} will be the wind speed within the vegetative canopy air-volume, u_c, if it is assumed that h_{cc} functions in a similar fashion to h_c.

It must be stressed that these equations merely indicate the controlling effects of certain independent variables on T. The equations themselves are not good models since they do not take into account the effects of radiant energy from L^+ on T and L^-.

Before a final list of relevant variables, properties and factors is identified for modelling T and L^-, it is advantageous to identify the controls of incoming long wave irradiance from the open sky, L^+_0, in order to correlate them with those mentioned previously for T and L^-. Also, it is desirable to analyze components of the urban canyon to understand more about urban surfaces and urban skies.

3. The Independent Variables for L^+_0 and T_0

Relevant independent variables, properties, and factors for L^+_0 and T_0 may be identified through statistical models and theory developed by other researchers. The models were identified and discussed briefly in Chapter 1. Some of the more commonly used clear sky models are listed in Table 2.4. The most prevelant variable in all these models is the air temperature, T_a. Using T_a appears logical because long wave irradiance is directly related to T^4. Often during the night, a radiation inversion is created where the driving-force

is surface long-wave radiative cooling and the inversion is based at the ground (or other active surface) and may extend up to heights of 50 - 100 metres above the surface (Oke, 1978). Radiation inversions are characteristic of the lower atmosphere on nights with little or no cloud, and light winds or calm. Figure 2.1 illustrates the temperature profile for such an inversion as it might exist above an open rural surface. It is unclear in the literature as to what time of day some of the statistical models were developed, or whether they were designed to estimate $L^{\downarrow}_{0}$ throughout the day or night. The constants used in the Idso & Jackson and Brunt models may be adjusted. This suggests that these models might have application in urban areas if the proper constants are used. These applications are open to verification in future research. The higher air temperatures associated with the smaller SVF of urban canyons noted by Bärring et al. (1985) do tend to overestimate $L^{\downarrow}_{0}$ in urban areas as suggested by Oke and Fuggle (1972). Based upon the average of 21 radiant sky temperatures (Data Sheet 11), the average T_0 = -16.3°C yields an $L^{\downarrow}_{0}$ = 247.0 Wm^{-2} when used directly in the Stefan-Boltzmann Law and ε = 1.0. The air temperature from Data Sheet 11 was 8.5°C . When this air temperature is used the Swinbank (1963) equation, $L^{\downarrow}_{0}$ = 257.5 Wm^{-2} .Used in the Monteith (1973) equation , $L^{\downarrow}_{0}$ = 259.0 Wm^{-2} . Both these models appear to overestimate the incoming long wave irradiance from the open sky.

The Brunt (1932) equation also identifies a vapour pressure variable, e_a, based on a T_a - T_w differential above a rural surface. Water vapour is an excellent absorber and emitter of long wave radiation. The higher the concentration of water vapour, the more incoming long wave irradiance from the open sky that

Figure 2.1: Temperature profile in an inversion

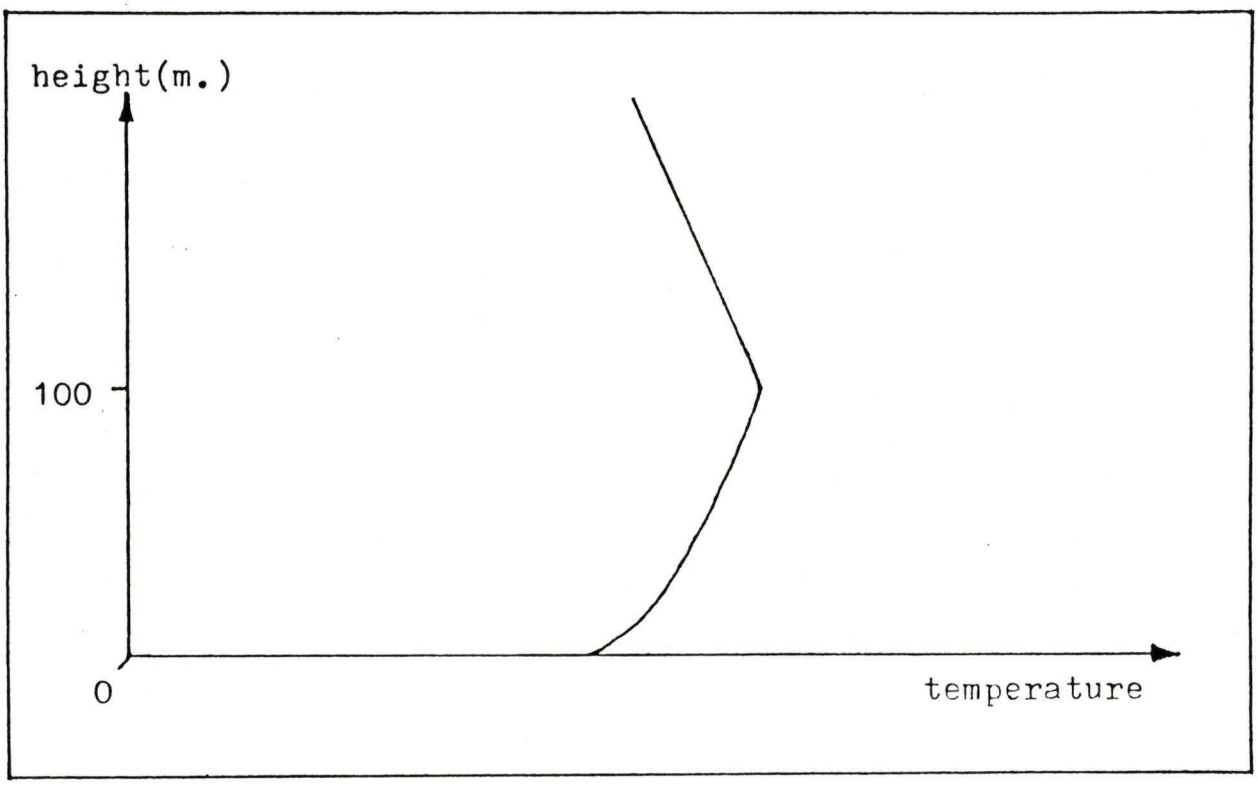

might be expected. Oke (1978) suggests that there is little difference in water vapour concentrations between urban and rural areas, however mid-latitude urban areas tend to have higher concentrations of water vapour at night. This fact would tend to support the observations of Oke and Fuggle (1972) and Aida and Yaji (1979) that L^{*}_{0} is greater in urban areas at night.

Air pollution concentrations in urban areas also tend to be higher than most rural areas. These higher concentrations might also be expected to increase the long wave irradiance from the open sky. However, Oke(1978) suggests that air pollution concentrations are probably not that significant.

To conclude, the models in Table 2.4 may be accurate in form and content, but the parameters in these models may require changing to more precisely predict L^{+}_{0} in urban areas at night. Models that predict a mean T_0 to be used in the Stefan-Boltzmann Law should probably also consider T_a and e_a(i.e. $T_a - T_{dp}$) as independent variables. As suggested in the previous section, a SVF may also be appropriate since L^{+}_{0} is one term in L^{*} which may have a bearing on T_a.

Table 2.4: Formulae used to compute incoming long wave irradiance from cloudless open skies (irradiance units = Wm^{-2})

1) Brunt (1932)

$$L^{+}_{0} = \sigma T_a^4 [a + b(e_a)^{1/2}]$$

where a,b are constants that vary with location;
T_a (°K); e_a (mb)

2) Swinbank (1963)

$$L^{+}_{0} = 1.20\sigma T_a^4 - 171$$

where T_a is limited to temperatures above 273°K;
T_a (°K)

3) Monteith (1973)

$$L^{+}_{0} = 208 + 6T_a$$

T_a (°C) valid over the range $-5\,°C \leq T_a \leq 25\,°C$

4) Idso & Jackson (1969)

$$L^{+}_{0} = \sigma T_a^4 \{1 - c \exp[-d(273 - T_a)^2]\}$$

where the constants c = 0.261, d = 7.77×10^{-4}
T_a (°K)

Source: from Oke (1978)

B. Types of Urban Canyon Components

Urban canyons have been identified as practical units of study in urban climatology, particularly in urban long wave radiation theory. Due to the variability and complexity of urban canyon surfaces, it is desirable to stratify and quantify these surfaces. This will permit an attenuation of the research and modelling format to specific surfaces or surface types. This section identifies urban surface elements, configurations and components, and introduces conditions affecting the emission of long wave irradiance from urban skies.

1. Urban Surface Elements

Urban surface elements are surface areas composed of homogeneous materials or conglomerates. They are the most basic areal units of the urban canyon that can be studied at a practical level. Elements construct all the active surfaces where radiative exchanges occur.

A list of elements found in a particular urban canyon may include concrete, glass, wood siding, asphalt, leaves and grass. The elements would construct the surfaces of buildings, streets, trees and lawns. Note that composition, titles or labels are of little concern to classification of elements. The best criterion for classifying elements is their thermal conductivity (Table A1, Appendix B.). Thermal conductivity reflects an element's ability to channel and store heat in its mass thus affecting, in part, the surface temperature of that element. The emissivity of a surface element can be affected significantly by simply changing the colour of the surface. The thermal conductivity is affected to a lesser extent by such a colour change. Thus, thermal conductivities tend to be more stable properties of elements than emissivities. As mentioned earlier, they are also significant to a surface's energy budget.

Elements may be best suited for the development of long wave radiation models. With some foreknowledge of the classes of elements, their location within an urban canyon and their surface areas, the long wave radiation regime could be constructed. It is highly impractical to develop models for each possible element found in urban canyons. However, a single model for each classification of elements listed in Table A1 (Appendix B) could be developed.

Although time-consuming initially, these models could prove the most practical and beneficial for simulating surface temperatures and long-wave radiation regimes once the developmental stage is completed.

2. Urban Surface Configurations

Urban surface configurations are combinations of surface elements. The presence of elements in a variety of areal sizes, orientations, and numbers can make identification or sampling of individual elements difficult at times. Thus, the surface configuration may serve as a more convenient surface unit. Three basic urban surface configurations can be identified: homogeneous, heterogeneous-even and heterogeneous- uneven.

Homogeneous configurations are defined here as surface areas composed of one homogeneous surface element. They are in fact a single surface element that covers a substantial area of the walls or floor of the urban canyon. Decorative strips or patterns may be present within the configuration but are generally insignificant features of the urban canyon. Figure 2.2 illustrates some homogeneous configurations.

Heterogeneous-even configurations are defined as surface areas composed of two or more surface elements where those elements occur with some pattern or regularity throughout the configuration. Generally, these configurations have a dominant element that surrounds the other elements giving the impression that these elements are imbedded in the dominant one. (Figure 2.3).

Heterogeneous-uneven configurations are defined as surface areas composed of two or more surface elements where those elements do NOT occur with some pattern or regularity. Again, elements can appear imbedded in a dominant element, but these elements might appear clustered in certain related areas or spread randomly throughout the configuration (Figure 2.4).

Often, distinguishing between a heterogeneous-even and heterogeneous-uneven configuration can prove difficult and confusing. Identification may be based upon the researcher's judgement where the only criterion available is the degree of complexity of the configuration as perceived by the researcher.

In the context of this research, surface configurations are best suited to identifying sampling procedures for combinations of surface elements where the researcher must sort through the elements and sample the relevant variables over larger surface areas.

Figure 2.2: Homogeneous surface configurations
a) vertical

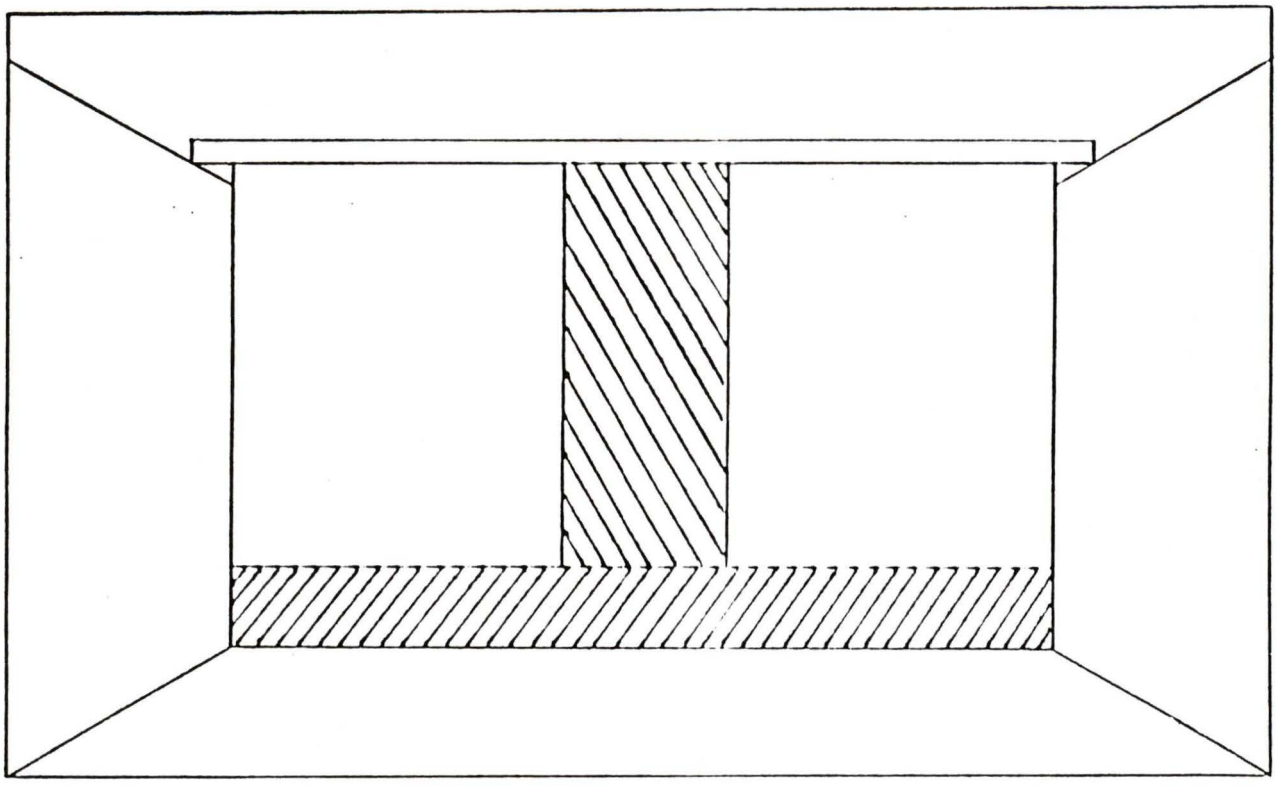

b) horizontal

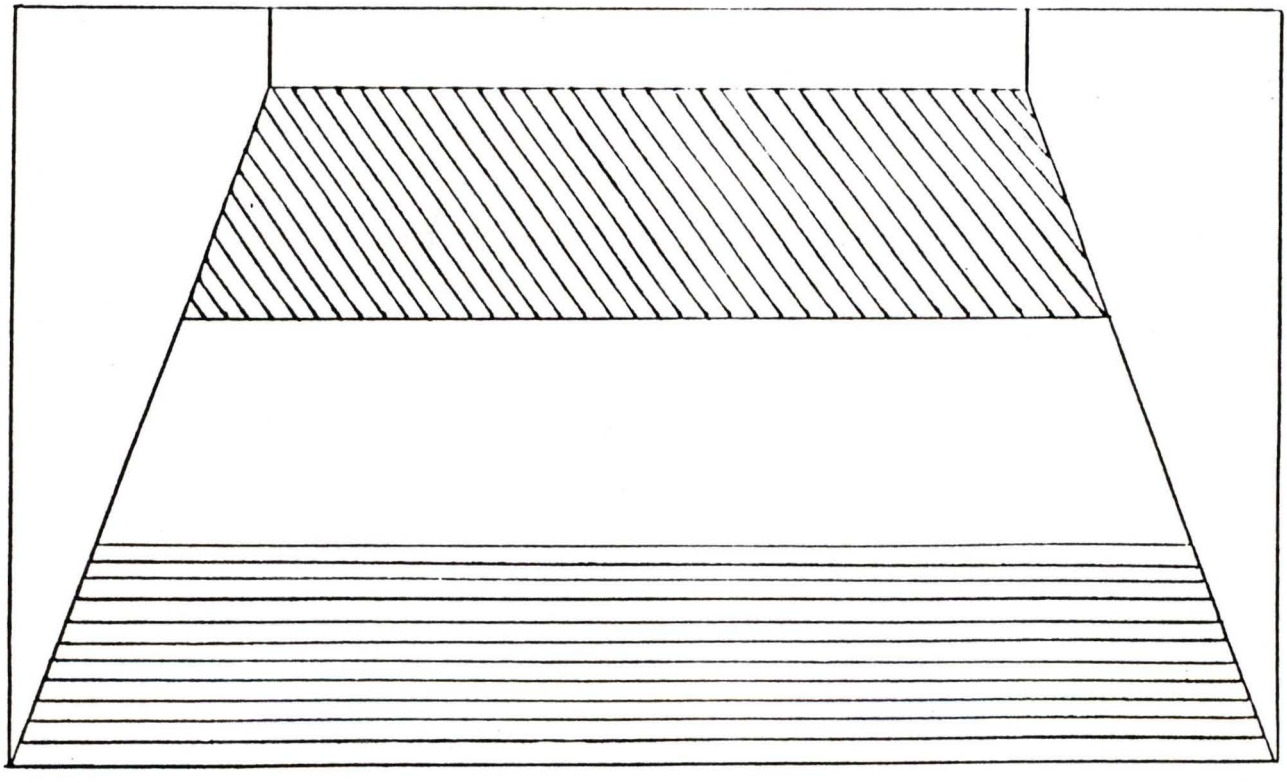

Figure 2.3: Heterogeneous - even surface configurations
a) vertical

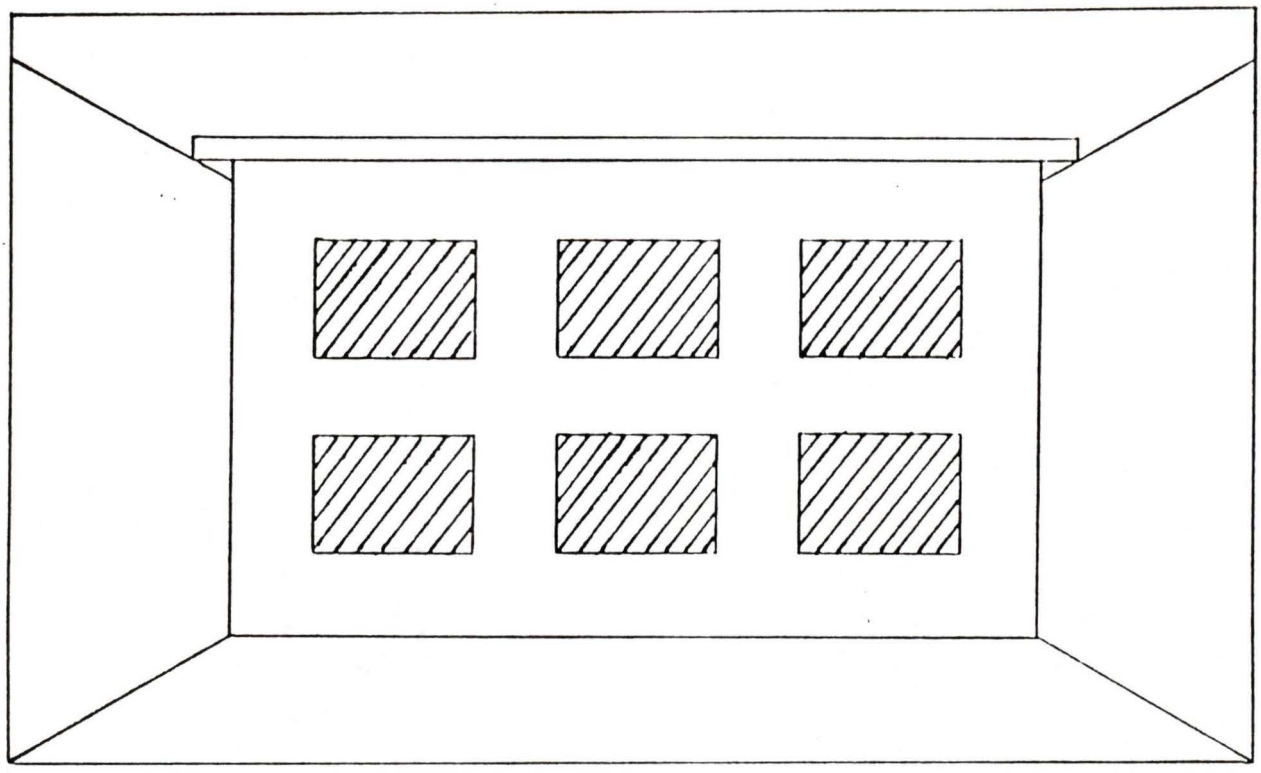

b) horizontal

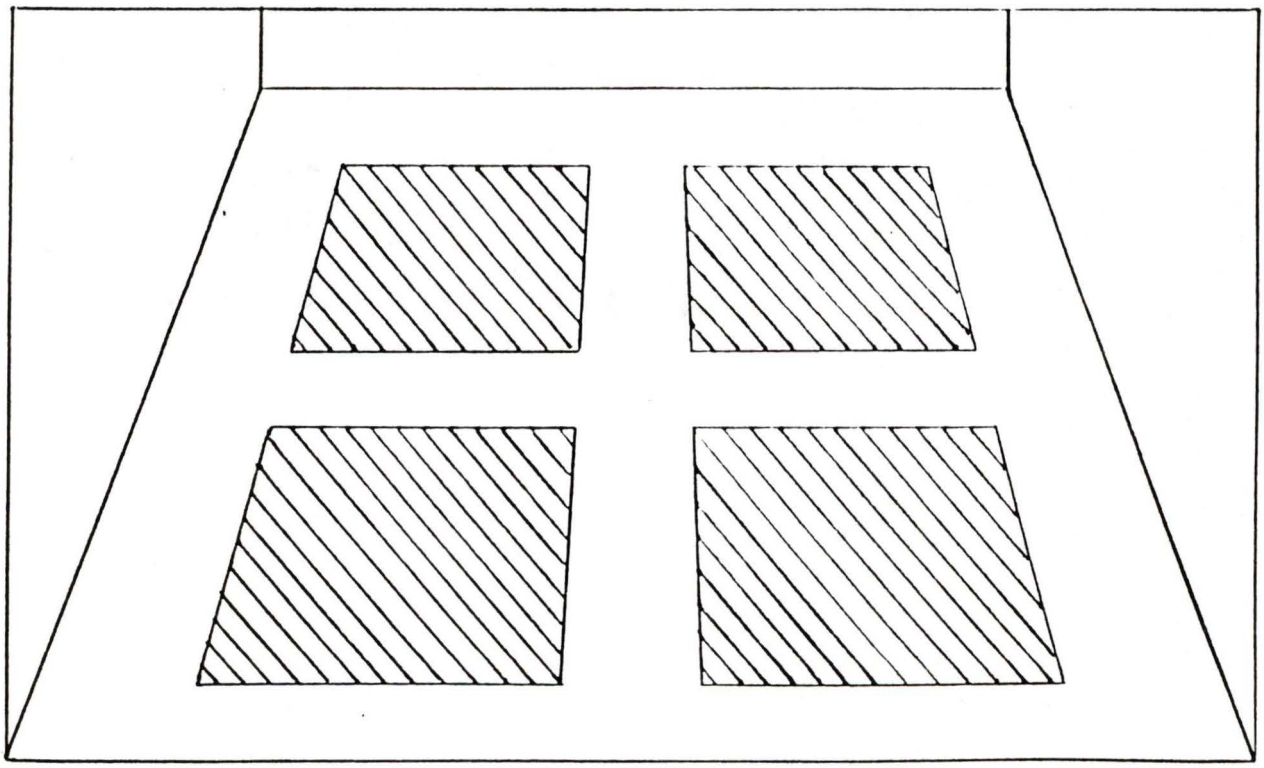

Figure 2.4: Heterogeneous - uneven surface configurations
a) vertical

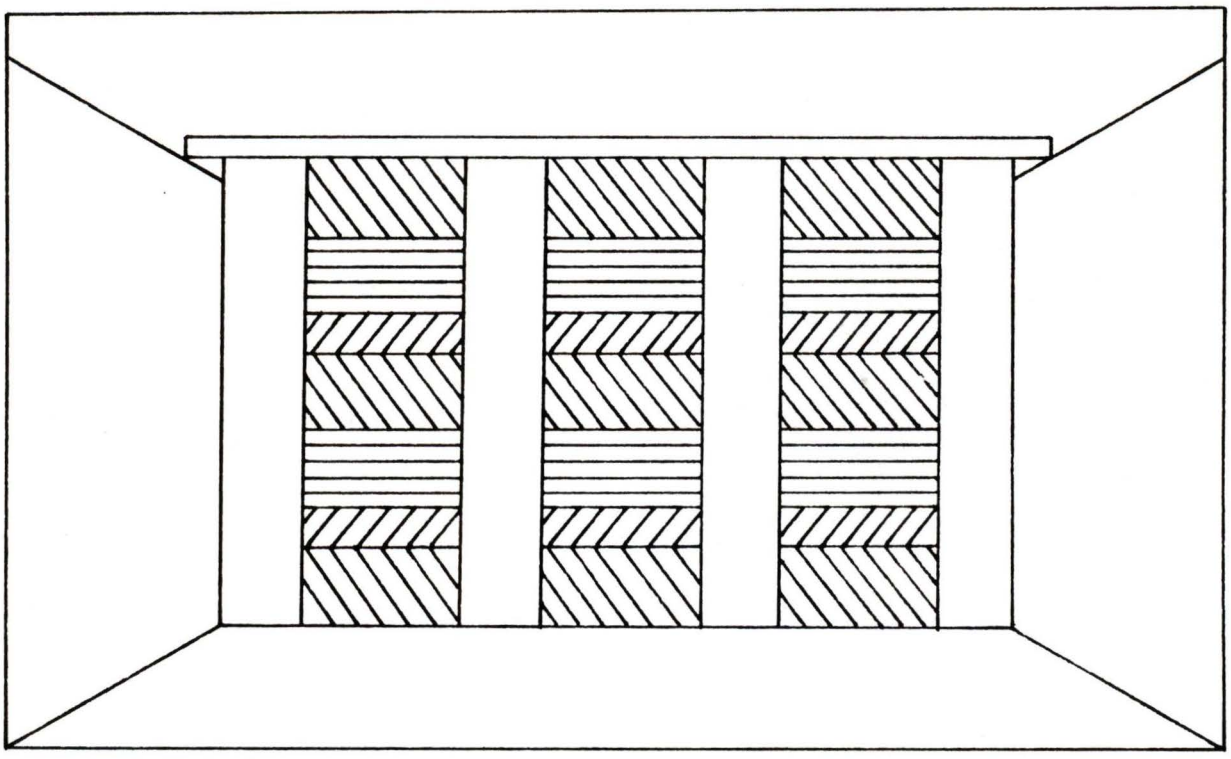

b) horizontal

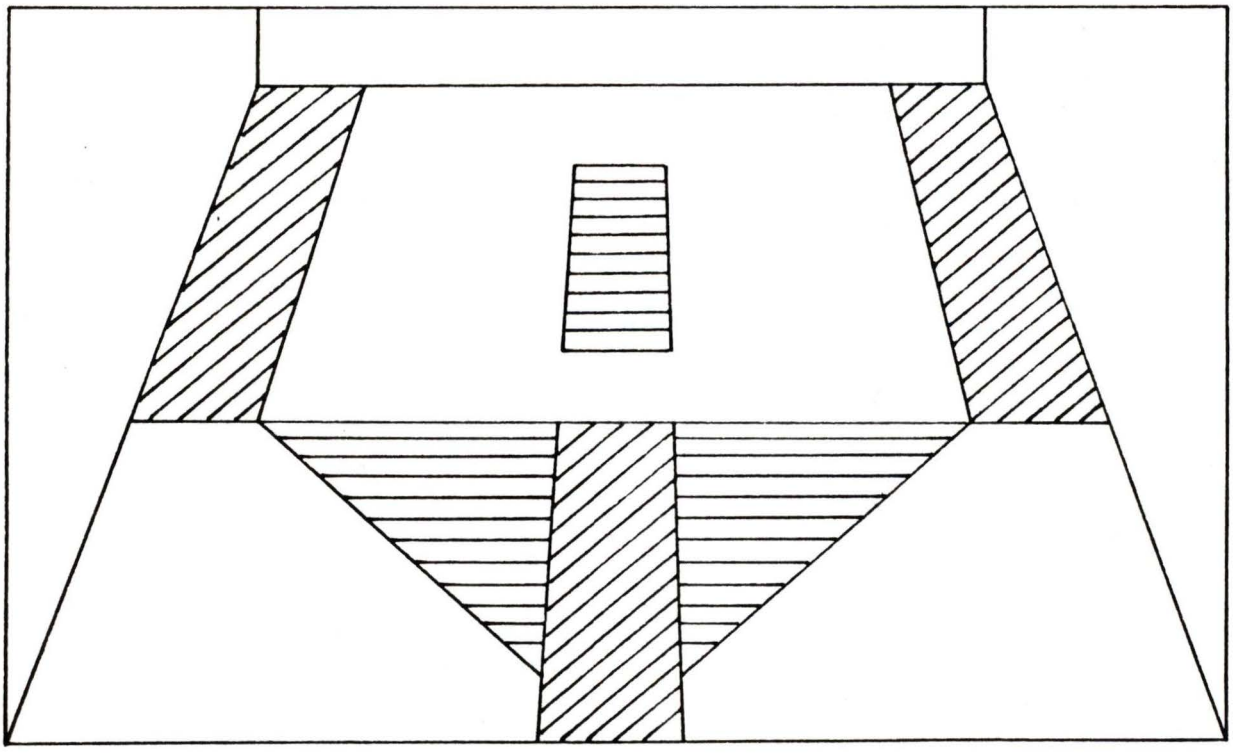

3. Urban Canyon Components

Urban surface components are the largest working units of the urban canyon. They generally describe the sides, floors and significant obstructions within the canyon. The five categories for urban surface components include:

a) buildings,

b) vertical non-vegetative surfaces,

c) vertical vegetative surfaces,

d) horizontal non-vegetative surfaces, and

e) horizontal vegetative surfaces.

The primary distinction between buildings and vertical non-vegetative surface components is that buildings have an internal air-volume that may or may not be heated. Horizontal components are generally on the floor of the canyon. Differences between the categories occur as a result of orientation (horizontal or vertical) and the presence of vegetation. Seldom will the researcher find it confusing to choose an appropriate category with the exception of vegetative surfaces overlying non-vegetative surfaces. Figure 2.5 is a visual aid for estimating the percentage of cover for vegetation. Where the vegetative cover equals or exceeds fifty percent (50 %) the designation of "vegetative surface component" may be used. Estimating vegetative cover requires practice and experience. Generally, all urban surfaces found in the urban canyon will fall into one of these categories.

The categories serve to initiate and focus study for modelling. The researcher should begin by classifying each subject surface into one of the com-

ponent categories. From there, the surface may be broken down into its relevant configurations or elements for sampling.

4. Urban Skies as Components

Urban skies, through the urban boundary layer, form the ceiling of the urban canyon and represent a component unique from the component categories previously identified. It is the only component that can change rapidly over time with cloud cover and cloud types, and with varying concentrations of water vapour and particulates. Even in the absence of clouds, water vapour and particulates may still be present. The study of cloud formation and the assessment of particulate concentrations lie in the realm of atmospheric science and are of minimal interest to this research. However, the determination of urban sky long wave irradiances must take into consideration the thermal and radiative characteristics of water vapour and the most appropriate method to estimate this variable.

Figure 2.5: Comparison charts for visual estimation of vegetative cover (white=vegetation)

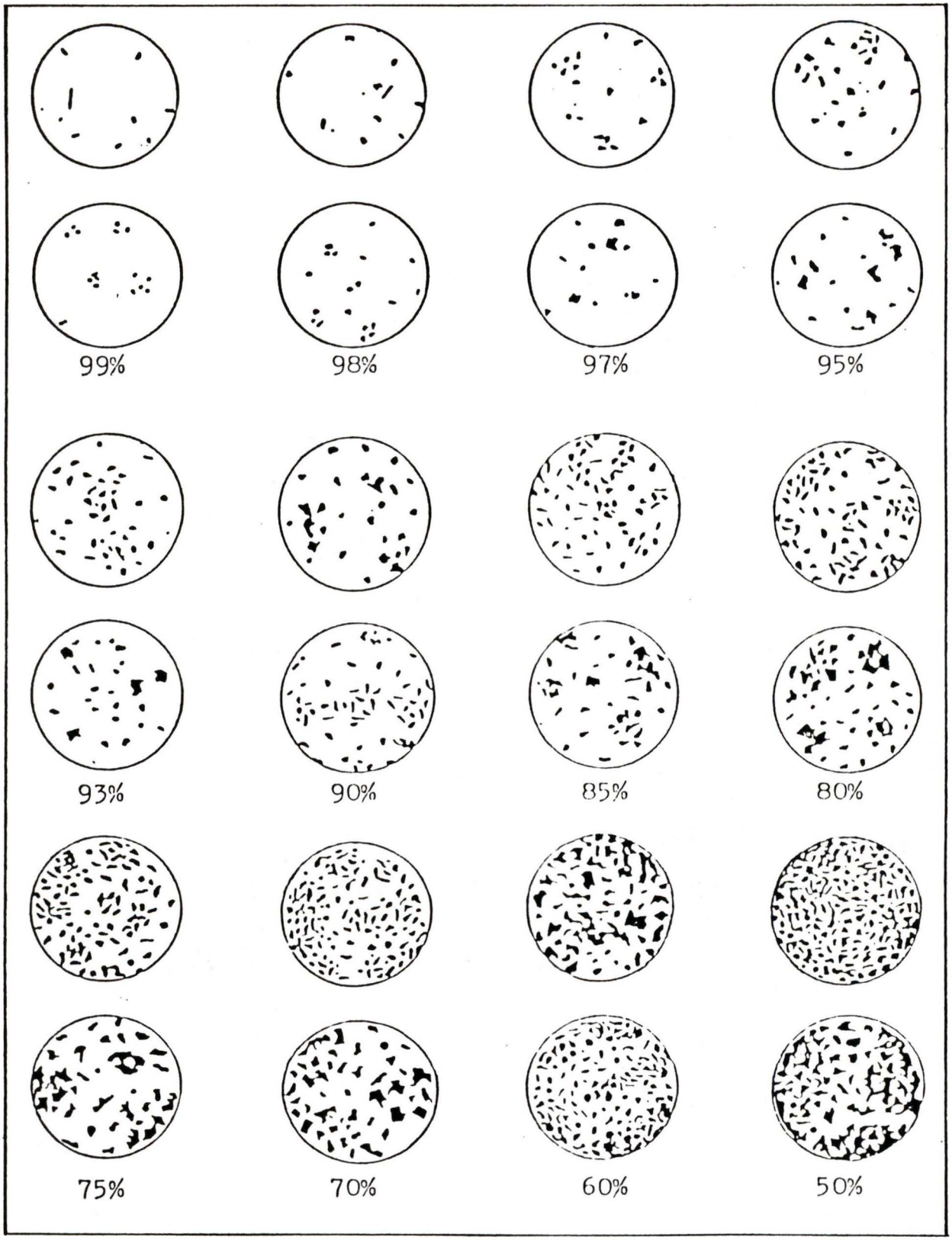

C. Relevant Variables, Properties and Factors for Modelling

The previous sections have identified several dependent and independent variables as well as some properties and factors that should be considered in model development. In order to develop sampling techniques for the variables and gain an understanding of the nature of the properties and factors, it is desirable to classify them and study their relevant dimensions. However, the urban canyon itself is a good place to begin. The items listed in Table 2.5 will be the focus of the remainder of this section.

1. The Urban Canyon

The urban canyon is the focal point of this research. The dimensions of all variables and the sampling methodologies are all linked in some way with the urban canyon dimensions. It is imperative that the researcher knows where each sampling station and surface is at all times within the urban canyon. The simplest method of tying everything together in the urban canyon is to relate them to the urban canyon centre, C.

The dimensions of the urban canyon are based upon a three-dimensional coordinate system where the canyon centre, C, is the origin (0, 0, 0). Figure 2.6 illustrates the urban canyon dimensions. The researcher must become familiar with each urban canyon in the study. This is important not only to the sampling methodologies that will be outlined in Chapter 4, but it is also important for tying all the relevant variables together for any single model.

Table 2.5: List of variables, properties and factors deemed relevant to modelling L^-, T, L^+_0 and T_0

Dependent Variables

L^-	outgoing long wave irradiance
T	surface temperature
L^+_0	incoming long wave irradiance from open sky
T_0	radiant sky temperature
L^*	net long wave irradiance

Independent Variables

T_a	air temperature of canyon air-volume
T_w	wet-bulb air temperature (canyon)
T_{ai}	air temperature of interior air-volume
T_i	interior temperature (substrata)
T_{ac}	air temperature of canopy air-volume
u	wind speed in canyon air-volume
u_c	wind speed in canopy air-volume
u_i	wind speed in interior air-volume

Properties

ε	surface emissivity
k	thermal conductivity of material

Factors

aspect	bearing which a surface faces
h	height (or depth) of vegetative canopy
SVF	sky viewfactor
z	thickness of substrata-sectional materials
EVF	urban surface viewfactor
c	vegetative canopy cover

Figure 2.6: Urban canyon dimensions

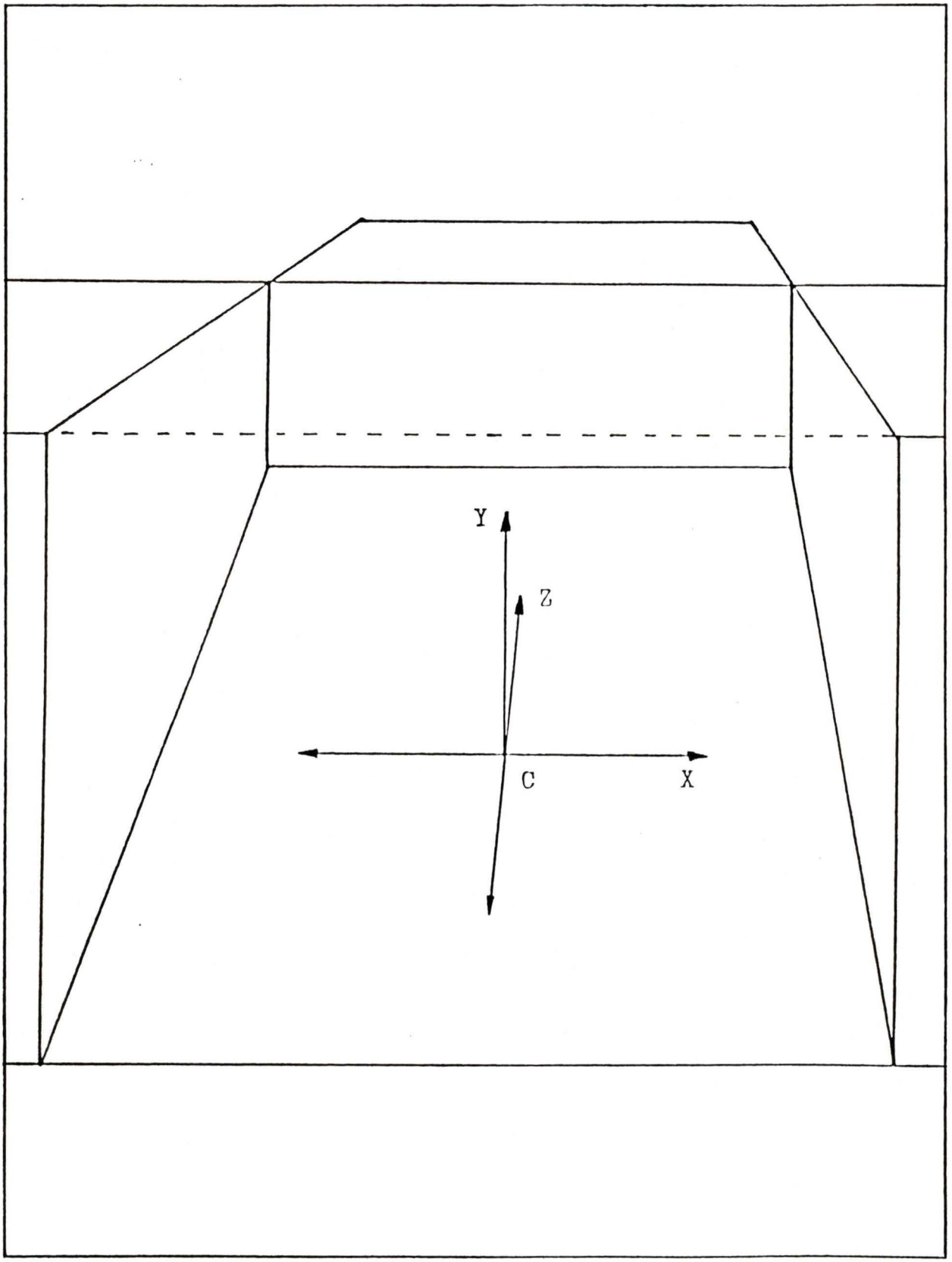

2. The Dependent Variables

Accurately locating and measuring the dependent variables is critical to the development and validation of models. Models are based upon the data collected for each dependent variable while the validity and reliability of the models are reflected in the accuracy and consistency of the data collection process. A standardized data collection procedure based on the coordinates at which these variables and the independent variables may be sampled will help validate models developed in one urban area for use in another.

a) L^*

The net long wave irradiance, L^*, has been discussed in some detail in Chapter 1. L^* at a surface is an irradiance characteristic of areal data. Therefore, for a horizontal surface, the dimensions will be the X, Y coordinates identified for the urban canyon. Similarly, a vertical surface will be identified with the Z dimension and either X or Y. This variable might be better suited as a test variable after models have been developed. Measuring L^* at a plane above or adjacent to a surface is relatively straightforward using simple instrumentation (Chapter 3) and sampling methodologies (Chapter 4). However, measuring L^* higher up in the urban canyon air-volume or on vertical surfaces is complicated by poor accessibility. Even when used as a test variable, measuring L^* is limited to the lower portions of the urban canyon.

b) T and L⁻

T and L⁻ are characteristic of areal data. These two variables lie in two dimensions of the urban canyon. As indicated in Figure 2.7, horizontal surfaces incorporate an X, Y coordinate system while vertical surfaces use Z and either an X or Y coordinate. Although most surfaces have distinct boundaries, the actual number of points at which T or L⁻ can be measured is infinite on any given surface. Since this research focusses on irradiances, measuring the entire surface area, or a portion of it, may be more appropriate. However, a point may prove useful for locating the centre of a sample area depending upon the instrumentation employed.

Figure 2.7: Coordinates of T and L⁻ sampling points

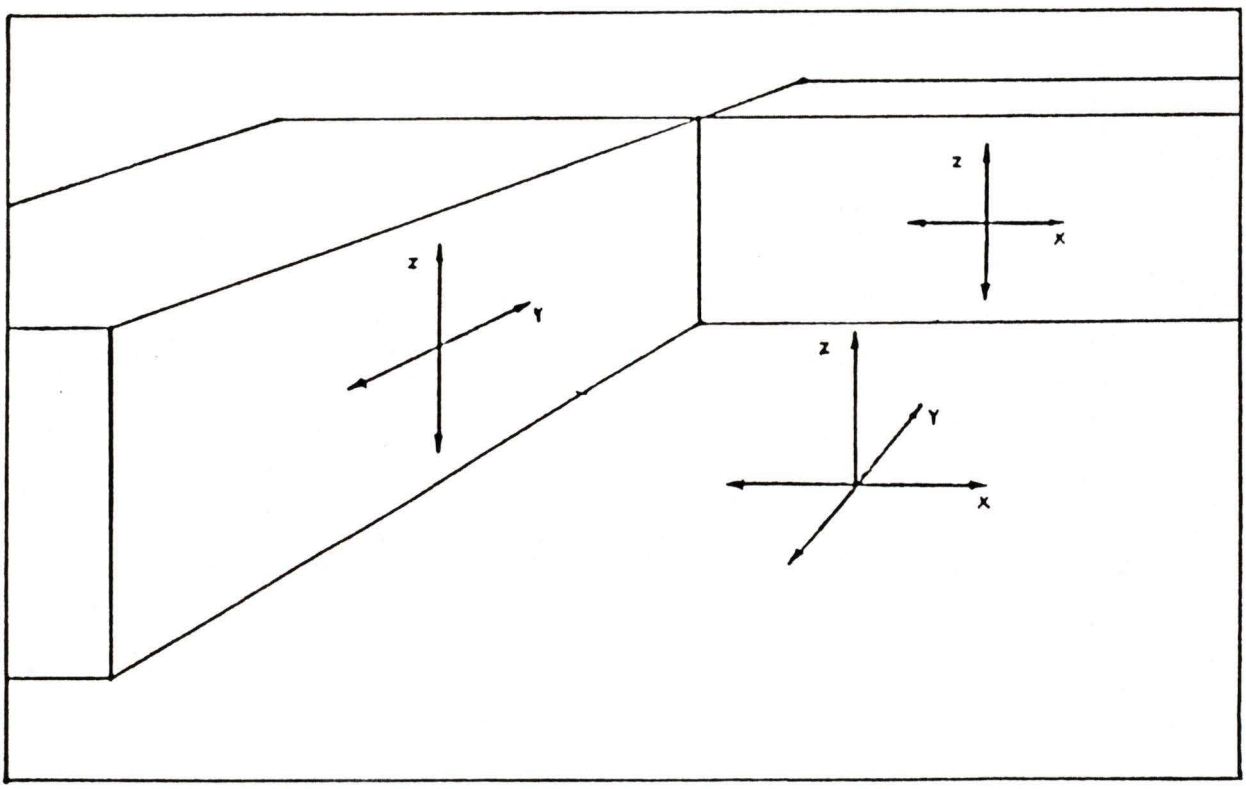

c) T_0 and L^+_0

Areal data also characterize T_0 and L^+_0 . In this case, the area can be visualized as lying at the surface of a hemispherical dome. The dome centre lies at the urban canyon centre, C. As with T and L , the surface area of the dome also has an infinite number of points. These points on the dome are best located using a system of azimuthal and zenith angles that are tied into the dome and urban canyon centres. The zero azimuth angle (0°) lies along the longest positive axis of the coordinate system where this long axis is based on the overall canyon dimensions (e.g. Y-axis along the street). The actual orientation of 0° along this axis is not important. Either direction will do as long as the bearing is recorded. The zero zenith angle (0°) lies directly over the canyon centre on the Z-axis. Using this system (Figure 2.8), all points on the dome have a unique azimuth angle ranging from 0° to just less than 360° and a zenith angle ranging from 0° to just less than 90° . This system is also more advantageous for accurately locating the centre of a particular surface area on the dome.

3. The Independent Variables

The independent variables are equally important to model development and validation. Many of these variable sampling surfaces share the same dimensions and can probably be co-sampled. However, all these variables are characteristic of the climates in various air-volumes with the exception of T_i which is characteristic of a volume of solid mass. These variables are not sampled over areas , but points can be accurately identified where each variable can be measured. Each variable has an infinite number of measurement points that can eventually be trimmed down to a manageable sample size unit.

Figure 2.8: Coordinates of T_0 and L^*_0 over a sampling surface

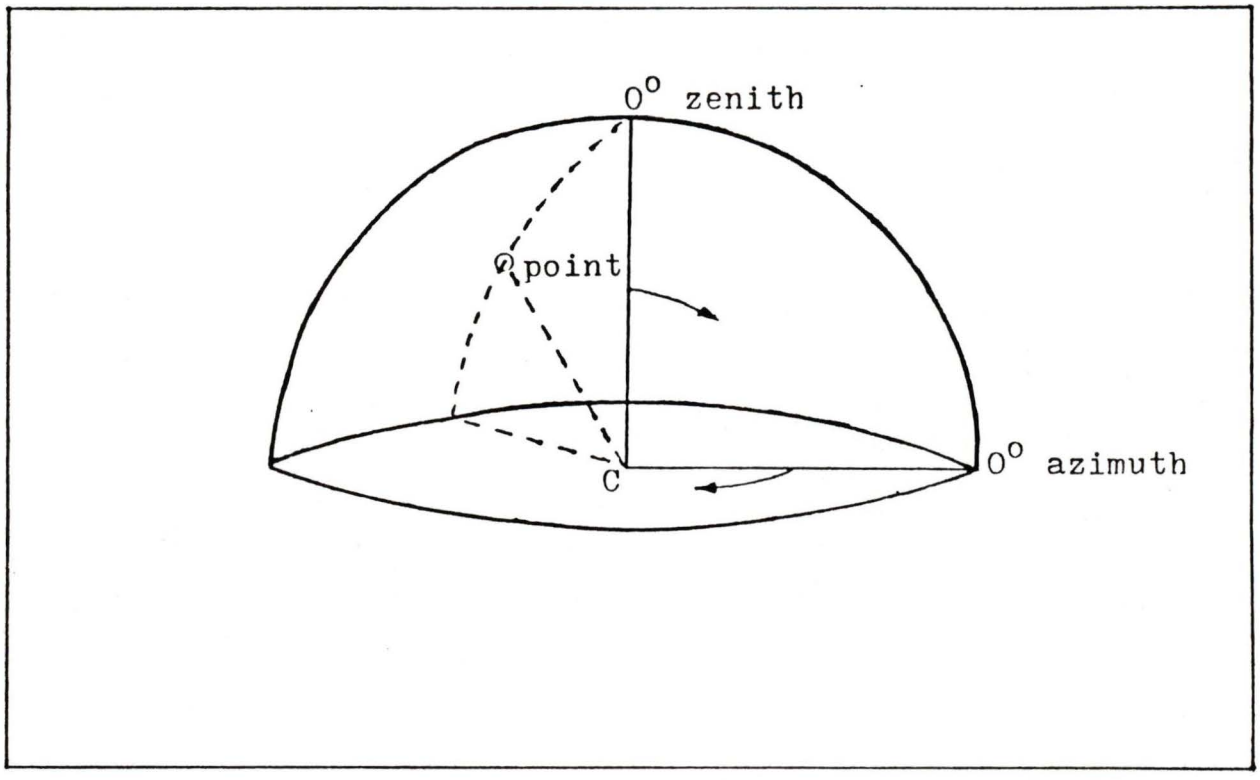

a) T_a, T_w and u

The air temperature, T_a, wet-bulb air temperature, T_w, and wind speed, u, are variables in the urban canyon air-volume that share a common coordinate system. Points for these variables lie in the three dimensions of the urban canyon air-volume and are tied to the canyon centre using the canyon's coordinate system (Figure 2.9).

Measuring T_a, T_w and u may be severely limited in the Z direction due to poor accessibility in the upper regions of the canyon air-volume. Although the

points for measuring these variables lie in three dimensions, actually locating these points may be limited to the X and Y coordinates. The Z dimension becomes the height of the instrument, HI, above the canyon floor.

Rarely will the researcher have the time or means to access vertical profiles of these variables that reach to the canyon ceiling. This limitation should not be detrimental to model development if the instrument height, HI, remains in a small range throughout the data collection processes for development and model use, and as long as it is specified. A screen height between 1.0 and 1.5 metres is commonly used in climatic studies (Oke, 1978).

Figure 2.9: Coordinates of T_a, T_w and u sampling points

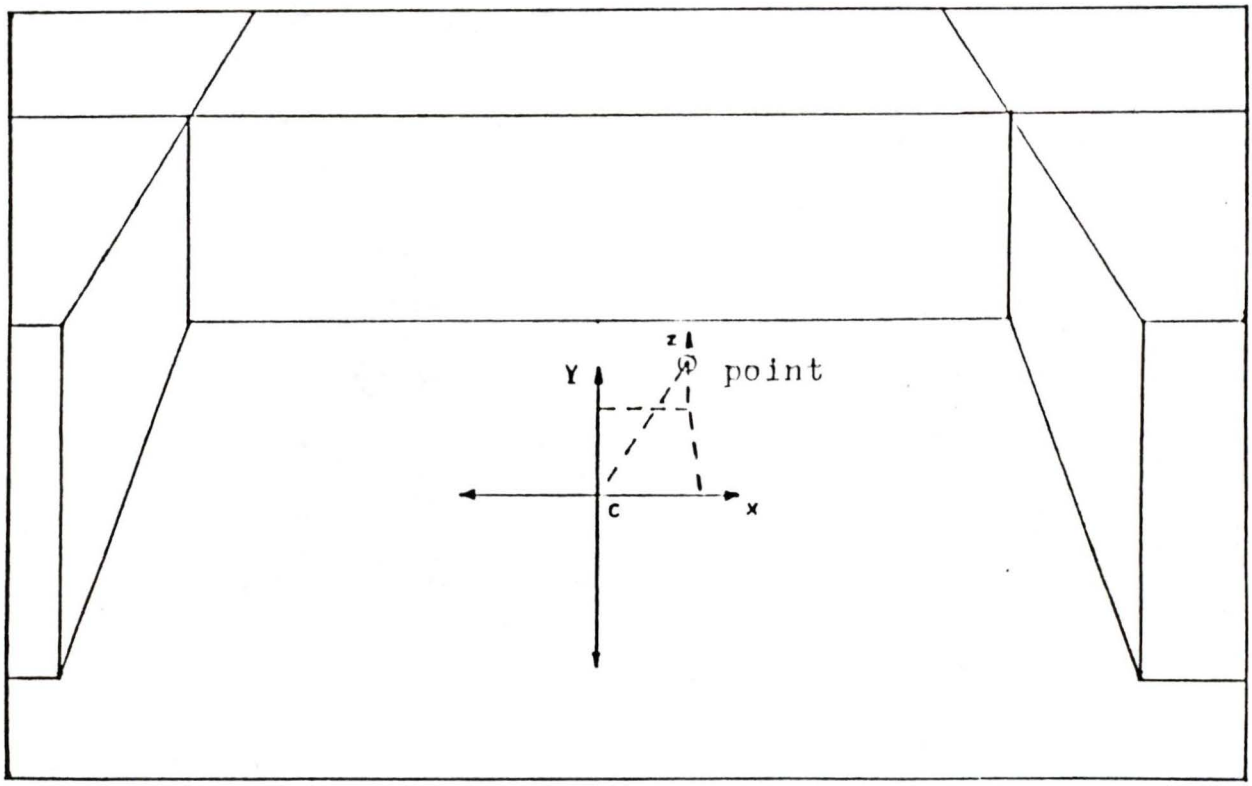

b) T_{ai} and u_i

The inside air-temperature, T_{ai}, and inside wind speed, u_i, are variables characteristic of a building air-volume. These variables also utilize a three dimensional coordinate system similar to that in the urban canyon air-volume. However, this coordinate system has its origin in the centre of rooms within a building. Some buildings house a single room and air-volume (e.g. warehouses) while others contain several rooms with their own air-volumes (e.g. apartments and offices). Large single-room buildings such as warehouses may pose the accessibility problem in the Z direction identified in the urban-canyon air-volume. Maintaining a constant screen height may overcome this problem. Multi-room buildings may require a sampling of rooms for T_{ai} and u_i if an average for the whole building air-volume is desired or if a surface element lies extensively over a building wall. Such a room sample is deemed necessary because the air-volumes in individual rooms are rarely confined and become linked to the total building air-volume (Figure 2.10).

c) T_{ac} and u_c

The canopy air temperature, T_{ac}, and the canopy wind speed, u_c, are variables in the vegetative air-volume contained within a vegetative canopy. Two types of canopies can be identified each with its own coordinate system: vertical vegetation and horizontal vegetation. Vertical vegetation (Figure 2.11a) has a three dimensional system of coordinates describing its canopy air-volume where the depth of the canopy, h, identifies the horizontal radial dimensions (i.e. X and Y coordinates) and Z identifies the vertical dimension of this

Figure 2.10: Coordinates of T_{a} and u_{i} sampling points

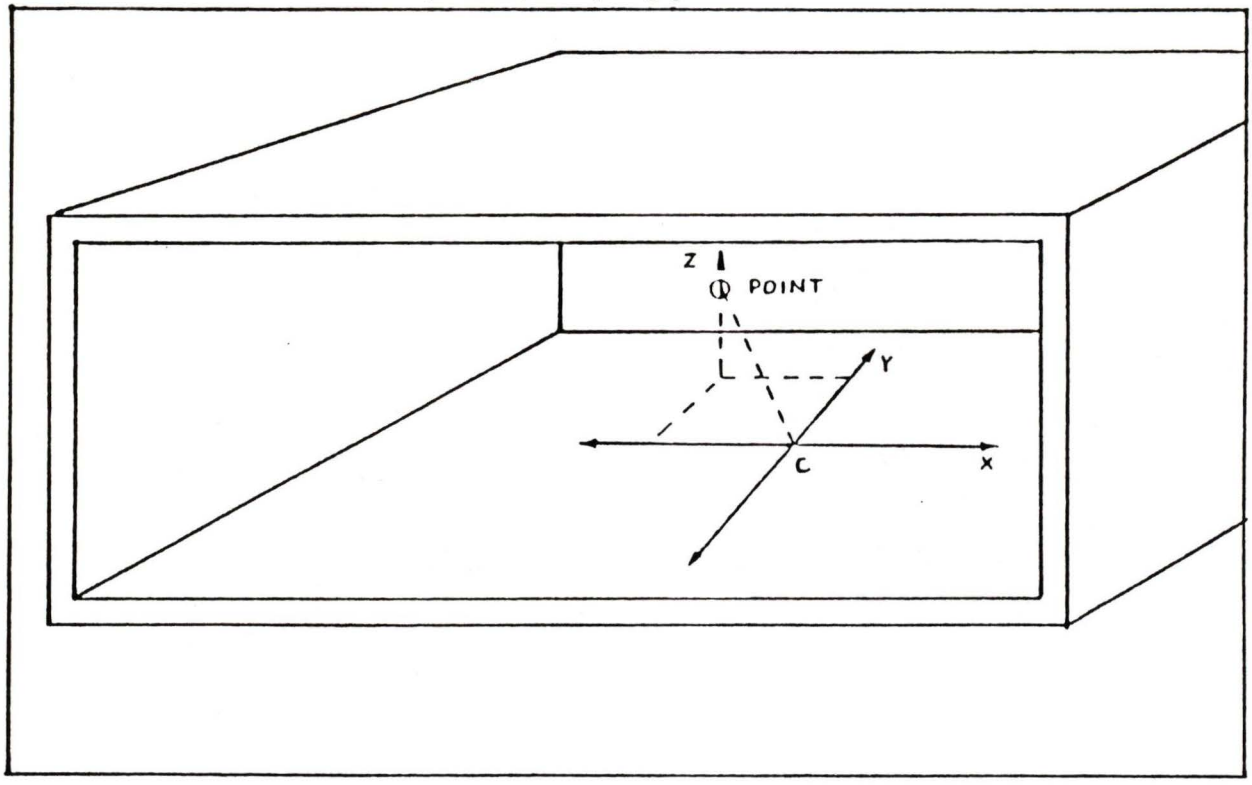

air-volume. As mentioned earlier, h can be averaged. T_{ar} and u_{r} are measured along a radial axis at a height, Z, within the canopy. Accessibility in both the Z and h dimensions can be problematic when the base of the canopy is above 1.5 metres or the canopy is very dense. The origin of this coordinate system is along the trunk between 1.0 and 1.5 m. above ground.

Horizontal vegetation (Figure 2.11b) also uses a three dimensional coordinate system based on the X, Y, Z dimensions used for T_{a}, T_{w} and u. Here, the Z dimension is limited by and is identified with the vegetation height, h. The coordinate system originates at the ground surface at the centre of the vegetative surface. It is difficult to determine when vegetation should be treated as vertical or horizontal. Often, this decision must be left to the discretion of the

researcher since accessibility as well as the factors h and vegetative canopy cover, c, are instrumental in the decision-making process.

Figure 2.11: Coordinates of T_{ac} and u_c
a) vertical

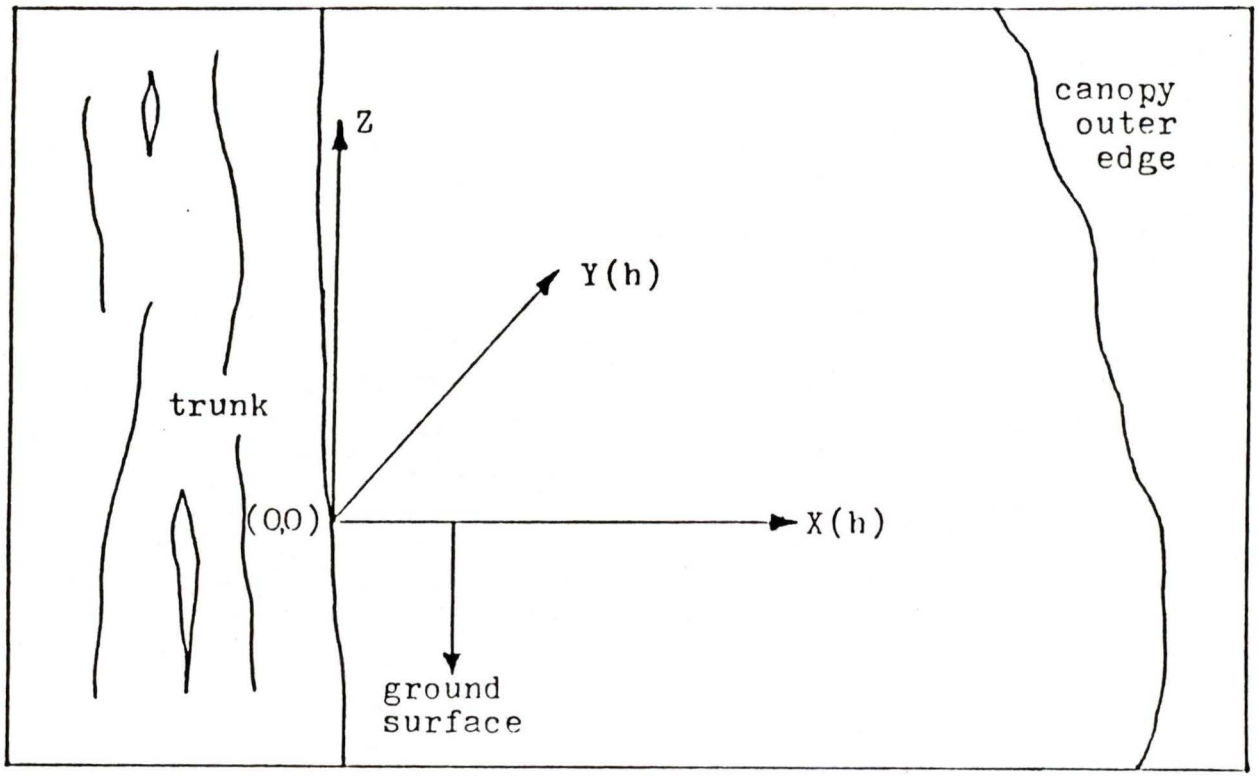

b) horizontal

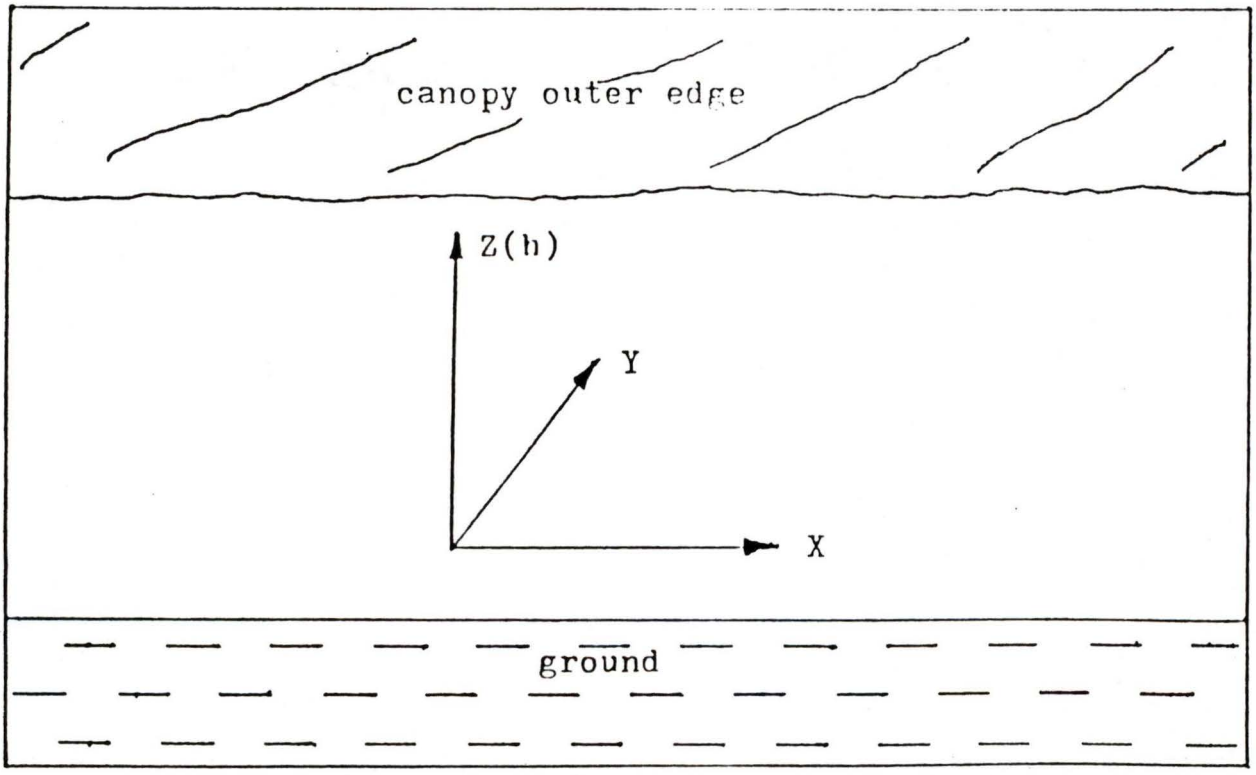

d) T_i

The interior temperature, T_i, of a solid volume or mass may also be measured at points in three dimensions (Figure 2.12). Reaching a point at which to measure T_i poses its own problems. Although T_i may be accessible to a researcher with the right tools and instruments (e.g. thermocouples), T_i may not always be accessible to the model user in the field. Municipalities generally do not appreciate others making holes in the middle of the street just to measure a T_i - T differential.

Figure 2.12: Coordinates for T_i sampling points

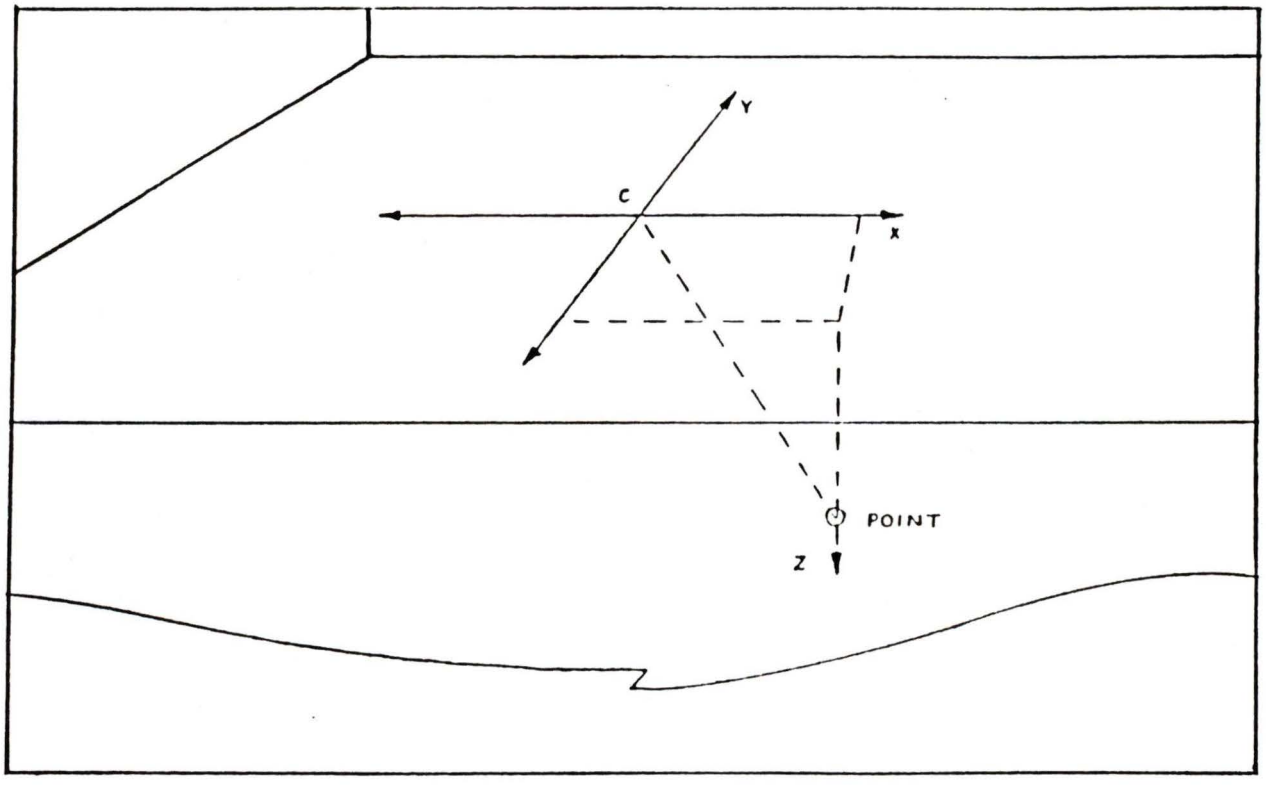

4. Properties

a) emissivity, ε

The surface emissivity, ε ,has been discussed in detail earlier in this chapter. Should surface temperatures prove more suitable as dependent variables than L , then ε is critical to the determination of long wave irradiances using the Stefan-Boltzmann Law. Typical values for ε are listed in Table A2 (Appendix B).

b) thermal conductivity, k

The thermal conductivity, k, of a material determines the rate of heat transfer through conduction. Since the controls placed by the energy budget on the dependent variables, T and L , are so closely linked to the flow of heat energy, k may provide the means by which surface elements can be classified for focussing model development. Table A1 (Appendix B) lists surface materials that share common values for k.

To save time and money, models for materials with each of these ranges of k could be developed. The surface emissivity, ε, displays too much variability due to paints or finishes to be a basis for focussing model development. Models for vegetation and clear skies should be developed separately and use other criteria (e.g. cloud & vegetative cover and cloud amount).

5. Factors

a) h

This factor is the height of the vegetative canopy for horizontal vegetation or the depth of the vegetative canopy for vertical vegetation. It affects the eddies and mixing of the air adjacent to vegetative surfaces.

b) z

The thickness of material, z, for each layer of substrata or a building shell is significant to the rate at which heat energy is conducted along with k.

c) aspect

The aspect of a surface has not been discussed in any detail so far. This factor indicates the direction a surface faces, whether it "sees" north, south, east, west, or a combination of these aspects. Assigning an aspect for vertical surfaces is usually quite simple since something like a wall actually faces the appropriate aspect. However, horizontal surfaces lying on one side of a canyon (e.g. north) do in fact face the opposite direction (e.g. south) and should be assigned this opposite aspect. This research outlines some preliminary investigations into the aspect factor (Data Sheets 6 to 9 in Appendix A) as it relates to surface temperatures. It was found that on average and over the course of the night, south and west facing surfaces of horizontal non-vegetative surfaces and building shells were warmer than north and east aspects. For horizontal and vertical vegetation however, T did not vary more than ± 0.5 °C between

aspects. Therefore, for building shells and horizontal non-vegetative surfaces (and probably vertical non-vegetative surfaces) it is recommended that aspect be considered in model development.

d) canopy cover

The cover for a vegetative canopy, c, has been discussed in some detail. It is crucial to the determination of canopy dominance during model development, and whether a vegetative surface or the material behind this surface (e.g. trunk, stem, or ground) should be modelled.

e) SVF

The sky viewfactor, SVF, may affect the air temperature in an urban canyon and overall surface temperatures (Bärring et al., 1985). The case study (Data Sheet 1) measured the air temperature over a single surface element type in three urban canyons within a 10 minute period at night. There is apparently an inverse relationship between T_a and SVF.

f) EVF

The environmental viewfactors, EVF, for surface elements, configurations or components are most relevant to testing the models. When models have been developed, they can be used in conjunction with EVF and SVF to construct the urban nocturnal long wave radiation regime for comparison with measured values of L^* in an urban canyon.

D. Chapter Summary

This chapter has gone to great lengths to identify the variables, properties, and factors relevant to modelling long wave irradiances at night in the urban canyon as well as give some justification as to why they are relevant and significant. The concept of surface elements, configurations and components was introduced. Surface elements are the recommended focus for models of T and L^{-}. Finally, a detailed list of these variables, properties and factors was presented and the sample point coordinates were identified. Variable and dimension identification will facilitate the analysis of the instruments to be covered in Chapter 3 and the development of sampling methodologies in Chapter 4.

Chapter III

INSTRUMENTS FOR MEASURING THE DEPENDENT AND INDEPENDENT VARIABLES WITHIN URBAN CANYONS

The second precondition in URBMAT is the identification and evaluation of those instruments that may be used in the measurement of the relevant variables outlined in Chapter 2. This includes not only the identification of appropriate instrument types and groups, but also their accuracies, calibration and practical considerations for their use.

Chapter 3 will begin by evaluating instruments for measuring long wave irradiances and radiant temperatures in the urban canyon. This will be followed by instruments for measuring air temperatures, humidities and wind speeds. The chapter summary will then correlate specific instruments with relevant variables in an attempt to choose the "best" instrument for measuring each. To help with the selection, the advantages, disadvantages and limitations of each instrument are considered when evaluating practical considerations for use.

A significant portion of the section on radiant temperature instruments is devoted to the analysis and use of these instruments. This research suggests that the use of these instruments has been poorly considered in the past, especially when measuring radiant temperatures on vertical surfaces. For this reason, an extensive Guide (Appendix D) has been developed to assist the researcher in

organizing and planning the measurement of these temperatures for vertical surfaces. This Guide is believed to be "one of a kind" and the first attempt at clarifying the use of radiant temperature instruments.

A. Instruments for the Dependent Variables

This section will introduce general instrument types that measure long wave irradiance and radiant temperature. Only those devices that display practical applications for urban canyons will be covered. Some instruments may not be portable, may require large power sources, or may be too expensive thus rendering them impractical. General instrument types, their principles of operation, calibration and any practical considerations for their use will be discussed rather than specific name brands and models.

1. Long Wave Irradiance Instruments

There are two general types of instruments suitable for the practical measurement of long wave irradiance: the net pyrradiometer and the net pyrgeometer. Both instruments rely in part on controlling the effects of evaporative, convective and conductive heat flux densities within the instrument housing. Nearly all operational radiation instruments use the temperature difference between a receiver surface upon which radiation is incident and a reference body as a measure of irradiance. These instruments are considered to be under a steady-state condition so that the thermal time constants of the instruments do not enter into the radiation analysis (Dobson et al., 1980).

a) Net Pyrradiometer

These instruments are designed to measure the total net radiation, Q^*, at a horizontal plane above a surface, although they may also be use for vertical and sloping planes. This means that emitted and reflected irradiances incident

upon the instrument from above and below are registered to yielded a net reading at the instrument. Both solar and long wave irradiances are measured by day, but at night, the pyrradiometer may be used to measure long wave irradiance in the absence of solar irradiance (Chapter 2). The response time, or the time it takes for these instruments to yield a stable and valid reading, is considered quick. This means that readings may be taken immediately.

For the purposes of this research, a net reading of long wave irradiance is desirable only as a validation for models of long wave irradiance or radiant temperature. These instruments measure irradiance over a hemispherical dome above the plane ($L^{\downarrow}$) and a dome below the plane ($L^{\uparrow}$). To isolate individual long wave irradiances from all the emitters in an urban canyon using these instruments would be nearly impossible unless they were put very close to the emitter. However, by using models and viewfactors to construct the urban nocturnal long wave radiation regime and L^{*} at a specific point in the urban canyon (e.g. urban canyon centre , C), the calculated value for $L^{\downarrow}$ could be compared to one measured by a net pyrradiometer.

A single reading for the nocturnal long wave irradiance emitted from a single surface element or type can also be obtained using these instruments. By attaching a black body cavity with a known emissivity (preferably 1.0) and surface temperature over the bottom sensor of the pyrradiometer, the incoming long wave irradiance to the other sensor can be calculated using:

$$L_{r} = Q^{*} + \varepsilon_{b}\sigma T^{4}_{k} \qquad \text{Eq. 3.1}$$

where

L_r is the long wave irradiance received by the net pyrradiometer's top sensor (equivalent to $L^{\uparrow}$ or $L^{\downarrow}$ in Wm^{-2}),

Q^* is the net radiation measured by the instrument (Wm^{-2}),

ε_b is the emissivity of the black body cavity, and

T_k is the surface temperature of the black body cavity (°K).

b) Net Pyrgeometers

Net pyrgeometers work on similar principles to those of net pyrradiometers. These instruments use a filter dome over the receivers that are intended to be transparent only for wavelengths greater than or equal to 3.0 micrometers thus measuring only long wave irradiance. Unfortunately, no filter material fulfills this conditions. Clear and black polyethylene as well a silicone crystals have been used (Dobson et al., 1980). During the day, some of the solar irradiances are able to penetrate the filters while at night, bands of long wave irradiance (i.e. terrestrial wavelength intervals) are blotted out totally by not being able to penetrate the filters.

These instruments also yield a "net" reading of long wave irradiances. Therefore, they may be used for either model validation or for single readings of long wave irradiances in a manner similar to that described for the net pyrradiometer. For a single reading of $L^{\uparrow}$ or $L^{\downarrow}$, Eq. 3.1 can be employed using L^* for the instrument reading in lieu of Q^*. Response times for these instruments are also quick.

c) Calibration

These instruments are easily calibrated for use in measuring long wave irradiances. Black body cavities of known emissivities and temperatures can be attached to both sides of the instrument to yield a known net reading or a reading of zero. However, although this method is easy not everyone may have the proper black body cavities available to them. By enclosing the instrument in a box with known emissivity and surface temperature, the instrument may be calibrated for zero.

d) Practical Considerations for Use

Measuring L at a horizontal plane over the urban canyon centre, C, is the easist when using these instruments to test the validity and capability of models to estimate the urban nocturnal long wave radiation regime. Using the screen height (instrument height HI = 1.5 metres), level the instrument so that the lower sensor is parallel to the surface. Often the sensors are mounted at the end of a probe which is connected to a meter or recorder via a cable. If possible, the probe and sensors should be mounted on a platform or tripod and the readings taken as far away from the sensors as the cable will permit. In this way, the outgoing long wave irradiance from the researcher will have a minimal effect on the reading.

For making single readings of incoming long wave irradiances, the "open" sensor (i.e. the one not covered by a black body cavity) can be placed in close proximity to a surface, or it can be made somewhat unidirectional. Since the

sensors generally measure irradiances over a [illegible] are by nature multidirectional in their sensing capabi[illegible]ery close to a surface, radiation "noise" can affec[illegible]lts from undesireable irradiances incident on the lower [illegible]ons of the domed filter (i.e. closest to the housing) being registered by the instrument.

Rendering these instruments unidirectional may not be difficult, but it can be impractical. A blackened tube can be placed over the "open" sensor so that only irradiances entering the tube or reflected by the inner tube walls will be measured. However, this requires that the emissivity, reflectance and surface temperature of the tube as well as the cosine relationships of the hemispherical sensing area between the tube and sensor are known.

Aside from the instruments' multidirectional properties, the filter domes over the receivers pose problems that may greatly affect the instrument's accuracy. The domes are not only imperfect filters of long wave irradiance, but they also deteriorate and must be replaced regularly. For this reason, the accuracy of most of these instruments is suspect unless frequently calibrated (Dobson et al., 1980) although many will yield a reading within $\pm$ 1.0 Wm^{-2}.

2. Instruments for Radiant Temperatures

Instruments that measure radiant temperatures are referred to as radiometers. They contain as essential parts a lens or mirror that focusses the sensory image, a detector, filters and electronic circuitry while some also incorporate a chopper. The detectors are the transducers which convert the radiant energy

emitted and reflected by a target (e.g. surface element) into an electrical signal. The lenses, detectors and filters have limited wavelength responses. Usually, they are attuned to long wave radiation.

An infra-red radiometer works on the principal of comparing the irradiance in a specified wavelength band from a target area with that of an internal reference cavity in the instrument housing. Some of these instruments (e.g. Stoll-Hardy and Barnes systems) measure the temperature increase caused by absorbed irradiance at the sensor compared to the temperature of an unexposed black body cavity in the housing. Others use a chopper to produce an alternating signal when irradiances come alternately from the target and cavity.

When semiconductor materials are heated, changes occur in their vibrational energy and their ability to conduct electricity. The conductivity of heat sensing thermistors within an instrument's detector increases with temperature in an exponential fashion (Dobson et al., 1980). A detector based upon this principle is called a bolometer and is the common detector mechanism in many commercially available hand-held radiometers. Bolometers are light-weight and use an internal power source. Their response times are also quick. Therefore, they are considered practical and are the only instruments for measuring radiant temperatures that will be considered here.

These bolometer detectors are mounted in an insulated and evacuated cavity. Since detection depends on heating caused by long wave irradiances incident upon the detector, heat losses from convection and conduction must be

controlled. Openings to the detector are covered by a "window" or a focussing lens which not only isolates the detector, but also provide wavelength limits by filtering the incoming irradiance. Detectors are made very small so that they can quickly respond to changes in the incident irradiance.

Although these instruments measure the incident long wave irradiance at the sensor or that emitted by the target, they usually indicate a radiant temperature. This radiant temperature is then used in the Stefan-Boltzmann Law to yield an outgoing long wave irradiance for the target. However, it must be stressed that these instruments yield an apparent radiant temperature, T_r. The irradiance "seen" by the instruments is that emitted by the surface plus any incoming irradiances in the same wavelength band reflected by the target. Thus, the target's outgoing long wave irradiance is:

$$\varepsilon\sigma T_r^4 = \varepsilon\sigma T^4 + (1 - \varepsilon)\, L^{\downarrow} \qquad \text{Eq. 3.2}$$

where T is the actual surface temperature (°K) that is the desired measurement. For most natural surfaces , including vegetation, ε is close to 1.0 and T_r can be considered equal to T. This approach is very helpful because no contact with the surface is involved and the irradiance "seen" is an integration of that emitted from an area. The effect of neglecting the variation of emissivities is of the order of 1°C for most natural surfaces (Oke, 1978). For man-made surfaces, no such generalization should be made. Where the range of surface emissivities for water, soil, natural and vegetative surfaces is 0.82 (old snow) to 0.99 (fresh snow, leaved deciduous trees and agricultural crops), the emissivities for man-made surfaces ranges from 0.13 (corrugated iron) to 0.98 (black paints) (Table A2, Appendix B).

The researcher should be aware of several sources of error which may limit the accuracy of an infra-red radiometer. A leak in the filter will admit undesirable radiation from outside the infra-red spectral range. Exposure to cold or wind can affect accuracy since normally the heating element of the temperature controlled cavity has limited power.

Frequent calibration checks of a radiometer are recommended for a variety of reasons. Amplifiers and other components have a limited lifetime. The optical materials may deteriorate. Mirrors and choppers may become scratched, dirty, corroded or wet in an adverse environment. All these reasons reduce the instruments' sensitivity and accuracy. Many of these instruments are capable of accuracies within ± 0.1°C (Dobson et al., 1980). However, the temperature scales generally read to an accuracy of ± 0.5°C. For this reason, ± 0.5°C is a reasonable accuracy for measuring surface temperatures since it appears to be well within the capability of these instruments.

a) Instrument Viewfactors and Spot Readings

Manufacturers of radiometers specify an instrument field-of-view, or viewfactor, ϕ . Thus far, these viewfactors are fixed and circular. The circular viewfactors of radiometers are generally considered to sense a circular area on a flat surface when the centre of the viewfactor is perpendicular to the target, hereafter referred to as a "spot". Nowhere in the literature are concessions made for variations in spot size and dimensions as the radiometer is moved off the perpendicular. It is desirable to know the spot size, dimensions and location when using radiometers both on and off the perpendicular. First, should random sam-

pling without replacement prove applicable in the sampling methodologies, then overlapping spots could violate this condition. Thus, knowing the spot dimensions and location would be essential. Second, with the limited spatial areas of many surface elements in urban canyons it is imperative that the spot be placed within the element. Should the spot "pour" over the boundaries of the element, gross inaccuracies could result in the T_r reading when an adjacent elemental surface is included in the measurement.

Figure 3.1 indicates the instrument setup for measuring temperatures at a horizontal surface and Figure 3.2 illustrates the elliptic shape of the spot when the instrument is off the perpendicular. The spot height, a, in relation to the vertical axis of the instrument can be calculated using:

$$a = HI[\tan(\gamma + \phi/2) - \tan(\gamma - \phi/2)] \qquad \text{Eq. 3.3}$$

where

HI is the instrument height (m), and

γ is the angle from the vertical plane of the instrument to the centre of the instrument viewfactor, ϕ.

The spot width, w, can be calculated using:

$$w = \frac{2\ HI\ (\tan\phi/2)}{\cos\gamma} \qquad \text{Eq. 3.4}$$

If the instrument were trained at a horizontal surface in the perpendicular (γ = 0°) with an instrument height HI = 1.5 m and an instrument viewfactor ϕ = 28°, then the spot dimensions would be a = 0.75 m and w = 0.75 m. However, if this surface were a narrow strip of concrete of width W = 0.60 m., then either the instrument would have to be lowered or the viewfactor narrowed. Since, the

Figure 3.1: Radiometer setup for horizontal surfaces

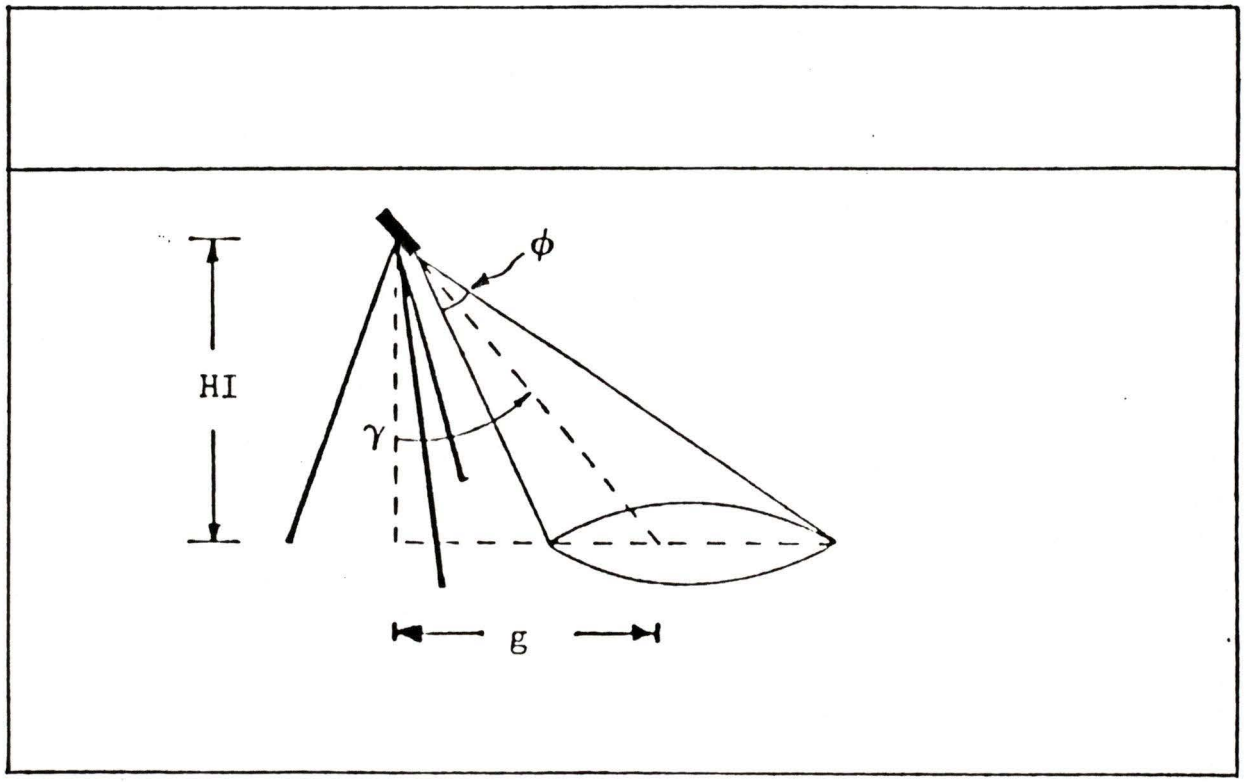

Figure 3.2: Spot dimensions

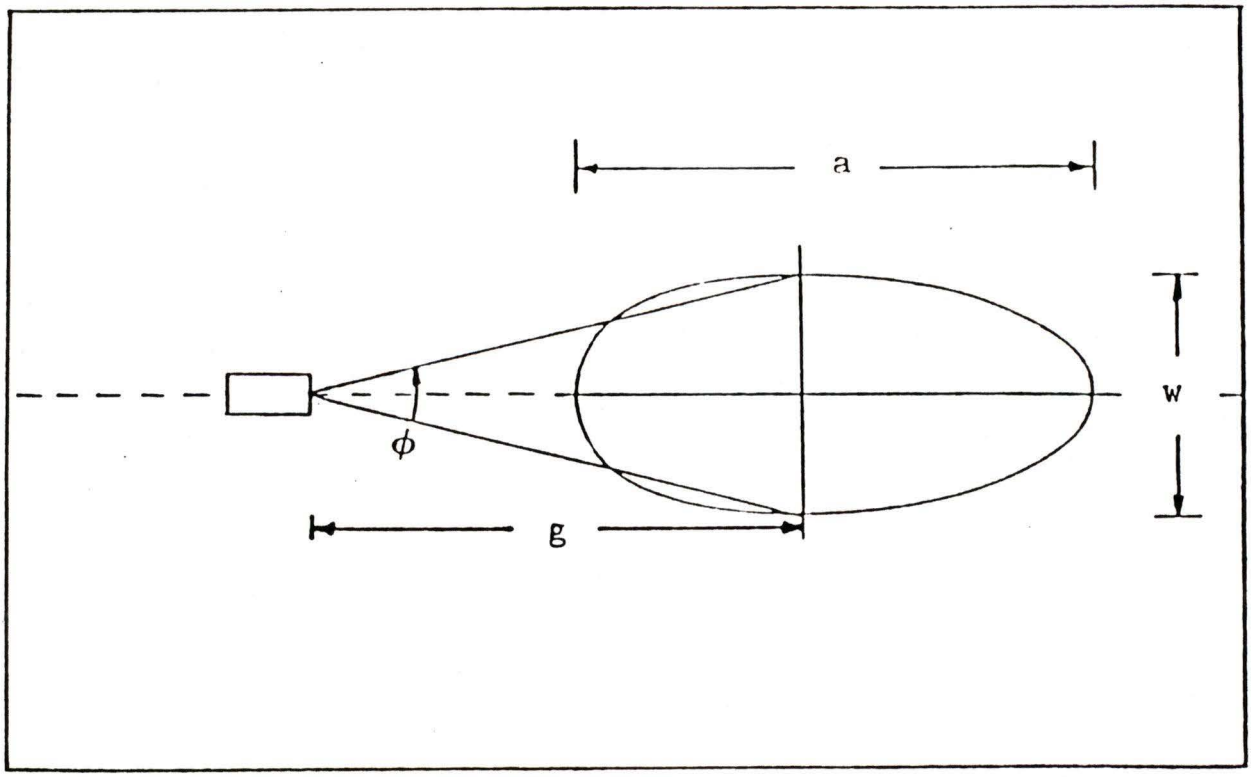

viewfactor is fixed, HI would have to be set at 1.2 metres so that the spot would "fit" into the concrete strip.

When the instrument is off the perpendicular, both the spot height and width increase. With $\gamma = 30°$, HI = 1.5 m and $\phi = 28°$, a = 1.02 m and w = 0.86 m. To emphasize how much changing γ will affect the spot, the area of each spot, A, can be compared where the spot is treated as an ellipse when off the perpendicular using:

$$A = \frac{\pi a w}{4} \qquad \text{Eq. 3.5}$$

Therefore, when HI = 1.5 m and $\phi = 28°$, A = 0.44 m^2 when $\gamma = 0°$ while A = 0.69 m^2 when $\gamma = 30°$. Clearly there are significant changes in a, w and A when the instrument is off the perpendicular.

The instrument setup is similar for vertical surfaces except that γ becomes the angle from the horizontal plane of the instrument to the centre of the instrument viewfactor, ϕ (Figure 3.3). The equations for a, w and A (Eq. 3.3, 3.4 and 3.5 respectively) can also be used for spots on vertical surfaces. However, rather than using HI in each of Eq. 3.3 and 3.4, the perpendicular distance from the instrument to the vertical surface, d, is used. Again, as γ is moved from the perpendicular the spot height, width and area increase with γ .

Similarly, as the instrument is moved closer to the surface or the instrument viewfactor is reduced, the spot dimensions and size decrease.

Figure 3.3: Radiometer setup for vertical surfaces

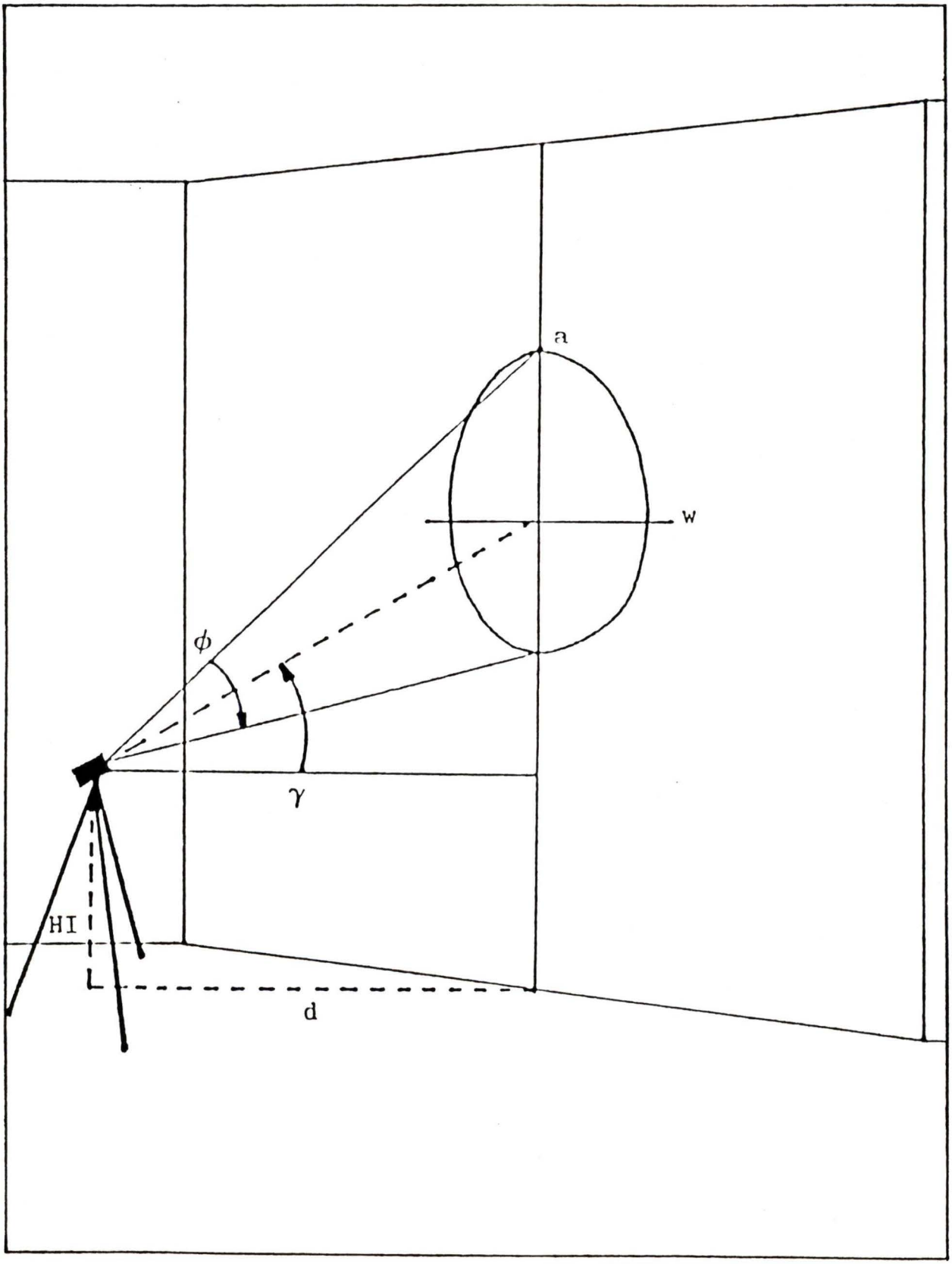

b) Calibration

Calibration of the radiometer can be performed in the laboratory by positioning a black body source of known temperature and emissivity so that it fills the instrument's field-of-view. It is important that the emissivity be as close to 1.0 as possible so that the apparent radiant temperature, T_r, can be set equal to the actual radiant temperature, T. Once the instrument is calibrated in the lab, a quick recalibration can usually be done in the field with either built-in or separate temperature sources provided with the instrument. Field recalibration is usually required after a few consecutive measurements or before the instrument is used each time if it has been turned off.

c) Practical Considerations for Use

There are several considerations involved in using radiometers aside from instrument viewfactors, spot dimensions and instrument setups.

One consideration is what these instruments measure. They do not measure points. They measure specific areas on a surface based on how and where they are pointed. It is important to know what part and area of a surface element is being sensed . Horizontal and vertical surfaces each require special considerations for sampling T.

For horizontal surfaces, HI and γ must be carefully considered and recorded. The instrument height, HI, must be set where the researcher can easily read the instrument without straining himself. Of course recording HI also has a bearing on calculation of spot dimensions. The instrument angle, γ, is

important to spot dimensions as well, but it is also important to spot location. If γ were retained at 0°, then in most cases the researcher would include his feet in the spot temperature measurement of a horizontal surface when the instrument is hand-held. Therefore, it is recommended that the radiometer be placed on a tripod and that γ be set at such an angle that no undesireable objects be included in the spot (e.g. feet). Mounting the radiometer has the added advantage of freeing the researchers' hands for recording as well as more accurately controlling γ when the tripod is fitted with a zenith angle scale (i.e. 0° to 90° in 2 directions).

Setting γ and HI for use in the field can be based in part on the distance along the surface from the instrument to the centre of the spot, g (Fig. 3.1), where:

$$g = HI \tan\gamma \qquad \text{Eq. 3.6}$$

When g is greater than one half of the spot height, then the presence of the researcher will not interfere with the surface temperature measurement. For example, with ϕ = 28° and HI = 1.25 m, g = 0.72 m and a/2 = 0.42 m when γ = 30° . There is no interference. However, using the same ϕ and HI, g = 0.31 m and a/2 = 0.66 when γ = 14° : there would be interference with either the researcher or the tripod. In this research (Appendix A), an HI between 1.0 and 1.5 metres was found to be very comfortable while γ = 30° seldom resulted in any interference.

Although a surface is considered to be covered with an infinite number of points, there are a finite number of spots that will cover a given surface area without overlapping the spots. The exact number of spots that will fit within

the limits of a horizontal surface area is based upon ϕ, HI, γ, the linear dimensions of the surface (X, Y) and the direction along the surface that the spots are measured (either in the X or Y direction).

A horizontal surface of dimensions X = 10 m and Y = 25 m is covered with 171 spots when HI = 1.5 m, $\gamma = 30°$ and $\phi = 35°$ where the instrument is pointed in the Y direction. This same surface is covered by 154 spots when the instrument is pointed in the X direction. In neither case are the spots permitted to overlap nor are there any partial spots. Of course using an instrument with a smaller viewfactor would increase the number of spots. When ϕ is changed to $2.8°$, 31250 spots are generated in the Y direction and 31200 in the X direction. The question arises as to which instrument viewfactor is preferable: a narrow ($2.8°$) or a wide ($35°$) viewfactor. Based on the spot area, A, that would be generated in the Y direction and using the above information, a $\phi = 2.8°$ provides a 79 % total areal coverage while $\phi = 35°$ provides a 76 % total areal coverage. Clearly, increasing the number of spots by decreasing the instrument viewfactor does not provide a great improvement in total areal coverage. In addition, during the course of this research, two instruments employing these instrument viewfactors showed no difference in the surface temperature readings they generated after they were calibrated. Therefore, choosing an appropriate instrument viewfactor becomes a case of convenience where smaller or narrower elemental surface areas are more easily measured for T using narrower instrument viewfactors. Of course, a researcher does not want to sample 154 spots for surface temperature let alone 31250 spots. Not only would sampling all these spots be undesirable, but one purpose of this research is to test the necessity of sampling all these spots.

For vertical surfaces, HI should also be held constant somewhere between 1.0 and 1.5 metres and well recorded. However, determining γ and the distance of the instrument from the vertical surface, d, requires special consideration so that the spots will fit into a confined elemental surface area and no overlapping of spots will occur. To this end, a Guide (Appendix D) has been developed to assist the researcher in accurately locating spots within elemental surface areas. The Guide not only generates appropriate values of γ and d based on HI, ϕ, the surface's dimensions, and overall height of a vertical component, but it also generates spot dimensions.

Aside from vertical vegetative surfaces (e.g. trees) there are several possible variations on a basic rectangular shape of vertical surface elements found on many urban canyon walls. The width of a surface element may be either less than, equal to, or greater than the height of this same element. Further, a single surface may range above or below the instrument height in the Z direction, or traverse the wall in the Y direction (Fig. 3.4). Each of these variations requires a different approach to sampling and the calculation of γ and d. Thus, the need for the Guide.

To maintain consistency in the spot temperature measurements, it is preferable to keep at least one of the spot dimensions constant, either width or height, when using the Guide. Generally, this is a simple process when the Guide is used correctly, however, problems can and will occur. Two scenarios will be presented that should illustrate the use of the Guide for rectangular surface areas on urban canyon walls.

Figure 3.4: Possible ranges of vertical surface elements

a) vertical orientation

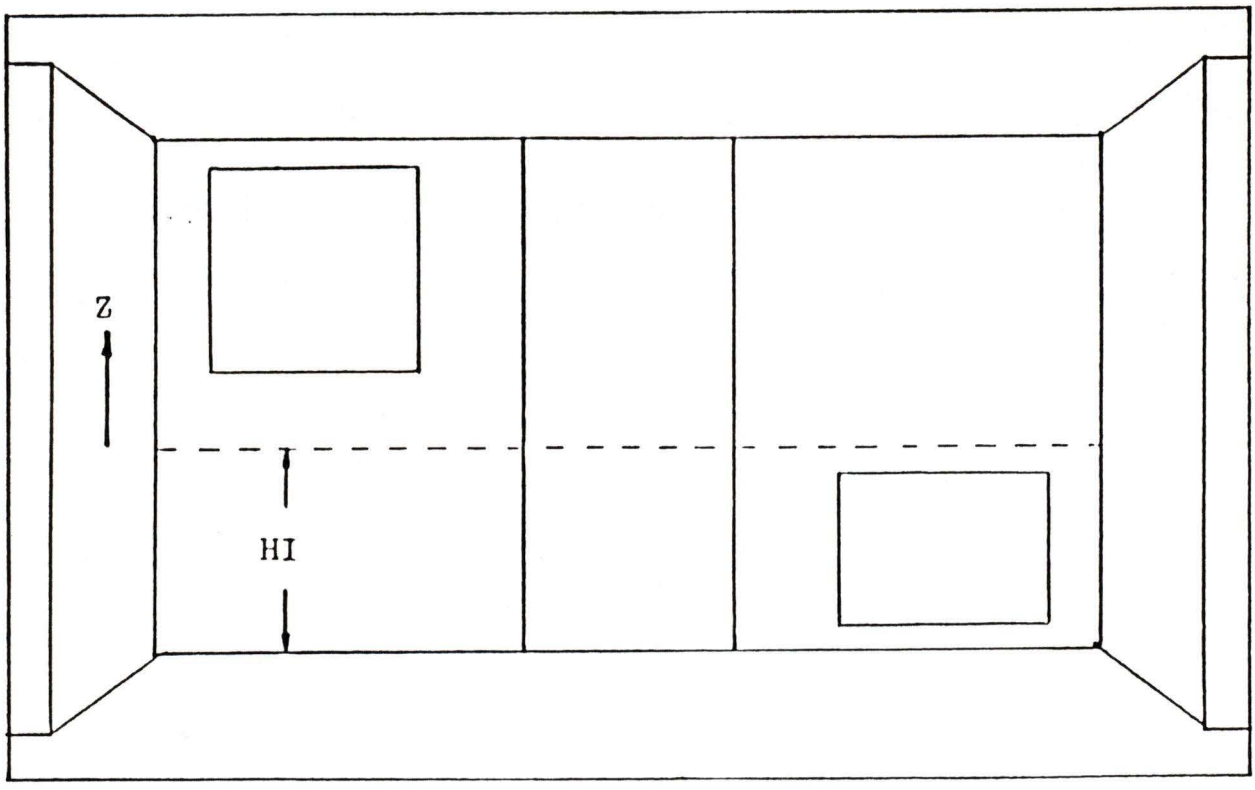

b) horizontal orientation

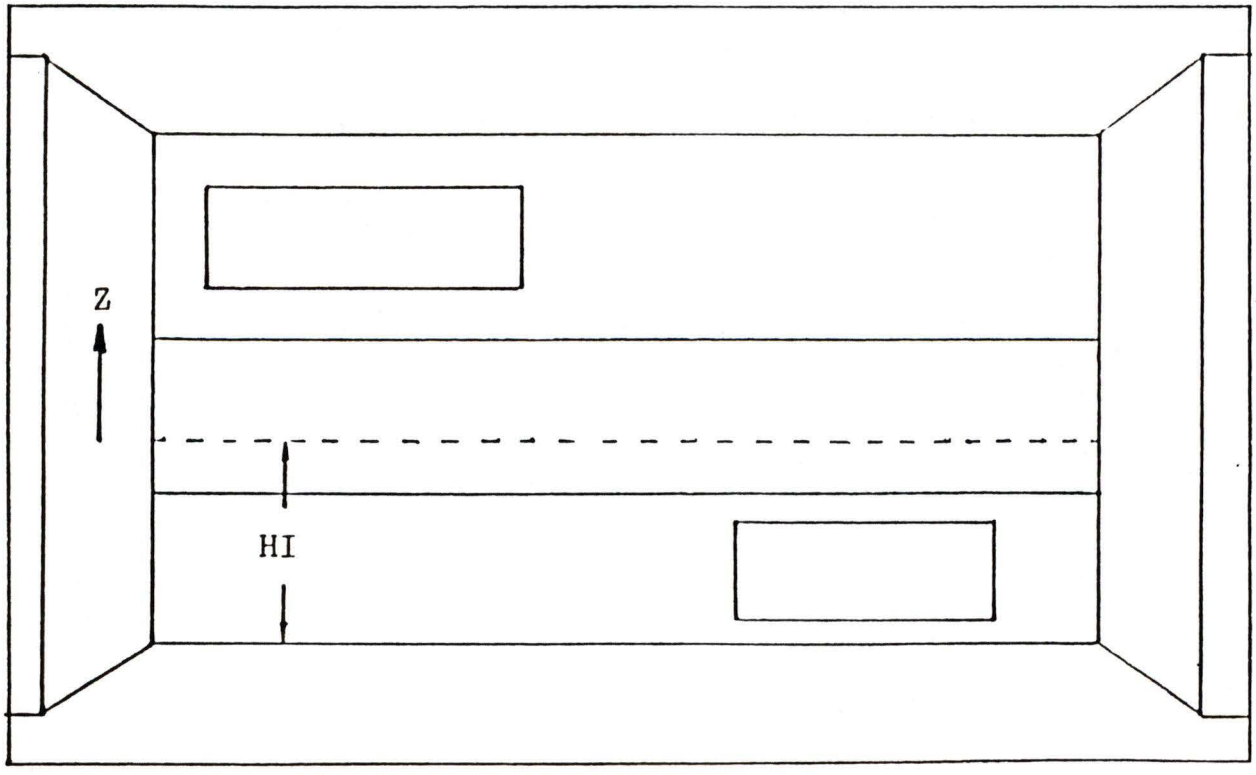

In the first scenario, an elemental surface area runs the full height of a building wall. The width of this surface is less than its height. For maximum areal coverage by the spots, set the spot width, w, equal to the surface width. This will produce a single, non-random traverse running the height of the surface and wall during sampling (Fig. 3.5). A tape measure is laid perpendicular to the centre of the surface area along the ground to enable the accurate location of the instrument from the wall, d.

The researcher then refers to Part I, Section A of the Guide to begin calculation of γ and d that will be employed during sampling. The Guide begins in reference to the highest point on the surface area and proceeds down the wall from there. As each spot is located on the wall within the confines of the elemental surface area, the researcher is referred to other sections in the Guide. Each section refers to an illustration of relevant angles and dimensions, and makes appropriate comments regarding each section.

Part I of the Guide can be used in all cases where the surface height exceeds the surface width regardless of whether the surface lies above, below or traverses the instrument height, HI. The researcher need only look at the illustrations in the Guide and choose the section that best suits his purpose. Of course variations are possible and likely. Therefore, the researcher can be more selective when using the Guide for variations such as locating a spot at the centre of an elemental surface area. The researcher is advised to make all his calculations of γ and d before entering the field in order to reduce the sampling time.

Certain limitations to maintaining a spot width equal to the surface width may occur. As the height to which the spot must reach, H, decreases the instrument distance, d, increases to maintain a constant w. The dimensions of the canyon may limit d as the researcher finds himself backed up against a wall. To prevent this from happening, the researcher can compare the maximum calculated d with the canyon dimensions before entering the field. In the field, a powerful flashlight with a cone-shaped cover matching the instrument viewfactor may be employed to check spot dimensions.

Figure 3.5: Vertical traverse over a vertical configuration

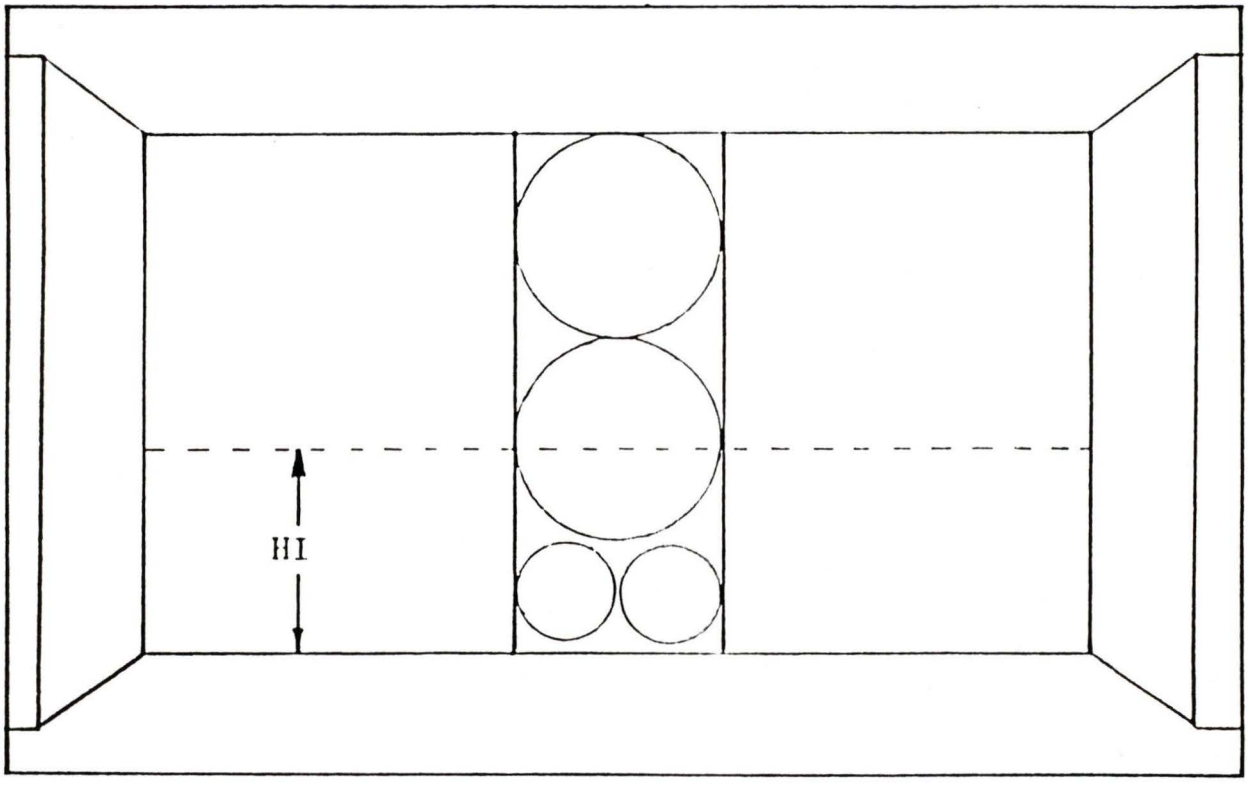

To overcome a limitation in d, the researcher may choose to reduce the spot width, w, so that two or more spots will fit across the surface. This may be done toward the end of the traverse and will require the researcher to shift the instrument station perpendicular to the tape measure at a precalculated distance d. Should this limitation be eminent, the researcher may choose to split the spot width before sampling begins thereby creating two or more vertical traverses.

Serious problems arise in the distribution of some surface elements. When an element is very high up on a wall and the instrument angle γ exceeds or equals $90° - (\phi/2)$, then the spot and surface limitations (i.e. γ and ϕ) render the surface temperature at that height unmeasurable. For example, the top of a surface element reaches a height H = 100 metres while the instrument viewfactor $\phi = 35°$. The minimum spot width at this height is 3.5 metres. Should the surface width be less than 3.5 metres, then T cannot be measured at this height with this instrument. Reducing the viewfactor may overcome this problem, but rarely will the researcher have two instruments available. A further problem arising from higher elements is the need to place the instrument close to the wall. Often, the proximity of the wall will affect the placement of the instrument or tripod.

Other problems involve obstructions and floor surfaces in the urban canyon. Trees or vertical obstructions may affect the viewing capacity of the instrument. Uneven floor surfaces can make instrument setup difficult. Such problems are most likely to hinder data collection, thus choosing urban canyons with even floors and vertical obstructions close to the canyon perimeter is very important.

The second scenario occurs when the surface's height is less than or equal to the surface's width. Ideally, the spot height, a, will equal the surface's height to permit the maximum coverage. Part II of the Guide covers elemental surface areas of the type where the entire surface lies above the instrument height, HI. When the surface area lies across or below HI, the Guide refers the researcher back to the relevant section in Part I.

Should the surface's width be two or more times wider than the surface's height, then a single non-random traverse can be conducted parallel to the elemental surface area (Fig. 3.6). The instrument distance, d, and instrument angle, γ, will remain constant while the researcher moves the instrument along the wall at intervals equalling the spot width to ensure the spots do not overlap.

These surfaces are subject to similar limitations and problems outlined in the previous scenario. When limitations in d occur, rather than splitting the spot width, the spot height may be split to give two or more horizontal traverses. Again, variations in the use of the Guide are possible.

Figure 3.6: Horizontal traverse over a vertical configuration

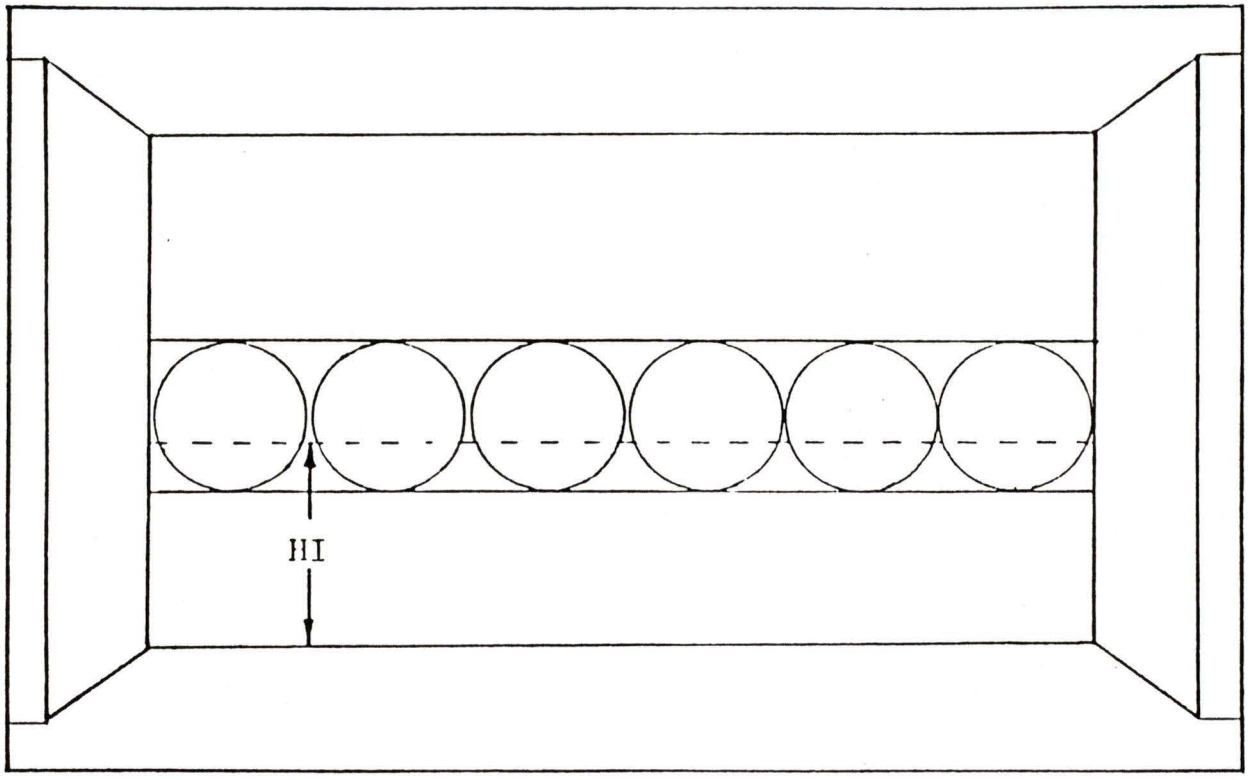

B. Instruments for the Independent Variables

General instrument types that measure air temperatures, interior temperatures, humidity and wind speed will be introduced in this section. Only devices with practical applications in urban canyons will be covered. Discussion will focus on instrument types, principals of operation, calibration and practical considerations for use.

1. Air Temperature Instruments

Several instrument types are suitable for measuring air temperatures in urban canyons, buildings and vegetative canopies. For this study, those instruments that may be used in transect studies (i.e. quick-response types) are preferred over those requiring recorders such as the graphic display in a thermograph. The instruments covered in this section include mercury thermometers, resistance thermometers and thermistors.

The theory behind the measurement of air temperature is that the instrument's sensor takes on an equilibrium temperature that satisfies its total energy budget. The idea is to get the sensor's temperature (T_{sensor}) to equal the air temperature. This is done by eliminating net radiation and evaporative and conductive heat flux densities. Then the convective heat flux density is maximized by aspirating the sensor until $T_{sensor} - T_a$ equals 0. A radiation shield around the sensor can minimize the effects of solar and long wave radiation at the sensor. Net long wave radiative exchange between the shield and sensor can be minimized by maintaining the shield at a temperature close to that of the air temperature and by making the shield from a low emissivity material such as polished metal. Evaporative heat exchange can be eliminated by ensuring that the sensor is dry. Conductive heat exchange between the sensor and the instrument housing can be controlled to some extent by insulating and isolating the sensor, or matching the internal temperature of the housing with the sensor temperature. The convective heat flux density at the sensor is directly proportional to the wind speed and inversely proportional to the size of the sensor. Thus, forcing air over the sensor

(aspirating it) or reducing the size of the sensor will help to maximize the convective heat flux density.

a) Mercury Thermometers

Conceptually, the mercury thermometer is the simplest sensor of air temperature. It is easily recognizable as a tube containing a quantity of mercury and covered with a gradient indicating temperatures. A good mercury thermometer can measure temperature with an accuracy of ± 0.1°C. They are easy to maintain and clean. Although, the gradations are not always accurate, they are easy to calibrate in the laboratory. These thermometers can be fitted with shields and aspirated to optimize convection using electric or mechanical motors. Due to the sensor size however, aspirating these instruments is strongly recommended. Response times for these instruments is considered moderate. Several minutes may be required for the instrument to stablize and yield a valid reading.

b) Resistance Thermometers

Resistance thermometers use a sensor which is often a wire of pure metal, such as platinum, whose resistance varies inversely with diameter and changes with temperature. These wires are stretched across a bridge where temperature variations at the wire cause voltage changes due to conduction through the wire. Since these wires can be made very thin, aspiration is less crucial to obtaining an air temperature reading. These instuments are often very sensitive with quick response times. Accuracies of $\pm$ 0.01 °C are possible (Dobson et al., 1980).

c) Thermistors

Thermistors use resistance elements in a similar fashion to resistance thermometers. However, these resistance elements are semiconductors that have either a very high positive or negative temperature coefficient of resistance. They are available in a variety of different forms including beads, rods and discs. Heat dissipates better from rods than from beads, so rods can give a greater sensitivity (Dobson et al., 1980). As with resistance thermometers, these sensors can be made very small thus reducing the need for aspiration. Response times are considered quick.

d) Calibration

These instruments may be calibrated using a liquid or other substance with a high specific heat such as water. Air is unsuitable for this purpose because air temperature changes too rapidly. The instrument can be placed in this liquid and the reading compared to some standard such as a thermometer used solely for the purpose of calibration.

Instruments such as the thermistor and resistance thermometers require regular calibration. The sensors (wires, films, etc.) may deteriorate with time while electrical circuitry has a limited lifetime. Mercury thermometers generally do not require calibration as often, however the gradations may be inaccurate and any discrepancies should be noted on the instrument (e.g. "reads + 0.2°C between - 10°C and 35°C").

e) Practical Considerations for Use

Thermistors and resistance thermometers can be made very sensitive and accurate. However, the level of accuracy demanded in field measurements need be no more accurate than those for the validation of radiant temperatures (i.e. ± 0.5 °C). These instruments can also be shielded and aspirated. Response times of 30 seconds are common. However, both instruments require a power source and regular calibration. They are most useful in measuring temperature differentials and gradients since they can be wired in series.

Mercury thermometers are probably most practical for use in urban canyons. They are reliable and portable. Often, two of these thermometers are placed in the same housing and are shielded and aspirated. When the sensor on one of the thermometers is covered with a wick moistened with distilled water, it measures the wet-bulb air temperature. This system describes a psychrometer that yields temperatures for calculating humidity (i.e. $T_a - T_w$ differential). Thus, two instruments in one housing can be used to measure both air temperature and humidity. Temperature readings may be taken at 30 second intervals until the readings stabilize (i.e. 2 consecutive readings are the same).

2. Interior Temperature Instruments

The thermistor and resistance thermometers identified in the previous section are probably the best instruments for measuring temperatures within substrata. They have quick response times and can be wired in series to obtain differentials between the substrata and surface temperatures (i.e. $T_i - T$). Calibration also follows that for air temperature instruments.

The concept of practically measuring interior temperatures is in serious doubt. Accessing substrata in the field in order to measure T_i may result in strong objections from local authorities. Investigating the link between T_i and T may best be conducted in the laboratory since the temperature sensor must be in contact with the substrata materials ($T_{material}$). For measuring substrata temperatures, T_{sensor} must equal $T_{material}$ and it is virtually impossible to guarantee this in pre-existing substrata (e.g. streets or walls). In the lab, the type and thickness of substrata can be controlled while accessibility to the substrata will not interfere with regular municipal operations. Models describing the $T_i - T$ link can then be used in conjunction with other models of T and L . For these reasons, T_i is not considered a practical variable for field sampling.

3. Humidity Instruments

Several instruments may be used to determine atmospheric humidity. These instruments may be classified under the following five categories: psychrometric approaches (thermodynamic methods involving the measurement of air temperatures); absorption methods (based on changes in the physical dimensions of substances due to moisture absorption); condensation approaches (determining the dew-point temperature at which a water film forms on a cooled surface); chemical and electrical approaches (based on changes in the chemical and electrical properties of substances due to moisture absorption); and radiation absorption approaches (utilizing the fact that water vapour absorbs radiation in specific bands) (Oke, 1978).

Of these five categories, the psychrometric approach is the most practical and commonly used, and therefore the only approach to be considered for use in urban canyons. Instruments in this category, called psychrometers, feature simplicity in use and a low cost. A brief description was offered in the section on air temperature instruments. A more elaborate description will now be offered.

The principle upon which a psychrometric system works is based on the fact that the saturation specific humidity at the surface of the wick, which is at the wet-bulb air temperature (T_w), is larger than the specific humidity of the incoming air (at T_a) unless the air is saturated. The temperature of the air coming into the instrument is measured with the other thermometer and referred to as the dry-bulb air temperature (i.e. T_a). Evaporation and cooling of the wetted thermometer occurs so that the wet-bulb temperature is finally less than the dry-bulb tempera-

ture unless saturation occurs (i.e. $T_a = T_w$) where the difference between T_a and T_w is dependent on the humidity of the air.

Psychrometric instruments using mercury thermometers range from the well known, inexpensive sling psychrometer to the fan-aspirated, radiation-shielded units such as the Assmann psychrometer. Their response times are moderate. Calibration of the thermometers follows the procedure outlined for air temperature where the wick is removed from the thermometer used for wet-bulb temperatures.

Practical considerations for the use of a psychrometer include the need for adequate ventilation , proper radiation shielding, and precise and accurate thermometry. Since the specific humidity relies on the temperature difference between T_a and T_w (Eq. 2.10 and 2.11), sensitivity of the thermometers is less critical than accuracy since inaccuracies are cumulative. It is also important that the thermometers are exposed for a sufficient period of time so an equilibrium temperature at the sensors can be reached. Some research applications have used small thermistors for temperature sensors so that radiation effects are lessened, response times are quickened, and continuous electrical output signals for mean and fluctuating humidity are obtained (Paulson et al., 1972; Polavarapu & Munn, 1967). According to Wexler (1970) however, the best absolute accuracy for psychrometers is ± 1 %.

The best reason for using the psychrometric approach in terms of this research is the elimination of an additional instrument. A psychrometer not only yields a differential between dry-bulb and wet-bulb air temperatures, but also an absolute value for air temperature.

4. Wind speed Instruments

General instrument groups for measuring wind speed include: cup anemometers, propeller anemometers, and heat-transfer devices (Oke, 1978). Several other wind speed devices were designed to work in confined spaces and are not considered here. These include laser anemometers and ion anemometers which are both expensive and finicky.

a) Cup anemometers

Cup anemometers are widely used. They are simple, sturdy, reliable and generally require only a minimum of maintenance. Horizontal air movement against the cups rotates a vertical shaft that may be used to provide voltage pulses or a continuously variable voltage signal (Oke, 1978). These pulses or signals can be translated into measurements of wind speed. The major operational advantage is that alignment into the wind direction is unnecessary.

There are inherent disadvantages in cup anemometers. Overspeeding, the cup-shaft assembly turning too quickly, is one of these disadvantages and is caused by nonlinear responses of the assembly to fluctuating winds. They also respond more quickly to an increase in wind speed than to a decrease of the same magnitude. Consequently, in a turbulent flow the mean wind speed will be overestimated if the instrument has been calibrated in a laminar flow (Dobson et al., 1980). The wind speed also has to be greater than a threshold value to overcome the friction in the bearings holding the vertical

shaft. Thus, in order to determine the correct mean wind speed it is necessary to identify the periods when the cup wheel did not rotate and the actual wind speed during these periods. Despite these disadvantages, cup anemometers are typically accurate to within ± 1 % of the actual reading above 5 m sec^{-1} and ± 5 cm sec^{-1} below (Dobson et al., 1980). However, due to the necessity of a threshold speed, wind speed readings are generally averaged over time and thus their response time can be considered moderate to slow.

b) Propeller anemometers

These anemometers can be used to measure wind speed in any dimension. Propeller anemometers must be aligned to the axis of the wind. Therefore, sensing wind speed in more than one dimension requires more than one of these instruments.

The speed of revolution of a propeller is linearly related to the magnitude of the wind component directed along the propeller axis. However, turbulent airflow causes the speed of rotation to become smaller than it would have been with the instrument action solely in a laminar airflow. Not only are these instruments susceptible to inaccuracies due to friction which require wind speeds greater than a threshold speed but they are mechanically frail when compared with most cup anemometers. Again, due to the necessity of a threshold speed, wind speed readings are generally averaged over time and thus their response time can be considered moderate to slow.

c) Heat-transfer devices

Hot-wire and hot-film anemometers fall into the category of heat-transfer devices. Sensors are heated wires or films that respond to fluxes in convection caused by wind speed (Chapter 2). They are used for measurements of fluctuations in the wind speed as well as the straight wind speed itself. The high frequency resolution of these sensors cannot be matched by any other anemometers (Dobson et al., 1980) and response times are quick.

Hot-film sensors have a more stable calibration than wires that probably results from their larger diameters compared to hot wires. Hot-wires have the advantage that temperature distribution along the wire is more homogeneous and thus the effect of flow not perpendicular to the wire is more predictable. At very low speeds, the flow around the wire is dominated by buoyancy due to overheating rather than by the mean flow of air.

These anemometers work well in confined spaces. The threshold speed is virtually zero and response times can be considered quick. They also have a use in open spaces but they respond to almost the complete wind field, not just horizontal or vertical components.

d) Calibration

Calibration of these instruments usually requires a wind tunnel. Wind tunnels can be a rare commodity and are complicated to design and construct. These tunnels usually produce a laminar flow of air with low-intensity turbulence. The high-intensity turbulence often encountered in the field can render an ane-

mometer inaccurate and under these conditions more than one anemometer is recommended (Oke, 1978). In lieu of a wind tunnel, one of the heat-sensor devices can be calibrated and used only to calibrate other anemometers.

e) Practical considerations

Choosing between the three instrument groups described can be difficult. Any one of them would probably give good results in an urban canyon. However, the calm or light wind conditions often associated with clear nights in urban canyons suggests the hot-wire anemometer may be most practical. The high resolution of these instruments is preferable and desirable. They are also very portable. Defining wind direction under light wind conditions in which to set up the hot-wire anemometer can be difficult. Also, the sensitivity of these instruments requires a time period over which the wind speed can be averaged.

C. Chapter Summary

This chapter, along with Chapter 2, provides the foundation of URBMAT upon which sampling methodologies for the dependent and independent variables can be developed. Using these chapters, identification of appropriate variables, "best" instruments, desired accuracies and practical uses are possible. The key instruments discussed in this chapter are summarized in Table 3.1 including their accuracies, applications, response times and other features.

$L^{\downarrow}$ is an appropriate variable for testing the validity and reliability of models that may be developed in subsequent research. At night, L can be measured using either a net pyrradiometer or net pyrgeometer. A desirable and practical accuracy that could be easily attained within the limitations of this research is ± 2.6 Wm^{-2} which is equivalent to ± 0.5°C at T = 10°C when ε = 1.0. Testing models does not require that $L^{\downarrow}$ be measured at any specific place within the urban canyon. Therefore, measurement can take place at an accessible instrument height of between 1.0 and 1.5 metres above the urban canyon floor.

The most appropriate dependent variables are T and T_0 . These variables are appropriate because by using an infra-red radiometer nearly all urban canyon components can be easily accessed for measuring these variables. Accuracies of ± 0.5°C are desirable and attainable using most radiometers. The Guide is an integral part of sampling T for vertical surfaces and the researcher is advised to become familiar with its uses. Measurement of T and T_0 is enhanced by using a tripod with both zenith angles and azimuthal angles marked on the tripod where the instrument height is set so that the researcher is comfortable and HI is always recorded.

Table 3.1: Summary of Climatic Instruments With Urban Canyon Applications

A. Longwave Irradiance Instruments

Net Pyrradiometer
- accuracy: ± 1.0 Wm^{-2}
- application: long wave application at night only
- response time: quick
- comments: net reading, all wavelengths
  multidirectional sensing

Net Pyrgeometer
- accuracy: ± 1.0 Wm^{-2}
- application: diurnal application
- response time: quick
- comments: net long wave reading
  multidirectional sensing

B. Surface Temperature and Radiant Sky Temperature Instruments

Bolometer (Infra-red Thermometer)
- accuracy: ± 0.1 °C
- application: remote sensing of surface temperatures
- response time: quick
- comments: preferred instrument
  no surface contact required
  unidirectional sensing

C. Air Temperature Instruments

Mercury Thermometer
- accuracy: ± 0.1 °C
- application: dry-bulb and wet-bulb air temperatures
- response time: moderate
- comments: preferred instrument for urban canyon air-volumes
  should be shielded and aspirated

Resistance Thermometers
- accuracy: ± 0.01 °C
- application: dry-bulb and wet-bulb air temperatures
- response time: quick
- comments: fragile and sensitive

Table 3.1: continued

Thermistors
accuracy: ± 0.01 °C
application: dry-bulb and wet-bulb air temperatures
response time: quick
comments: preferred instrument for enclosed air-volumes

D. Humidity Instruments

Psychrometer
absolute accuracy: ± 1 %
application: dry-bulb and wet-bulb air temperature differential
response time: quick to moderate
comments: preferred instrument
also yields absolute value for air temperature
should be shielded and aspirated

E. Wind Speed Instruments

Cup Anemometer
accuracy: ± 1 % above 5 m s^{-1}
accuracy: ± 0.05 m s^{-1} below 5 m s^{-1}
application: moderate to strong winds
laminar or turbulent air flow
response time: moderate to slow
comments: require speeds greater than threshold to operate

Propeller Anemometer
accuracy: ± 1 % above 5 m s^{-1}
accuracy: ± 0.05 m s^{-1} below 5 m s^{-1}
application: light to moderate winds
unidirectional air flow
response time: moderate to slow
comments: require speeds greater than threshold to operate
frail instrument

Heat Transfer Devices
(Hot-wire and Hot-film Anemometers)
accuracy: ± 0.05 m s^{-1} below 5 m s^{-1}
application: respond to complete wind field
especially good in confined spaces
response time: quick
comments: preferred instrument under calm and light wind conditions

Most of the independent variables identified in Chapter 2 are appropriate for sampling. These include T_a, T_w, u, $T_{a'}$, u_i, T_{ac} and u_c .

T_a and T_w can be measured easily within the urban canyon using a psychrometer where an accuracy of $\pm$ 0.5°C is both desirable and attainable. This accuracy can be applied to either absolute temperature values or temperature differentials between T_a and T_w. The recommended height at which T_a and T_w should be measured is between 1.0 and 1.5 metres above the floor of the urban canyon. The air temperature profile over a non-vegetative surface (Data Sheet 2, Appendix A) shows a decrease in temperature with height before midnight between 0.01m and 2.0m above the surface. After midnight, there is very little vertical change in air temperatures with height, with the exception of the profile around 2:25 A.M. The wet-bulb air temperature over a non-vegetative surface (Data Sheet 2) shows a decrease in T_w from 0.1m to 1.0m both before and after midnight, and an increase from 1.0m to 2.0m on either side of midnight. However, when these temperatures are averaged over the whole night for each height, the maximum difference of the averages is 0.5°C for T_a and 0.33°C for T_w.

The urban canyon wind speed, u, can also be measured within the prescribed instrument height for T_a and T_w using a hot-wire or hot-film anemometer (Data Sheet 4). An accuracy of $\pm$ 0.05 m sec^{-1} is desirable in this case based on Dobson et al., (1980). The sensitivity of these instruments is great and poses difficulties that must be overcome during sampling (Chapter 4). However, these instruments are most appropriate for calm wind conditions because there is no threshold wind speed required to activate them.

The other air temperatures, $T_{a'}$ and T_{ac}, can be measured using a small thermistor thermometer. These instruments can also easily measure to an accuracy of

± 0.5 °C . Further, where a psychrometer or aspirated thermometer may not work in the confines of a room or canopy, thermistors can be used in a stationary position. Sampling T_{ac} will be discussed in Chapter 4. The instrument height for T_{ai}, however, can also be set between 1.0 and 1.5 metres above the floor, this time above the room floor (Data Sheet 20). The wind speeds u_i and u_c should also be measured using a hot-wire or hot-film anemometer with an accuracy of ± 0.05 m sec^{-1} . An instrument height between 1.0 and 1.5 metres is also appropriate for u_i .

This study concentrates on these variables and instruments when developing the sampling methodologies for URBMAT and modelling urban nocturnal long wave radiation regimes. It is important to note that interior temperatures for substrata are not included due to the poor accessibility of this variable in the field. Therefore, Chapter 4 will identify sampling methodologies for L↑, T, T_0, T_a, T_w, u, T_{ai}, u_i, T_{ac} and u_c .

Chapter IV

SAMPLING METHODOLOGIES FOR URBAN CANYONS AND THE VARIABLES WITHIN URBAN CANYONS

Clearly outlining the best and most practical sampling methodologies for the relevant variables makes up the third and final step in URBMAT. The methodologies described in this chapter are based upon data collected in the field where both time and cost savings were considered to be as important as accuracy. In geography, statistical tests using a 95% confidence interval are often used (Matthews, 1981). However, these tests are usually based on finite values for sampled variables and do not take into consideration the systematic errors created by the limits of accuracy for individual instruments. For this reason, the choice of a "best" sampling methodology will be based upon a range delineated by the instruments' limits of accuracy rather then a statistically based confidence interval. The limit of accuracy for temperature measurements will be ± 0.5 °C and for wind speed this accuracy will be ± 0.05 m sec^{-1} . These accuracies are deemed both appropriate and attainable.

L^* will be treated as a test variable in this chapter. The dependent variables are identified as T and T_0 although L will be included as a dependent variable. The independent variables are identified as T_a, T_w, T_{al}, T_{ac}, u, u_l and u_c . In Chapter 3, a Guide for correctly using infra-red radiometers was introduced that

permitted the accurate location and calculation of spots on vertical surfaces when measuring T. Aside from employing the Guide during the field study and analysis of sampling methodologies for T, the sampling methodologies for temperatures of elemental surface areas will be based on both homogeneous and heterogeneous configurations. Each configuration requires a different approach to the sampling of T.

Chapter 4 will begin by outlining sampling procedures for the urban canyons themselves followed by sampling methodologies for each of the dependent and independent variables. Finally, formats will be introduced to assist the researcher in planning a data collection session based upon the variables, properties, factors and methodologies outlined in this and previous chapters.

Throughout this chapter, reference will be made to data sheets found in Appendix A. The data provided in these sheets represents information typical of several data collecting sessions. Additional data will be referred to in the text that is listed briefly in the Data Sheets in Appendix A. In all cases, inferences and decisions on the "best" sampling methodology for a particular variable are based on the more detailed data provided in Appendix A. The additional data merely backs up any inferences or decisions.

A. Sampling the Urban Canyons

The researcher must first become acquainted with the city being studied by learning the characteristics of individual districts. Cities never serve one function but are broken up into commercial, retail, industrial, warehouse and residential districts each of which may display unique canyon characteristics. These districts may have distinct locations within the city based on function that will affect the overall macroclimate of the city. Finally, access to many of the urban canyons may be limited due to traffic, security or function.

To begin researching radiant temperatures, a sample of urban canyons is required. The researcher should familiarize himself with the various districts and mark their location on a good, recent map of the city. Note features of each district such as function, traffic patterns, accessibility and general surface element types. A brief daytime field survey through each district may reveal an abundance or lack of specific surface elements.

The districts marked on the map are suitable strata for employing a stratified-random sampling approach of urban canyons. Each canyon in a stratum is assigned a single, unique number. A random sample of canyons is drawn using these numbers. There are no hard and fast guidelines for determining the size of the canyon samples in each district. Each urban canyon must be intensively and extensively studied. It is preferable to keep the number of canyons to a minimum while covering as many surface element types as possible.

There are several criteria placed on the urban canyon that will determine its suitability for study. The floors and walls of the canyon should be relatively flat. There should be few protrusions from the components and the canyon floor should be clear of large vertical components that may restrict data collection. Larger vertical components, including trees, should be located toward the perimeters of the canyon where the obstruction of other vertical surfaces may be kept to a minimum. The researcher must feel certain that the security of his person and equipment will not be in jeopardy. Finally, the researcher must acquire permission to conduct research in the canyon and adjoining buildings.

Drawing a random sample of urban canyons is relatively simple. Accepting a canyon into the sample requires a field survey to see if the canyon is suitable and the desired surface elements are present. To retain some researcher objectivity, a larger sample of canyons should be drawn than the researcher requires. With a list of "desirable" surface elements and the canyon "suitability" criteria, the researcher should then randomly visit each canyon selected in the larger sample. Should a canyon meet all the criteria, then it should be accepted into the sample. If a single canyon houses all the desired elements, then one canyon is enough for the sample. Often, more canyons will be required to cover all the desired elements. When the desired elements are covered, the field survey should stop. If the researcher looks for more "suitable" canyons, then all randomness and objectivity are removed.

Following this procedure of urban canyon selection can remove at least some of the researcher bias associated with many case studies. There is a combination of randomness with good areal coverage and researcher judgement. Although total researcher objectivity is unlikely, the random element should partially offset the intrusion of researcher bias by limiting the selection process.

B. Sampling the Dependent Variables

The key to success in the development and validation of models is the ability to duplicate the collection of data reliably and consistently. This section will describe sampling methodologies that should accurately and consistently measure the dependent variables L^*, T, and T_o. These techniques have been proven effective in the field (Appendix A) and can be applied in most urban canyons. They are designed to make the data collection process as quick and easy as possible. Factors that may bias the results will also be considered.

1. Sampling L^*

As mentioned previously, the net long wave irradiance, L^*, is an ideal test variable. It presupposes that surface temperature models for each classification of element thermal conductivity are already developed. In order for the testing or model validation to proceed, the researcher must also be familiar with the urban canyon where the test will take place as well as one of the viewfactor modelling techniques.

L^* is probably most easily measured at the urban canyon centre, C, using either a net pyrradiometer or net pyrgeometer. Set the instrument sensor (i.e. dome) in a horizontal position above C at an instrument height between 1.0 and 1.5 metres. Mounting the sensor on a tripod should not significantly affect the L^* reading while at the same time it will enable the researcher to take notes and record the reading. It is critical that the researcher stand as far away from the sensor as possible so as not to affect the reading by imposing a L^- from the human body into the reading.

Model validation can proceed after L^* and any independent variables relevant to the models have been measured. It is important to note that a L on a horizontal plane is being measured. Therefore, L^+ to the top of the plane and L to the bottom of the plane should be treated as separate entities. If a viewfactor model based on a hemispherical dome is employed (e.g. Appendix C), then viewfactors for L^+ must be calculated separately from those for L (i.e. two hemispherical domes, one for each of L^+ and L^-).

2. Sampling T

Surface temperature, T, can be the most complex variable to sample. Sampling this variable is seldom a problem thanks to the remote sensing devices designed for this purpose (e.g. infra-red radiometers). For this reason, T is a more practical dependent variable than L where sampling can often be difficult because of the wide field of view of some hemispherical radiometers. This means that generally all the surface elements may be included in an urban canyon sample. The multitude of possible sample surfaces and variations in temperature reveals more factors for consideration than the other variables and exemplifies the complexity of sampling this variable.

In order to identify the best method for sampling T, a "complete" coverage for each of several homogeneous configurations was measured which yielded an average value for T, $\bar{T}$, over the entire surface area. This value for $\bar{T}$ was compared to the average of T measurements taken along one or more traverses that crossed the surface area. These traverses were selected at random from the "complete" coverage data. $\bar{T}$ was also compared to single readings for T centred at the surface element centre. The random traverse method and the single-reading method were compared to see whether either or both fell within the $\pm$ 0.5 °C accuracy range specified in this research.

Based upon the field data and the spot dimensions for radiometers introduced in Chapter 3, it became apparent that covering larger horizontal homogeneous surfaces completely was time consuming and totally impractical. Some method of assigning the number and size of intervals at which to sample

horizontal T measurements was required that would give the impression of a "complete" coverage. However, no method exists that will lead to assigning the total number of intervals for this particular application. This research assigned the number of intervals along the X dimension, n_x , and along the Y dimension, n_y . Based on the number of intervals for each dimension and the length of each dimension, equal interval spacing was created along which sampling was conducted. For example, if $n_x = 3$ and X = 10 m, then the size of the intervals is X/n_x or 3.33 m. Similarly, if $n_y = 4$ and Y = 15 m, then the size of the intervals is Y/n_y or 3.75 m. The first interval along each dimension should start at one half of the interval size and then proceed at full intervals from that point. Figure 4.1 illustrates these intervals for the X, Y dimensions used in this example and indicates the points at which T would be measured (i.e. spot centres).

When assigning the number of intervals along each dimension, the overall dimensions of the subject surface and the desired accuracy of surface temperature measurements were considered. More intervals were sampled as the subject surface increased in size or if more accurate results were desired.

a) horizontal homogeneous non-vegetative surface

A concrete surface of dimensions 17 x 19 metres was measured for T using N = 8 intervals (Data Sheet 10, Appendix A). The average surface temperature, $\bar{T}$,for a complete coverage was 19.1 ± 0.5°C. $\bar{T}$ for a single random traverse was 19.4 ± 0.5°C while $\bar{T}$ for two random traverses, one along each of X and Y dimensions with the intersection T measured only once, was 19.0 ± 0.5°C. A single reading was taken at the centre of this surface element yielding T = 19.5 ± 0.5°C.

Figure 4.1: Traverses over a horizontal homogeneous surface configuration

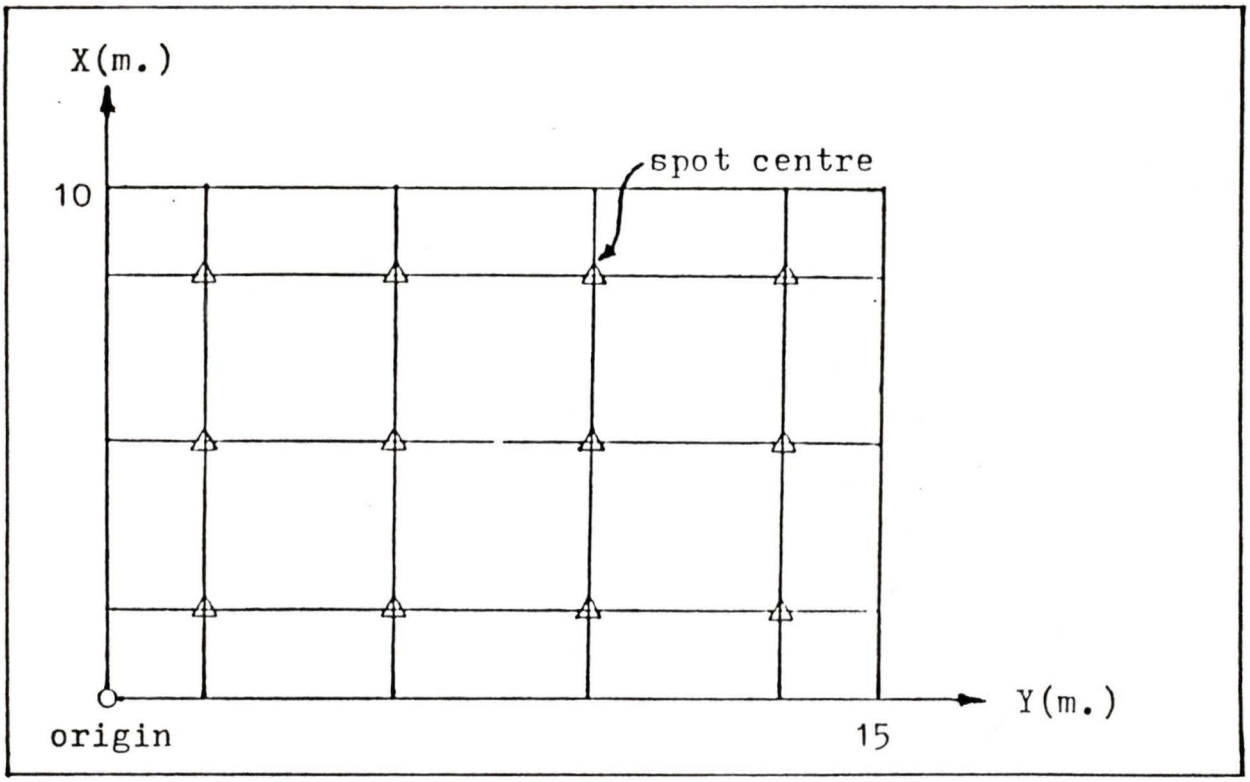

This research indicates that both traverse methods and the single reading at the centre were equally representative of the $\bar{T}$ for complete coverage. Here and in the rest of this chapter, representative means that either the average of traverse measurements or the average of single measurements at the centre of a surface fall within the range of average complete coverage measurements when using the limits of accuracy specified by the instruments. In this section for example, the range for a complete coverage $\bar{T}$ was 18.6°C to 19.6°C while the range for a single measurement of T at the centre of the surface element was 19.0°C to 20.0°C . Since these two ranges overlap, the single measurement of T at the centre of the surface is deemed "representative" of a complete coverage $\bar{T}$. Rather than traversing the entire surface taking measurements of T at prescribed inter-

vals, a single measurement of T at the centre can be used. This method is quickest, easiest and apparently accurate.

Three additional surfaces were measured for both complete coverage and centre surface temperatures. These measurements, along with those in Data Sheet 10, also supported this sampling methodology. The $\bar{T}$ for complete coverage ranged from 19.1 to 9.5°C while T measured at the centre of these surfaces ranged from 19.5 to 9.0°C . The average of the differences between these measurements was 0.43°C which is within the "representative" range of ± 0.5 °C for each temperature.

Based upon the aspect test (Data Sheet 6), it is recommended that the aspect of these non-vegetative surfaces be noted. A stratification of these surfaces, and those sharing the same thermal conductivity, can be based on south/west and north/east strata. Where the surface element spans the urban canyon floor, such a stratification is deemed unnecessary since the effects of exposure on one side of the canyon are offset by exposure on the other side (i.e. north offsets south; east offsets west). Therefore, a single sample point at the centre of the surface is sufficient.

b) horizontal homogeneous vegetative surface

A surface of short grass with dimensions 14 x 17 metres was measured for T using N = 8 intervals (Data Sheet 11). $\bar{T}$ for complete converage was 14.7 ± 0.5°C. Single traverse $\bar{T}$ was 14.8 ± 0.5°C and two random traverses yielded $\bar{T}$ = 14.3 ± 0.5°C. T was equal to 15.0 ± 0.5°C at the centre of this surface. It

should be noted that the vegetative cover for this surface was 100 %. No ground showed through.

Two other grass surfaces within urban canyons were sampled to test this methodology. The range for complete coverage $\bar{T}$ over all three surfaces was 14.7 to 7.1°C and the range for centre measurements of T was 15.0 to 6.5°C . The average of the differences between these temperatures was 0.43°C which is within the representative range and supportive of the sampling methodology.

Based on this study, both traverse methods and the single reading at the centre were deemed to be equally representative of the complete coverage $\bar{T}$. Again, it is recommended that a single reading for T be measured at the centre of these, and other, vegetative surface areas. This method is also quickest, easiest and apparently accurate.

The aspect test for these surface configurations (Data Sheet 7) indicated that aspect does not significantly affect surface temperature. However, it is important to note the vegetative cover, c, since the surface temperature of the underlying material will dominate temperature readings as cover decreases. It is recommended that models be developed for horizontal homogeneous vegetative surfaces when the vegetative cover exceeds 80 %. These models, along with those for non-vegetative surfaces, could be used with the vegetative cover, c, to yield a weighted average estimate of the surface temperature.

c) vertical homogeneous building and non-vegetative surfaces

The surface of a building shell measuring 5 m by 6 m and composed of light brown blocks was measured for T (Data Sheet 12). Spot widths were held constant at 1.0 metres so that the width gave 5 spot measurements of T. Using the Guide (Appendix D) and a Barnes Instatherm infra-red radiometer ($\phi = 2.8°$) gave 6 spot measurements through the height. The total number of spot measurements for T required to attain a complete coverage was 30. $\bar{T}$ for complete coverage was 15.6 ± 0.5°C. $\bar{T}$ for a single vertical random traverse was 15.8 ± 0.5°C, while $\bar{T}$ for two random traverses, one along each of the width and height with the intersection T measured only once, was 15.6 ± 0.5°C. A single large spot of w = 5 metres centred on the surface element yielded a single surface temperature reading T = 16.0 ± 0.5°C.

This study indicates that both traverse methods and the single large spot measurement centred on the surface element are equally representative of the $\bar{T}$ for complete coverage. To test this methodology, four buildings were sampled for both a complete coverage surface temperature and a single large spot temperature measurement. The complete coverage $\bar{T}$ ranged from 19.5 to 12.4°C while the range of single large spot temperature measurements was 19.0 to 12.0°C . The average of the differences was 0.28°C. Therefore, it is recommended that a single large spot measurement of T be used for vertical homogeneous building and non-vegetative surfaces. The spot centre should match the centre of the elemental surface area while the spot dimensions should be based on the narrower of either the surface width or height. The Guide can be used to assist the

researcher in accurately calculating the instrument distance from the wall and the angle at which the instrument should be set.

The aspect test for these types of configurations (Data Sheet 8) suggests that the aspect of these surfaces be noted. A stratification for vertical homogeneous building and non-vegetative surfaces can be based on south/west and north/east strata.

d) vertical vegetative surfaces

Two vertical vegetative surfaces were measured for T: a plum tree and a cedar hedge (Data Sheet 13). The plum had a canopy depth h = 2.0 metres and a canopy cover c = 60 %. Two traverses of spot surface temperatures were measured. One traverse was taken through the vertical axis passing through the centre of the canopy. The other traverse was measured along a horizontal axis that also passed through the centre of the canopy. These traverses resulted in 12 individual spots approximately 1 metre across and the measurements of T associated with each were used to derive a complete coverage $\bar{T}$. $\bar{T}$ for this complete coverage was 13.5 ± 0.5 °C . Treated separately, the vertical traverse resulted in an average $\bar{T}$ = 13.6 ± 0.5 °C while the horizontal traverse $\bar{T}$ = 13.6 ± 0.5 °C . Based on the largest spot that would fit within the canopy, the T for this spot measurement was 14.0 ± 0.5 °C .

The cedar hedge was 14 metres long and 2 metres high with a canopy cover c = 90 % and a canopy depth h = 1.0 metres. A single horizontal traverse of spots approximately 2.0 metres in diameter was used to measure the complete

coverage $\bar{T}$ which was 14.3 ± 0.5 °C . A single spot at the centre gave T = 14.5 ± 0.5 °C .

Based upon the surface temperature measurements for each of these vegetative surfaces, surface temperature is adequately represented by a single large spot temperature measurement at the centre of the vegetative canopy. The average of the differences between these two complete coverage and single spot surface temperature measurements was 0.35 °C which supports this conclusion since it is within the representative range. However, the vegetative cover, c, should be considered a significant factor. Both these surfaces were backed by clear sky and the air temperature was 9.5 °C. The surface temperature for the plum tree (c = 60 %) was 0.5 °C cooler than that for the cedar hedge (c = 90 %). Although this temperature difference is within the defined range of accuracy, this difference suggests that vegetative surface temperatures may be affected directly by a change in cover. It may be preferable to develop vegetative surface temperature models for vegetative covers greater than 80 % and, as for horizontal vegetative surfaces, use a weighted average estimate of T based on cover. Finally, the aspect for these surfaces (Data Sheet 9) is deemed to be insignificant to the surface temperature.

e) horizontal heterogeneous configuration of surfaces

For a horizontal heterogeneous configuration of surfaces, several of the sampling methods for surface temperatures can be employed. Where a surface element is embedded in a more extensive element, a single T measurement at the centre of the elemental surface area is adequate. However, for the sur-

face element in which these elements are embedded, the surface centre may not be accessible. The case study has revealed that traverses are equally representative of overall surface temperature. It is recommended that two random traverses, one in each of the X and Y dimensions be used to sample for an average surface temperature using the intervals previously outlined (Figure 4.2). By using this two traverse method, the effects of aspect on a non-vegetative surface would be offset.

Often there may be several horizontal surface elements of the same type or same thermal conductivity, k, on the urban canyon floor. Since measuring all of these surface elements may be time-consuming, it may be desirable to draw a sample of these elemental surface areas to measure T. The size of this sample can be based on an accuracy formula (Williams, 1984) such that:

$$E = z_{\alpha/2} \frac{s}{M} \qquad \text{Eq. 4.1}$$

where

E is the desired accuracy of T,

$z_{\alpha/2}$ is the z-score of the desired confidence interval,

s is the standard deviation of a small sample of surface temperature measurements, and

M is the number of individuals to be sampled.

In this case, the desired accuracy is $E = 0.5\,^{\circ}C$. The confidence interval in most geographical research is 95 % where $z_{\alpha/2} = 1.96$ (Mathews, 1981). The standard deviation of a sample may be derived using surface temperature measurements along a traverse where the number of intervals (N) is based on:

Figure 4.2: Traverses over horizontal heterogeneous surface configurations

a) even

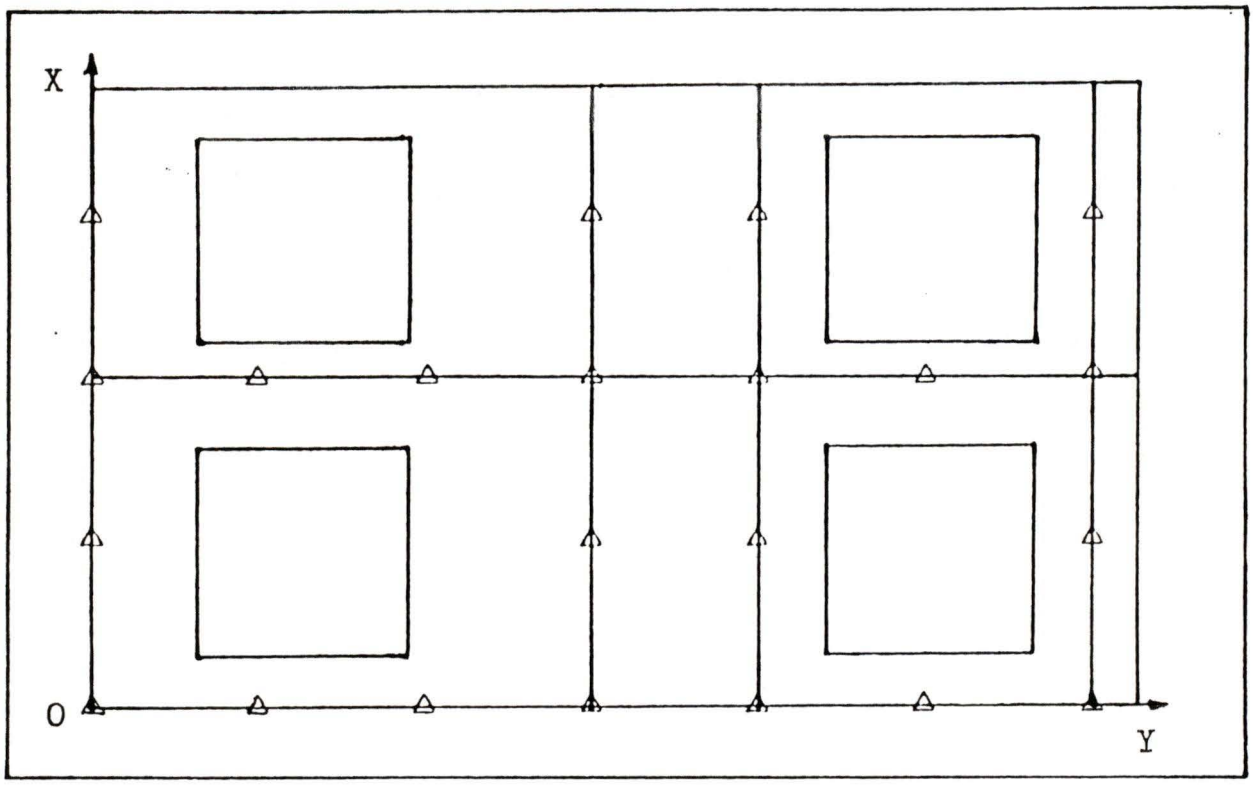

b) uneven

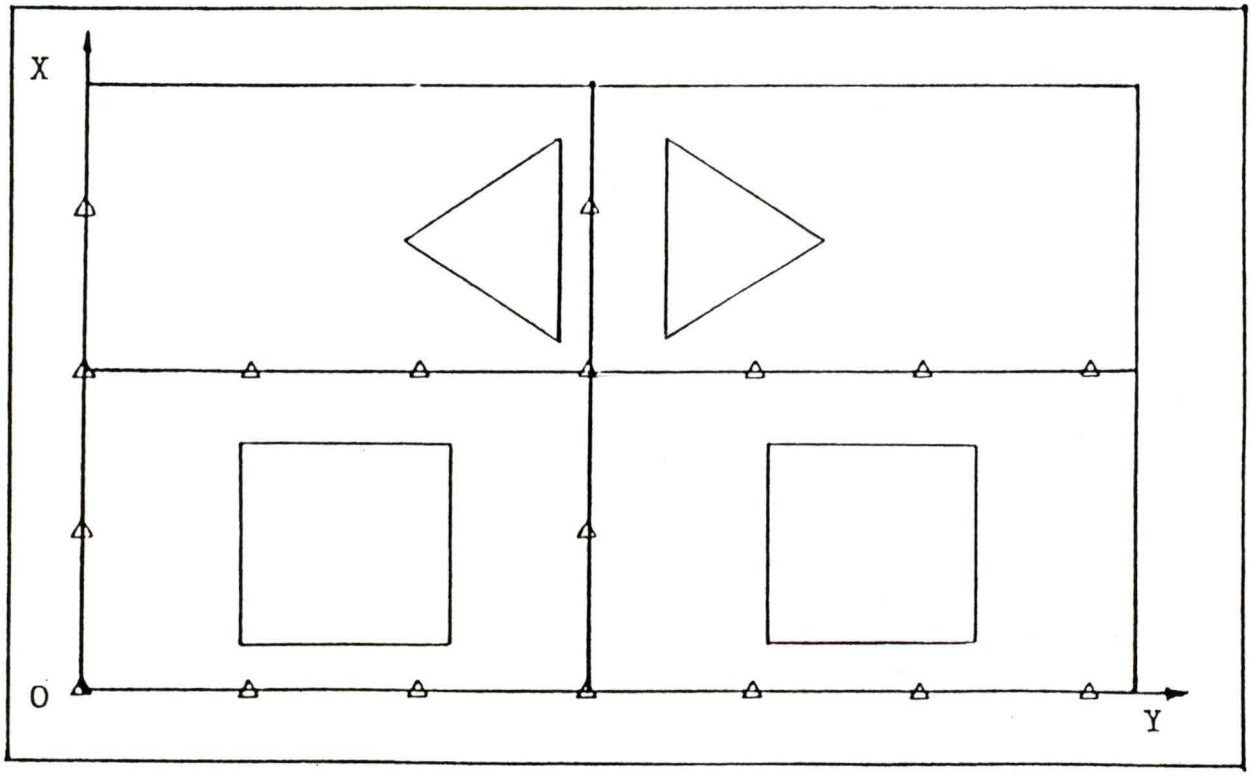

$$N = \left(\frac{X}{E}\right)^{1/2} \qquad \text{Eq. 4.2}$$

when the X-axis is used. The Y-axis can be used as well. The choice should be based on the variability in the particular element of interest. The standard deviation, s, can be calculated using:

$$s = \left(\frac{\sum (T - \bar{T})^2}{t_m}\right)^{1/2} \qquad \text{Eq. 4.3}$$

where

T is an individual surface temperature reading,

$\bar{T}$ is the average of all the T readings, and

t_m is the number of T readings based on the intervals.

The number of individuals to be sampled , M, of all similar or like surface elements would be:

$$M = z_{\alpha/2} \frac{s}{E} \qquad \text{Eq. 4.4}$$

derived from Eq. 4.1. For example, should s = 0.5 °C and E = 0.5 °C, then the sample size would be M = 3.8 ≃ 4 based on a 95 % confidence interval. This sample size can be used regardless of the number of similar surface elements present on the canyon floor. In this case, should there be 4 or less similar surface elements then all would have to be sampled.

f) vertical heterogeneous building surfaces

Many of the same sampling methodologies outlined for horizontal heterogeneous configurations, can be employed for vertical heterogeneous building surfaces. An embedded surface element can be measured using a single large spot surface temperature measurement. Similarly, for the surface element in which these others are embedded, traversing can be used when the centre is not accessible. It is recommended that a single traverse be used in this case where the traverse straddles the longest dimension of the surface, either width or height (Figure 4.3). The aspect of these surfaces must be considered in this case.

When several vertical building surface elements of the same type or k are involved, all need not be sampled for T. Equations 4.1 through 4.4 can be used to obtain a sample size. The standard deviation can be based on surface temperatures measured along a traverse that crosses the width or height of the element where the most varied number of elemental types are covered. Traverses should be based on the Guide (Appendix D).

3. Sampling T_0

The radiant sky temperature, T_0, was measured on a clear night in an open area over an asphalt surface when T_o at the zenith was -24.0°C (Data Sheet 14). Complete coverage for T_0 was based on measuring T_0 at zenith angles 0°, 15°, 30°, 45°, 60° and 75° in the north, east, south and west directions. Azimuth angles can be based on North being equal to 0° . The zenith angle 0° was used only once to measure T_0 . The average radiant temperature, $\bar{T}_0$, based on this

Figure 4.3: Traverses over vertical heterogeneous surface configurations
a) even

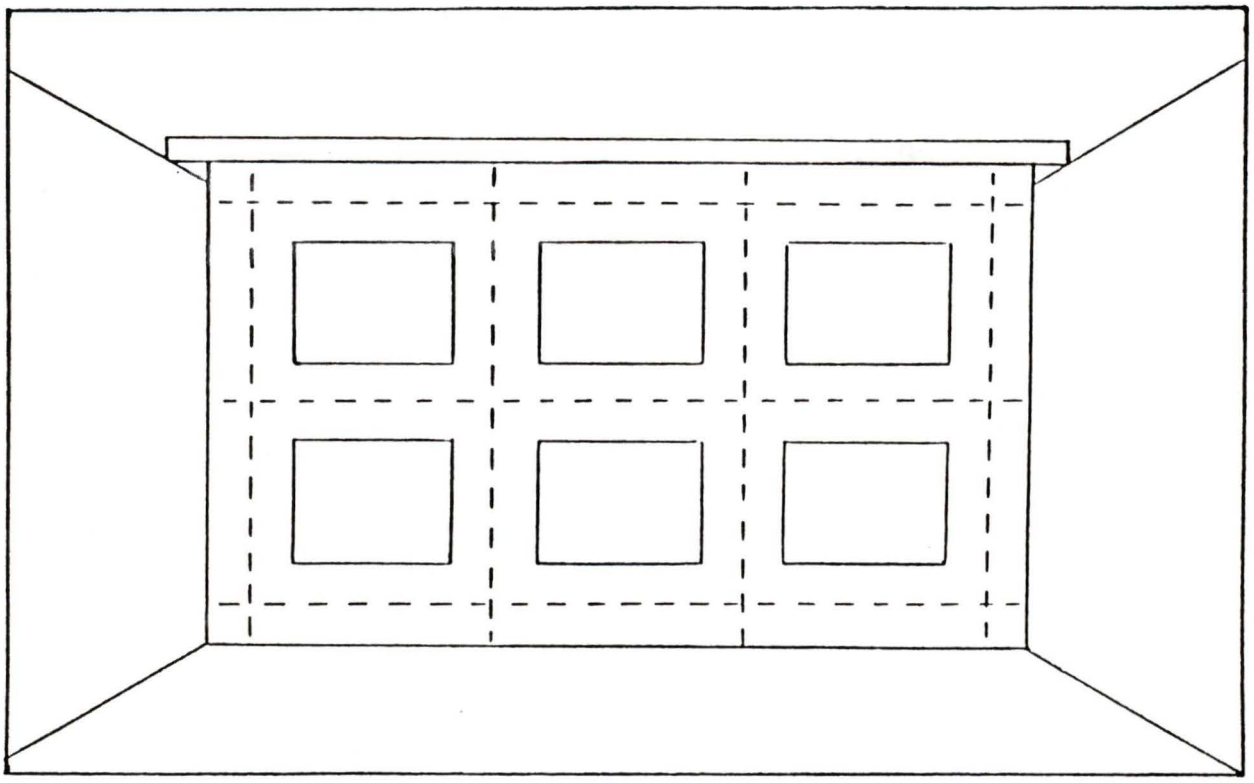

b) uneven

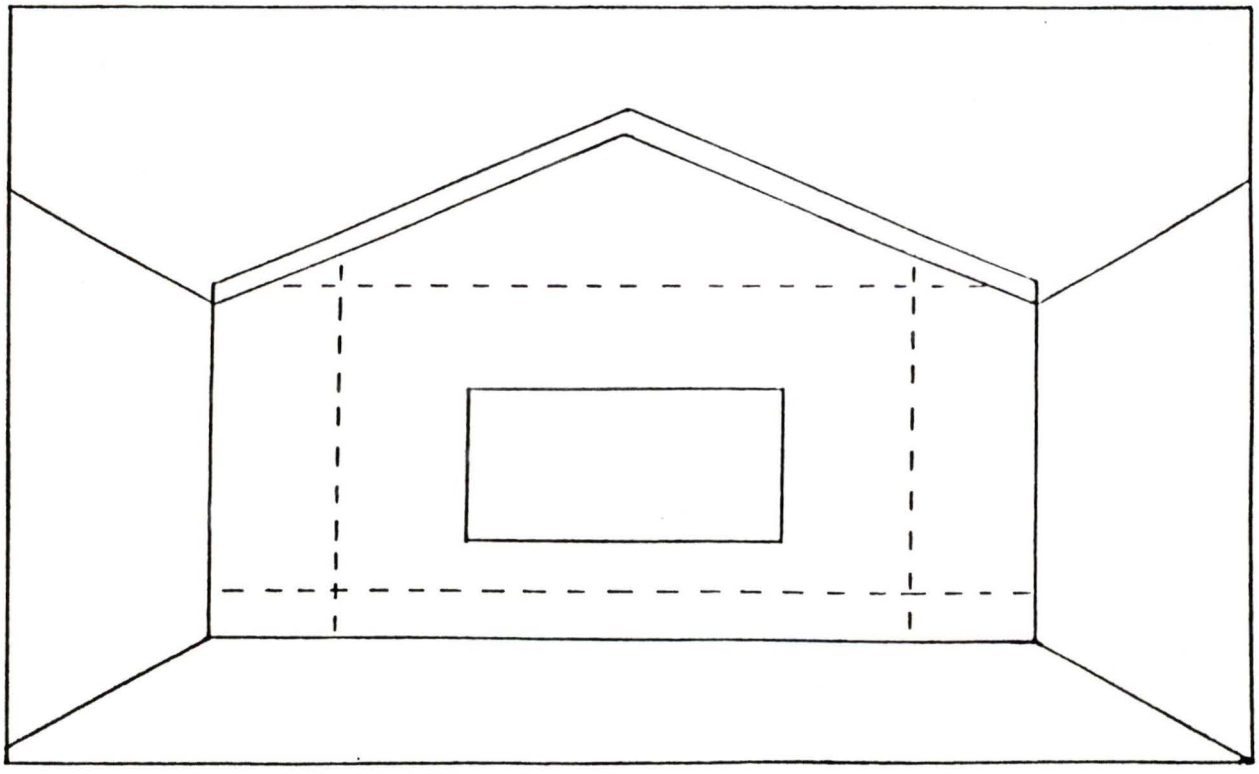

complete coverage was -16.5 ± 0.5°C. This complete coverage $\bar{T}_0$ was compared to a system of zenith angles and bearings that was less complicated and time consuming. This second method used zenith angles at 0°, 41°, 60° and 76° in the north, east, south and west directions where the zenith (0°) is measured only once. These angles mark the edges of bands that divide a hemispherical dome into 4 bands of equal surface area (Figure 4.4). Omitted from this list of zenith angles is 90° from the zenith since the horizon will often interfere with any measurement of T_0 . $\bar{T}_0$ for this second method was -15.6 ± 0.5°C and is deemed representative of the complete coverage $\bar{T}_0$.

T_0 was sampled on another evening where T_0 at the zenith was -31.0°C . Using both sets of data, the average of the complete coverage radiant temperatures was -17.5°C and the average of the radiant temperatures using the simplified coverage (i.e. 0° , 41° , 60° , 76°) was -17.55°C . The average of the differences between the two radiant temperatures was 0.48°C which supports the use of the second,and simpler, methodology.

Applying the second, and recommended, method in an urban canyon requires that the instrument be placed at the urban canyon centre, C, and that the height of all vertical components is known. Since urban canyons are not always oriented in N-S or E-W directions, it is more appropriate to perform the sampling methodology along the canyon axis and a line perpendicular to the axis such that both axes run through the urban canyon centre. This helps to maximize the number of potential sampling points that are open to the sky and not obstructed by vertical buildings and vegetative surfaces. The instrument viewfactor, ϕ, is also

required to ensure that a portion of a vertical component is not accidently sensed. Two examples are illustrated in the following figures.

In Figure 4.5, the height of the vertical component above the instrument height (HI = 2.0 metres) is 13 metres while the distance to this component is 15 metres. The angle from the zenith (0°) to the top of the vertical component is 49.1° . This means that zenith angles 0° and 41° can be used when measuring T_0 as long as the the radiometer viewfactor is < 16° .

In Figure 4.6, the height of the vertical component above the instrument height is 5 metres while the distance to this component is 15 metres. In this case, the angle from the zenith to the top of the vertical component is 76.9.°At first glance, it appears that 0°, 41°, 60° and 76° can be used. However, when considering the instrument viewfactor (e.g. ϕ = 2.8° for the Barnes Instatherm) 76° cannot be used. The instrument will sense an arc centred on 76° which ranges between 74.6° and 77.4° . Since 77.4° is greater than 76°, 76° is not appropriate.

The average of the radiant temperature measured at these zenith angles and bearings (or azimuths) should yield the effective L'_0 when $\bar{T}_0$ is used in the Stefan-Boltzmann Law. Not only are the urban canyon dimensions important factors for deciding on appropriate zenith angles, but these same dimensions will be instrumental in determining the sky viewfactor, SVF, and the link between T_a, SVF and $\bar{T}_0$.

Figure 4.4: Equal quarters on a hemispherical dome

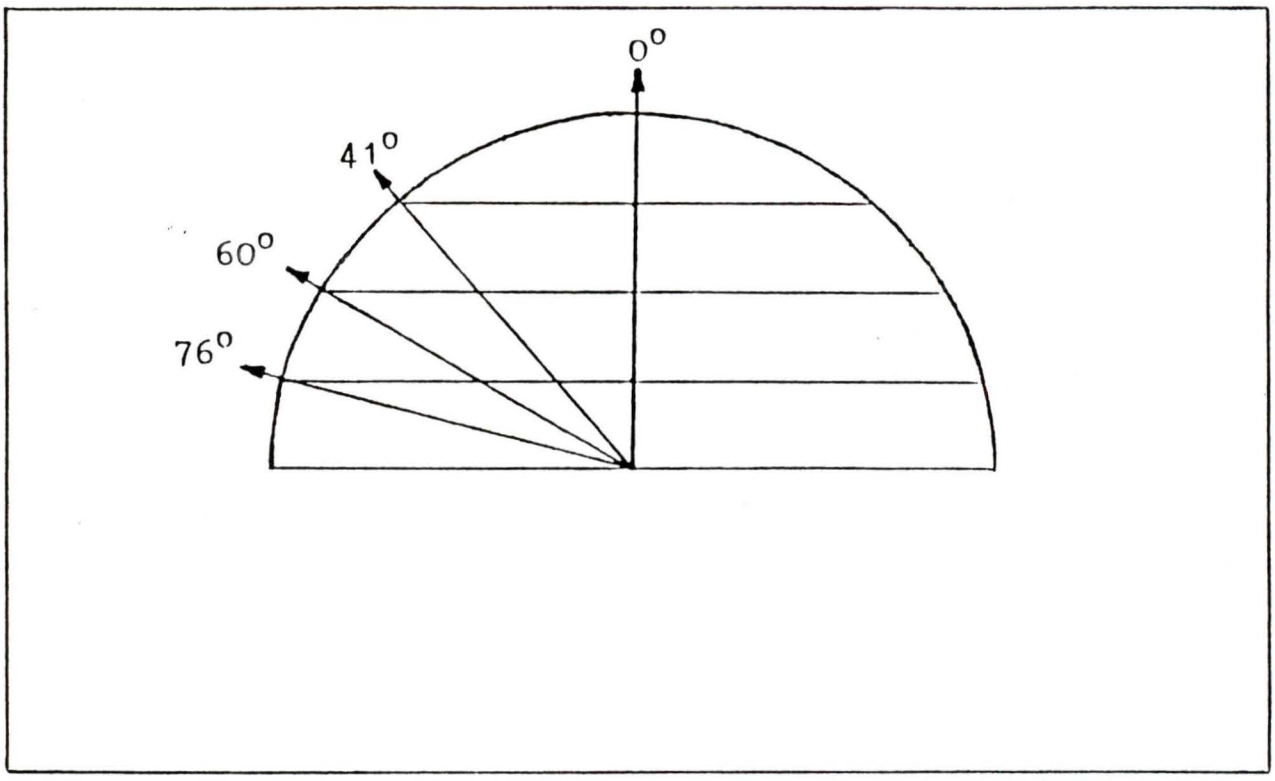

C. Sampling the Independent Variables

Reliability and consistency in the collection of data for the independent variables is also necessary for the development and validation of models. This section will describe sampling methodologies for the independent variables T_a, T_w, T_{ai}, T_{ac}, u, u_i and u_c . As with the dependent variables, an accurate yet simple method of sampling each will be identified based on field data (Appendix A). Factors to consider during the collection of data will also be discussed. The methodologies that will be described here will be discussed in terms of hori-

Figure 4.5: Unblocked instrument viewfactor

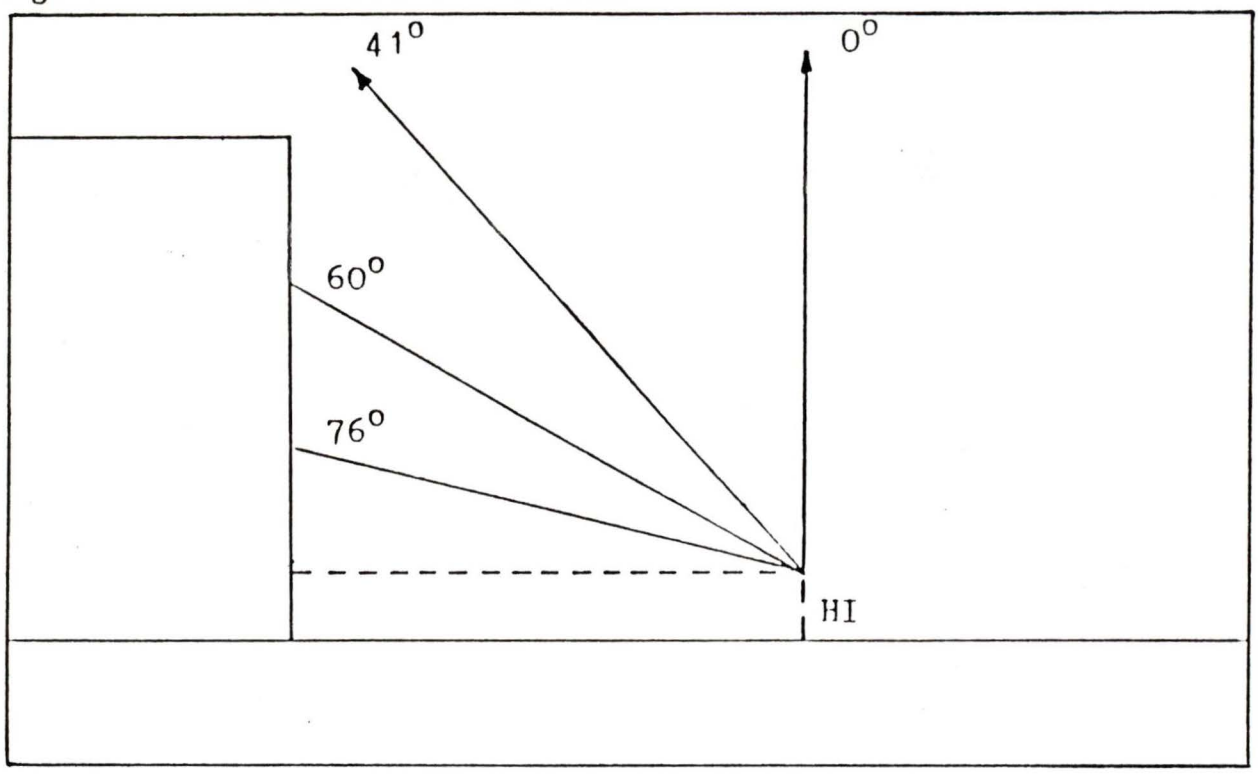

Figure 4.6: Blocked instrument viewfactor

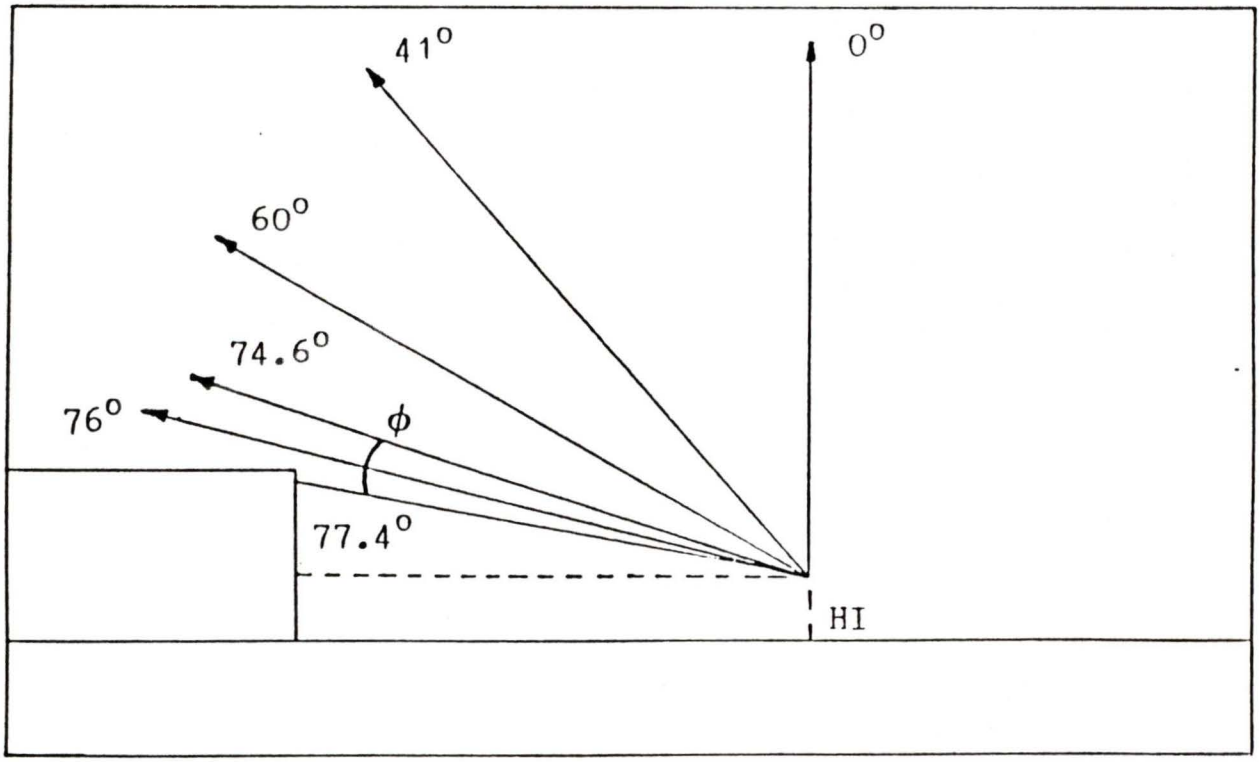

zontal homogeneous configurations with applications to horizontal heterogeneous configurations for T_a, T_w and u.

1. Sampling T_a, T_w and u in the Urban Canyon Air-Volume

T_a, T_w and u were sampled over a homogeneous short grass surface (Data Sheet 15) and a homogeneous concrete surface (Data Sheet 16). The grass surface was the one described in Data Sheet 11 (14 x 17 metres) while the concrete surface was that described in Data Sheet 10 (17 x 19 metres). A complete coverage for each of these variables was based on measurements taken at intervals using the interval method discussed in Section B of this chapter. These measurements were made at an instrument height HI = 1.5 metres.

Over the grass surface, the average air temperature based on complete coverage was $\bar{T}_a = 9.3 \pm 0.5°C$ and the average wet-bulb temperature was $\bar{T}_w = 6.9 \pm 0.5°C$. A single measurement for each of T_a and T_w was also taken at the centre of this surface where $T_a = 9.0 \pm 0.5°C$ and $T_w = 6.5 \pm 0.5°C$. For a complete coverage over the concrete surface, $\bar{T}_a = 15.7 \pm 0.5 °C$ and $\bar{T}_w = 11.4 \pm 0.5 °C$. Measurements at the centre of the concrete surface gave $T_a = 16.0 \pm 0.5 °C$ and $11.5 \pm 0.5 °C$.

For both surfaces, a single measurement of T_a and T_w over the centre of the elemental surface area at HI = 1.5 metres can be considered representative of T_a and T_w over the entire surface.

T_a and T_w were also sampled over two other grass surfaces and concrete surfaces, all within urban canyons. Combined with the data provided in Data Sheets

15 and 16, the ranges for complete coverage $\bar{T}_a$ were 9.9 to 5.3°C over the grass surfaces and 15.7 to 12.6°C over the concrete surfaces. The ranges for T_a measured over the centre of these same surfaces were 10.0 to 4.5°C over grass and 16.0 to 12.5°C over concrete. The average of all the differences between complete coverage and centre measurements was 0.32°C. Similarly, the ranges for complete coverage $\bar{T}_w$ were 7.4 to 2.7°C and 11.4 to 9.7°C for grass and concrete, respectively. The ranges for single measurements of T_w at the surface centres were 7.5 to 3.0°C for grass and 11.5 to 9.0°C for concrete. The average of all these differences was 0.33°C. It would appear that single measurements for T_a and T_w taken at the centre of surface elements are representative of the complete coverage air temperatures.

The wind speed, u, over these surfaces was also measured at the same intervals under seemingly calm conditions. Due to the sensitivity of the hot-wire anemometer, an average wind speed at each sampling point identified by the intervals was based on high and low readings of u over specific time periods. A complete coverage average wind speed, $\bar{u}$, was derived using the average wind speeds from each of the sampling points based on HI = 1.5 metres for each measurement. These complete coverage average wind speeds were then compared to single readings taken at the centre of each surface using the same instrument heights over the same time periods.

A 10 second time period was used for complete coverage $\bar{u}$ and the centre reading. Over the grass, $\bar{u} = 0.22 \pm 0.05$ ms^{-1} and the centre $u = 0.14 \pm 0.05$ ms^{-1} (Data Sheet 17). The concrete $\bar{u}$ was 0.25 ± 0.05 ms^{-1} and the centre $u = 0.19 \pm$

0.05 ms^{-1} (Data Sheet 18). Again, a reading for wind speed taken at the centre of the surface element was deemed representative of the complete coverage wind speed when a 10 second time interval is used.

Wind speed measurements over these and the two other concrete and grass surfaces were compared. For the grass surfaces, the range of the average complete coverage $\bar{u}$ was 0.45 to 0.22 ms^{-1} while for the concrete surfaces the range of average complete coverage $\bar{u}$ was 0.33 to 0.19 ms^{-1} . The ranges for u measured at the centre of these surfaces were 0.52 to 0.14 ms^{-1} and 0.40 to 0.15 ms^{-1} for grass and concrete, respectively. The average of the differences between complete coverage and centre wind speeds over all these surfaces was 0.054 ms^{-1} which is close to the representative range for wind speed. Due to the unpredictable nature of urban canyon winds, this average difference is deemed supportive of the use of wind speed measurements over the centre of surface elements. Time periods of 20 and 30 seconds were also tested with results no more representative than the 10 second time interval.

To test the usefulness of centre readings of T_a, T_w and u, traverses over a horizontal heterogeneous surface configuration of concrete and short grass were used to measure these variables based on the configuration's dimensions (20 x 25 metres) and a desired accuracy E = ± 0.5 °C and u = ± 0.05 ms^{-1} (Data Sheet 19). For a complete coverage, $\bar{T}_a$ = 15.9 ± 0.5 °C, $\bar{T}_w$ = 12.5 ± 0.5 °C and $\bar{u}$ = 0.28 ± 0.05 ms^{-1} . These complete coverage estimates were compared to the weighted average of these variables measured at the approximate centre of each surface element where the weighting was based on the area of each element. These

weighted averages yielded T_a = 16.2 ± 0.5 °C, T_w = 12.8 ± 0.5 °C and u = 0.25 ± 0.05 ms^{-1} . These three variables were also measured at the urban canyon centre where it was determined that T_a = 16.5 ± 0.5 °C , T_w = 13.0 ± 0.5 °C and u = 0.23 ± 0.05 ms^{-1} . The differences between the complete coverage measurements and the weighted average measurements were 0.4°C for T_a , 0.3°C for T_w and 0.03 ms^{-1} for u. Between the complete coverage measurements and the single measurements at the canyon centre, the differences were 0.6°C for T_a , 0.5°C for T_w and 0.05 ms^{-1} for u. For heterogeneous urban canyon floors, the recommended method for sampling T_a, T_w and u is to use the weighted average method. Where the centre of the surface element is not accessible, the point of closest proximity may be used.

A factor strongly related to T_a is the sky viewfactor, SVF (Bärring et al., 1985). For homogeneous urban canyon floors, this viewfactor should be determined for the urban canyon centre, C, since the sampling methodology for T_a specifies measurements at the canyon centre. The sky viewfactor is greatest at the centre of the urban canyon and the effects of the open sky on T_a are maximized. For heterogeneous urban canyon floors, a single sky viewfactor could be determined at the urban canyon centre. However, since the sampling methodology for T_a over these configurations specifies a weighted average of T_a based on relative surface areas and their locations, the researcher should consider applying a weighted average to sky viewfactors determined at the centre of each surface element making up the heterogeneous configuration.

2. Sampling T_{ai} and u_i in a Building Air-Volume

T_{ai} and u_i were sampled in a variety of rooms. Typical values for these variabes in one room are given in Data Sheet 20. Here, complete coverage was based on measurements at points identified using the interval method in Section B where the room dimensions were X = 4 metres, Y = 5 metres and E = 0.5°C. The instrument height HI = 1.5 metres.

The complete coverage average air temperature, $\bar{T}_{ai}$, was 19.8 ± 0.5 °C and the complete coverage wind speed, $\bar{u}_i$, was 0.13 ± 0.05 ms^{-1} .These values were compared to single readings at the centre of the room. The room centre values were T_{ai} = 20.5 ± 0.5 °C and u_i = 0.15 ± 0.05 ms^{-1} . These wind speeds were also based on the average of high/low readings over a 10 second time period. The room centre values in this and most cases were deemed representative of the complete coverage T_{ai} and u_i .

The air temperature distribution throughout a room will vary markedly both horizontally and vertically. At night, air temperatures at interior walls will generally be warmer than air temperatures at exterior walls except over a heat source. Since hot air rises, air temperatures at ceilings will generally be higher than those at floors. However, the air temperature data given in Data Sheet 10 suggests that air temperature measurements taken at the room centre where HI = 1.5 m adequately represent typical room temperatures. Similarly, convection currents created by the warming of air above a heat source can be measured for wind speed at the room centre (HI = 1.5 m) of a typical room. In this research, a typical room is based on standard construction practices for Victoria which often

include one or two exterior walls and a single heat source along one of these walls. Where the researcher encounters a different room scenario or layout, complete coverage measurements of air temperature and wind speed are recommended since the distribution of air temperatures and wind speeds becomes less predictable.

Four other rooms with single heat sources along one of their exterior walls were also sampled for T_{ai} and u_i . One of these had a ceiling approximately 3 m above the floor and was unheated. The range of complete coverage $\bar{T}_{ai}$ in these rooms and the room described in Data Sheet 10 was 24.,1 to 8.3°C while the range for complete coverage wind speed was 0.32 to 0.13 ms^{-1} . The ranges for room centre T_{ai} and u_i were 24.0 to 8.0°C and 0.28 to 0.17 ms^{-1}, respectively. The average of the differences for T_{ai} was 0.46°C while the average of the differences for u_i was 0.052 ms^{-1} . These differences are very close to the representative range for each variable. This research concludes that a single measurement at room centre be used for each of T_{ai} and u_i (10 second time interval) using HI = 1.5 m.

When modelling for a single surface element in a building shell, only the room immediately adjacent to the centre of the spot in which T is measured needs to be sampled for T_{ai} and u_i . However, when several similar or like surface elements are spread over a building shell in a heterogeneous configuration, the random sample of surface elements should dictate which rooms will be sampled.

3. Sampling T_{ac} and u_c in the Vegetative Canopy

T_{ac} and u_c were measured along a linear axis extending from the trunk through to the outer edge of the canopy for a pine tree with canopy depth h = 2.0 metres and canopy cover = 70% (Data Sheet 21). Measurements of these variables were taken in the air-volume enclosed by the canopy at the trunk and outer edge of the canopy. T_{ac} at the trunk was 9.5 ± 0.5 °C compared to T_{ac} = 9.5 ± 0.5 °C at the centre of the canopy and T_{ac} = 9.0 ± 0.5 °C at the canopy edge. Over a 10 second time interval for each measurement, u_c at the trunk was 0.10 ± 0.05 ms^{-1}, at the canopy centre u_c = 0.15 ± 0.05 ms^{-1},at the canopy edge u_c = 0.23 ± 0.05 ms^{-1} and just outside the canopy u = 0.28 ± 0.05 ms^{-1} . The average of these canopy air temperatures was 9.3°C while the average of the canopy wind speeds was 0.16 ms^{-1} .

A measurement for T_{ac} halfway through the canopy is recommended for representing the canopy air temperature based upon the previous data. Four other trees were measured for canopy air temperature and wind speed along linear axes running from their trunks to their canopy edges. The canopy covers ranged from approximately 55% to 75% and the canopy depths ranged from 1.5 to 3.5 m. Using data for the pine tree (Data Sheet 21) and the four other trees, the range for the average linear axes $\bar{T}_{ac}$ was 17.5 to 4.8°C while the range of canopy centre T_{ac} measurements was 18.0 to 5.0°C. The average of the differences between the linear axis $\bar{T}_{ac}$ and centre T_{ac} was 0.18°C.

It is recommended that the wind speed in the canopy also be measured at the centre of the linear axis. When wind speeds in the canopies of all five trees were

evaluated, the range of the average linear axes $\bar{u}_c$ measurements was 0.34 to 0.16 ms^{-1}. The range of canopy centre u_c was 0.30 to 0.15 ms^{-1}. The average of the differences between the linear axis $\bar{u}_c$ and centre u_c was 0.024 ms^{-1}. It is also worth noting that there appears to be some linearity in u_c where the canopy wind speed takes on the characteristics of the canyon wind speed toward the outer edge of the canopy.

These same methodologies should apply for horizontal vegetative surfaces (Data Sheet 22). Here, the canopy air temperature at the ground was T_{ac} = 14.5 ± 0.5 °C while at the canopy centre T_{ac} = 14.5 ± 0.5 °C and T_{ac} = 13.5 ± 0.5 °C at the canopy edge. The average of these three temperatures was 14.2°C which is well within the representative range for air temperature when compared to the canopy air temperature measured at the centre. The canopy wind speed at the ground was u_c = 0.15 ± 0.05 ms^{-1} while at the canopy centre u_c = 0.20 ± 0.05 ms^{-1} and u_c = 0.30 ± 0.05 ms^{-1} at the outer edge of the canopy. The average of all the three canopy wind speeds was 0.22 ms^{-1} which also closely approximates the wind speed at the canopy centre. Unfortunately, there are few horizontal vegetative surfaces in urban canyons that are tall enough to provide backup data supporting that in Data Sheet 22. The researcher must ensure that the vegetation height, h, is tall enough to accurately measure T_{ac} and u_c. When h is less than 0.5 metres, sampling these variables may be difficult while the canopy air-volume will have less of an effect on the vegetative T than the temperature of the ground surface underlying it.

D. Planning Data Collection Sessions

The key to successfully employing URBMAT is the careful planning of any and all data collection sessions. Before entering the field, the researcher must be familiar with the dimensions and location of the urban canyon chosen for study on any particular night. The surface elements and configurations must be measured and classified by their thermal conductivities (with the exception of vegetative surfaces). The sky viewfactor, SVF, at the urban canyon centre must also be determined, but this can be done before or after the session. Finally, the instruments required for any one session must be prepared (i.e. batteries charged and instruments calibrated). It is also recommended that the researcher wear warm clothing including a bright orange golf hat and bring a thermos of hot coffee spiked with brandy.

Aside from choosing a particular element or configuration on which to focus the collection process, it is important to have some sort of guide to direct the course of the session. In the following table (Table 4.1), the variables and factors associated with a variety of configurations are listed in the recommended order that they should be measured and recorded. Based on nocturnal changes in the surface temperature for a short grass and concrete surface (Data Sheet 2 and 3), it was determined that surface temperature decreased by approximately 0.5°C every 30 minutes from dusk until dawn. Thus, it is recommended that each of these sessions should run no longer than 30 minutes. Should the 30 minute time limit be exceeded, then the independent variables measured toward the start of the session must be remeasured and averages over the whole session used

for model development. During this research, sampling was conducted throughout the year and little variation in these procedures was deemed necessary.

Of course, several variations of these plans are possible some of which are based on the need to traverse surface elements to obtain values for surface temperature. Other variations can result from combining plans, especially for vertical surfaces. For example, once the urban canyon T_a and u have been measured (depending on the nature of the canyon floor), then the measurement of these variables need not be repeated for each surface sampled within a 30 minute time frame. However, this time limit must also include measurements of T_{ai}, u_i, T_{ac} and u_c where they are applicable.

Table 4.1:Session Plans

A. Horizontal Homogeneous Vegetation

1. determine h and c at centre
2. measure T_a and u at centre
3. measure T_{ac} and u_c where h $\geq$ 0.5 metres at centre
4. measure T for top of canopy at centre

B. Horizontal Homogeneous Non-vegetative

1. determine aspect at centre
2. measure T_a and u at centre
3. measure T at centre

C. Vertical Homogeneous Building Shell

1. determine aspect for particular wall
2. a) homogeneous canyon floor
   - measure T_a and u at centre of floor

   b) heterogeneous canyon floor
   - measure T_a and u at centre of each element for weighting
3. measure T at centre of element
4. measure T_{ai} and u_i in room adjacent to element centre

D. Vertical Homogeneous Non-vegetative

1. determine aspect at centre
2. a) homogeneous canyon floor
   - measure T_a and u at centre of floor

   b) heterogeneous canyon floor
   - measure T_a and u at centre of each element for weighting
3. measure T at centre of element

E. Vertical Homogeneous Vegetation

1. determine h and c at canopy centre
2. a) homogeneous canyon floor
   - measure T_a and u at centre of floor

   b) heterogeneous canyon floor
   - measure T_a and u at centre of each element for weighting

Table 4.1: continued

3. measure T_{ac} and u_c where $h \geq 0.5$ metres
4. measure T for canopy at centre

F. Open Portion of Sky

1. a) homogeneous canyon floor
   - measure T_a and T_w at centre of floor
   b) heterogeneous canyon floor
   - measure T_a and T_w at centre of each element for weighting
2. measure T_0 from centre

E. Chapter Summary

This chapter completes the third and final precondition required to develop "good" models of urban nocturnal long wave radiation regimes through URBMAT. By using data collected in the field (Appendix A), sampling methodologies for each dependent and independent variable were identified that collected data will be accurate. These methodologies also consider time and cost limitations faced by many model developers and users.

Chapter V

RESEARCH SUMMARY

This thesis has striven to identify a data collection format that may lead to the development of practical models for simulating urban nocturnal long wave radiation regimes. Before models can be developed and used, such a format becomes a requisite. That many researchers have overlooked the advantages of a standardized format reveals the major shortcoming in much of the literature and where some models are difficult to reproduce or validate for other areas.

A format has been identified in this thesis that can set the foundation for model development in the field of urban climatology, specifically urban nocturnal long wave radiation regimes. This is accomplished by following a series of logical steps identified as the three preconditions in URBMAT.

This chapter will briefly review the new approaches and concepts introduced in this research that relate to URBMAT and urban nocturnal long wave radiation regimes. The sampling methodologies described in Chapter 4 will also be briefly summarized since this is the point at which URBMAT culminates. Finally, some suggestions for future and related research will be offered as well as trends leading to the improvement of URBMAT and model development.

A. New Approaches and Concepts Introduced

Several new approaches and concepts were introduced in this research. Some are conceptually simple but never before clearly stated. All facilitate URBMAT and the development of practical models.

It has been shown that the long wave radiation regime of the urban canyon is constructed of radiatively active surfaces each displaying their own properties of temperature and emissivity. The concept of elements, configurations and components seeks to reinforce the construction of long wave radiation regimes. Introducing such a concept was necessary. The multitude of surface types and combinations of these surfaces necessitates that a basic surface unit (i.e. elements) be identified. Elements are easy to identify in the urban canyon and facilitate model development. Just as elements construct configurations and components, so too can models based on elements construct the long wave radiation regime of the urban canyon by piecing together configurations and components, respectively.

Identifying relevant variables, factors and properties from other models is not a new concept. However, the literature review suggests that this procedure is often poorly described. A researcher cannot enter the field to collect data without some preconceived list of variables upon which to base his data collection as well as some idea of the factors that may be relevant to the success of the field work and the model development. It is essential that a significant variable NOT be excluded from sampling or model development. However, sampling every possible variable that is indicated by other models, or

simply comes to mind, is inefficient and impractical. Thus, a large portion of this thesis has been dedicated to identifying those variables, factors and properties with the greatest relevance to urban nocturnal long wave radiation models.

Investigating the dimensional properties of variables has several purposes. First, it allows the researcher to plan for the sampling methodology to be employed. The researcher is better able to conceptualize the sampling procedure by understanding the dimensional nature of the variables under study. Secondly, variable coordinates reveal limitations that the researcher will encounter in the field. Often, accessibility severely limits the number of points at which a variable can be sampled. Finally, points at which variables are sampled may be accurately located using the variable coordinates.

The sampling techniques identified in this research refer to methods of drawing a sample and determining a sample size. A population of urban canyons may be stratified according to districts. The number of urban canyons to be sampled is still dependent upon the variety and number of surface elements present in the canyons. Districts are used to simplify this procedure since many districts display a propensity for particular elemental types. Vegetative surfaces are stratified into vertical or horizontal categories while open skies comprise a category of their own. The basic surface elements are also stratified into vertical and horizontal categories based on configurations. Further stratification is based on thermal conductivities, k, of surface materials. The actual sample size taken from each category is a function of the

desired accuracy of surface temperature readings, standard deviation of surface temperature measurements and a 95 % confidence interval. The sample of radiant sky temperature is based upon the canyon dimensions and proportions of a hemispherical dome lying over the canyon.

The sampling methodologies for each variable are extremely important to URBMAT. These methodologies will be reviewed briefly in the following section. However, several important approaches and concepts have been introduced through these methodologies. The sampling intervals are essential to the sampling methodologies which identify the locations where some variables should be sampled. Instrument height, HI, in particular should remain constant. It is important to note that models based upon one HI are valid only if HI remains the same (i.e. between 1.0 and 1.5 m) throughout the development and use of these models. The spot sampling techniques for horizontal and vertical surface temperatures have never been fully developed before this research. Spot temperature readings were treated as point readings. This treatment is false and dangerous. Spots have areas and average temperatures are sensed by the instruments. The Guide, in particular, is a totally new aid to researchers to assist in sampling radiant surface temperatures on vertical surfaces. Finally, planning the duration of the data collection session seems implicit. Yet, this procedure is often poorly performed because there are no set guidelines. This research sets guidelines for ensuring a well planned and performed session.

B. Summary of the Sampling Methodologies

URBMAT culminates in the prescription of sampling methodologies based on field data and experience. Chapters 2 and 3 were intended to lead to up to the methodologies by identifying relevant variables, factors and properties as well as instruments that are affordable and accurate. This section will briefly summarize the sampling methodologies for the dependent and independent variables.

1. Sample of Urban Canyons

A research summary is not the place to go over sampling methodologies in detail. However, there are several key points to note when drawing a sample of urban canyons. First, become familiar with the city in which the research is being conducted. This means not only familiarizing oneself with the districts and their elemental characteristics, but also noting key features of the city itself. Such features might include the functions of the city, its latitude and longitude, its surrounding geographical features, local relief, land and water distribution, and its size and area. Knowing the city well will dictate, in part, the applicability of models to other cities. Second, base the stratified random sample on the districts. Third, follow closely the urban canyon suitiblity criteria. Finally, know your canyons. Not only are the canyon dimensions important, but also the elemental types, their thermal and radiative properties, and the function of the buildings.

2. Sampling Dependent Variables

There are several basic steps that can be identified when sampling radiant surface or sky temperatures. Other steps are specific to certain surfaces and should be covered separately.

Before sampling radiant temperatures, the researcher must know the instrument he has selected. The researcher must be aware of the accuracy of the instrument (e.g. ± 0.5 °C). It is critical that the researcher knows the viewfactor, ϕ, of the instrument in order to calculate spot dimensions or use the Guide. The batteries should be charged and a spare set kept handy. Recalibration of the instrument in the field should be performed before each reading is taken.

Wherever possible use a good tripod with azimuth and zenith angles to speed up the sampling process. When changing instrument stations always relevel the instrument. Retain a constant instrument height, HI, throughout sampling and always record HI for reuse and validation by other researchers or model users.

a) Radiant Surface Temperatures of Horizontal Surfaces

The surface temperature, T, for horizontal homogeneous configurations can be sampled using one measurement at the centre of the configuration. Non-vegetative surfaces require stratification by aspect (i.e. N-E; S-W). Vegetative surfaces require measurement of the vegetative height at the point at which T is measured as well as the estimation of the vegetative cover, c. Models for T of horizontal vegetative surfaces should be based on a vegetative

cover greater than 80 % so as to minimize the effects of background temperatures.

For horizontal heterogeneous configurations, T can be sampled with a single measurement at the centre when the centre is accessible. Stratification for non-vegetative surfaces should also be based on aspect while vegetative height and cover should be considered for vegetative surfaces. When the centre is not accessible, two random traverses should be conducted, one in each of the X and Y directions. Aspect need not be considered for vegetative surfaces, while an average of height and cover should be estimated based on the points along the traverse.

b) Radiant Surface Temperature of Vertical Surfaces

The surface temperature, T, for vertical homogeneous configurations can also be sampled with a single measurement at the centre of the configuration using the largest spot possible based on the element's configurations. Non-vegetative surfaces such as building walls should be stratified by aspect. Vegetative surfaces should have the vegetative canopy depth, h, estimated based on an average of depths measured at N, E, S, and W. They should also consider vegetative cover where models are based on a cover greater than 80 %.

For vertical heterogeneous configurations, T can be sampled for each element with a single spot measurement when the centre of that element is accessible. When the centre of an element is not accessible, a single traverse along the longest dimension of the subject element should be conducted. Since these

configurations are generally associated with building shells, aspect should be used as a stratification.

c) Radiant Sky Temperatures

Radiant sky temperatures, T_0, should be measured in four directions corresponding to the urban canyon axis (i.e. along the street) and the axis perpendicular to the street axis where the instrument station is over the urban canyon centre,C . Measurements should be made at the zenith angles 0°, 41°, 60° and 76° at each bearing where the zenith (i.e. 0°) is sampled only once. The accessibility of these angles is based on urban canyon dimensions in relation to the urban canyon centre, C. The measurements of T_0 at each point should be averaged to yield a single estimate of radiant sky temperature.

3. Sampling Independent Variables

The air temperature and wind speed can generally be cosampled. Both display similarities in their sampling methodologies as they relate to urban canyons, rooms and vegetative canopies. Instrument familiarity is essential as are calibration techniques for each instrument. Using a solid instrument mount where possible will facilitate the sampling process and help ensure the instrument height is held constant. The locations for sampling these variables are related to the dimensions of the urban canyon floor where the horizontal distribution of these variables dictates the sampling methodology.

a) Dry-bulb air temperature, Wet-bulb air temperature and Wind Speed in the Urban Canyon Air-Volume

T_a, T_w and u over a homogeneous urban canyon floor can be sampled using a single measurement at the urban canyon centre, C. The instrument height should be held constant within the range HI = 1.0 to 1.5 metres. Wind speed, u, is the average of high-low readings over a 10 second interval if a hot-wire or hot-film anemometer is used.

Over a heterogeneous urban canyon floor, T_a, T_w and u are measured at the centre of each surface element. A weighted average for these climatic variables is determined based on the area of each elemental surface area. The instrument height, HI, remains in the range of 1.0 to 1.5 metres and u is averaged over a 10 second interval. Note, the sky viewfactor, SVF, should be determined for the canyon centre, C.

b) Air temperature and Wind Speed in a Building Air-Volume

Both T_{ai} and u_i can be sampled at the room centre with a single measure at HI = 1.5 metres. The room wind speed, u_i, is also based on the average of high-low readings over a 10 second interval. The rooms to be sampled should be those that lie immediately adjacent to the centre of the subject vertical elemental surface area. For a heterogeneous surface configuration, the room lying adjacent to the approximate centre of a particular surface area can be used.

c) Air temperature and Wind Speed in a Vegetative Canopy

T_{ac} can be sampled using a single measurement at a point halfway between the trunk or stem and the outer edge of the canopy for vertical vegetative surfaces, or the ground and the upper edge of the canopy for horizontal vegetative surfaces. This point should be adjacent to the centre of the spot used to sample T wherever possible. If this spot centre is not accessible, then a point as high as possible within the canopy (i.e. vertical vegetation) should be used.

The wind speed, u_i, can be sampled in a similar manner. However, two measurements are required, one close to the trunk or ground and one close to the outer edge of the canopy. High-low readings over a 10 second time interval at each point are averaged, then these two point measurements are averaged to obtain a u_c for the vegetative canopy.

These sampling methodologies are based on data collected in the field (Appendix A). They are the simplest and easiest methods for accurately sampling each variable identified in Chapter 2 with the exception of interior temperatures for substrata. Sampling can be conducted with reasonably inexpensive and easy-to-use instruments evaluated in Chapter 3. Chapters 2 to 4 outline URBMAT and although it is attuned to urban nocturnal long wave radiation regimes, the principals of the three preconditions can be applied for any and all model development.

C. Future Research and Development

There are several considerations that imply the need for future research and development in conjunction with this research.

There appears to be a need for more research into the interdependencies between air temperature, surface temperature and interior temperatures of the horizontal substrata of urban canyons. The nature, function and aesthetics of the urban environment dictates the need for placing services and utilities beneath the surface. Services include such items as subway tunnels and storm drains while utilities include gas and water mains, electrical and telephone wiring. Such services and utilities have the potential for raising the surface temperatures above them. Surface temperatures may respond more to peak and slow periods of these functions than to diurnal variations of air temperature. Even if mean temperatures could be established for these functions, the researcher would require the thickness and thermal conductivities of all materials lying between these functions and the surface. Further, knowledge of their exact locations would be necessary. Models of surface temperatures as they relate to interior temperatures could be used in conjunction with air temperature-surface temperature models to provide a more accurate simulation of horizontal radiant surface temperatures.

Vegetation, especially trees, may be better treated as a separate temperature generating and retaining entity unto itself. This suggests that a tree might have surface temperatures on a layer of air surrounding the entire tree. These surface temperatures could vary at the layer as a function of air tempera-

ture within the canopy, thickness of the canopy from the air layer to the canopy centre (e.g. trunk of the tree), canopy composition, season and plant species. As for interior temperatures beneath urban surfaces, models of canopy temperatures as they relate to vegetative air layer surface temperatures could be used in conjunction with air temperature-surface temperature models to improve simulation of vegetation radiant temperatures. Some research in this area has already been started at U.C.L.A. (Terjung & O'Rourke,1980d), but the applicability of these models to this research remains to be evaluated.

Further improvements to and development of some of the instruments would greatly facilitate this and future research. An infra-red radiometer with a fully adjustable viewfactor aperture may not necessarily eliminate the need for the Guide. It would certainly reduce the number of spots necessary to sample a vertical surface while giving better areal coverage over horizontal elements. Further, such an instrument could eliminate some of the limitations associated with canyon dimensions that prevent a researcher from getting far enough away from a vertical surface to get a temperature reading. Another improvement might include a device that would change the spot dimensions so that the spot could fit into elongated strata. Other improvements could include a built in light source that shows the researcher the surface area being sampled at night and a leveling bubble.

A hot-wire anemometer with a sensitive wind direction device would also be an improvement. Such a device would allow orientation of the hot-wire sensor with respect to the direction of the airflow in the horizontal plane. This could

decrease the frustration associated with trying to find the wind direction in light wind conditions. If fitted to a revolving base that could be set on a stand or tripod, further insight into urban wind regimes could be obtained.

The sampling methodologies outlined in this thesis are not definitive. Further study and assessment of these methodologies should be conducted in as many diverse urban canyon scenarios as possible. These studies should be conducted not only in Victoria, B.C., but in other cities displaying both maritime and continental climates.

The next logical step implied by this thesis, assuming the sampling methodologies prove to be valid, would be to collect data and construct models for radiant surface and sky temperatures. Temperatures derived from these models can then be used to simulate the urban nocturnal long-wave radiation regime. Indeed, this research was intended to be the first stage for this model development. To this end, it has fulfilled its purpose. That it raises more questions and identifies certain inadequacies is to be expected. In light of new research and commencement of data collection, this format and guide will change. Hopefully, the changes will lead to the development of practical and useful models and modelling.

BIBLIOGRAPHY

Aida, M, and M. Yaji (1979): Observations of Atmospheric Downward Radiation in the Tokyo Area, Boundary-Layer Met. , 16; 453-465.

Arnfield, A.J. (1975): Surface and Atmospheric Controls on the Heating Coefficient, Boundary-Layer Met. , 8; 109-123

Bärring, L., J.O. Mattsson and S. Lindquist (1985): Canyon Geometry, Street Temperatures and Urban Heat Island in Mälmo, Sweden, J. of Climatology , 5; 433-444.

Brunt, D. (1932): Notes on Radiation in the Atmosphere, Quart. J. Royal Meteorol. Soc. , 58; 389-420.

Burt, J.E., P.A. O'Rourke and W.H. Terjung (1982): View-factors leading to the Simulation of Human Heat Stress and Radiant Exchange: an Algorithm, Arch. Met. Geoph. Biocl. , Ser. B 30; 321-331.

Chorley, R.J. (1968): Geography and Analog Theory, Spatial Analysis. Prentice-Hall, New Jersey; 42-52.

Critchfield, H.J. (1974): General Climatology , 3rd ed. Prentice-Hall, New Jersey.

Dobson, F., L. Hasse and R. Davis (1980): Air-Sea Interaction. Plenum Press, New York.

Fanger, P.O. (1970): Thermal Comfort: Analysis and Applications in Enviromental Engineering. McGraw-Hill, New York.

Idso, S.B. and R.D. Jackson (1969): Thermal Radiation from the Atmosphere, J. Geophys. Res. , 74; 5397-5403.

Jacobs, P.A.M. (1984): Measurement of Longwave Sky Radiance Distribution, Arch. Met. Geoph. Biocl. , Ser. B34; 257-265.

Johns - Manville Engineering (1971): Engineering extra: data on building products. New York.

Johnson, G.T. and I.D. Watson (1984a): The Determination of Viewfactors in Urban Canyons, J. of Climate and Applied Meteorol., 23; 329-335.

Johnson, G.T. and I.D. Watson (1984b): Person View-factors in the Urban Environment, Arch. Met. Geoph. Biocl., Ser. B34; 273-285.

Kraus, E.B. (1972): Atmosphere-Ocean Interaction. Claredon Press, Oxford.

List, R.J. (1966): Smithsonian Meteorological Tables, 6th ed. Smithsonian Instit., Washington, D.C.

Mathews, J.A. (1981): Quantitative and Statistical Approaches to Geography. Pergamon Press, Oxford.

Minnis, P. and E.F. Harrison (1984): Diurnal Variability of Regional Cloud and Clear-Sky Radiative Parameters Derived from GOES Data, J. of Climate and App. Met., 23; 993-1051.

Monteith, J.L. (1961): An empirical method for estimating long-wave radiation exchanges in the British Isles, Quart. J. Royal Meteorol. Soc., 87; 170-178.

Monteith, J.L. (1973): Principles of Environmental Physics. Edward Arnold, London.

Myrup, L.O. (1969): A Numerical Model of the Urban Heat Island, J. of App. Met., 8; 896-907.

Novak, M.D. and T.A. Black (1985): Theoretical Determination of the Surface Energy Balance and Thermal Regimes of Bare Soil, Boundary-Layer Met., 33; 313-334.

Nunez, M. and T.R. Oke (1976): Long-Wave Radiative Flux Divergence and Nocturnal Cooling of the Urban Atmosphere, Boundary-Layer Met., 10; 121-135.

Nunez, M. and T.R. Oke (1977): The Energy Balance of an Urban Canyon, J. of App. Met., 16; 11-19.

Nunez, M. and T.R. Oke (1980): Modelling the Daytime Urban Surface Energy Balance, Geog. Analysis, 12; 214-223.

Oke, T.R. (1974): Review of Urban Climatology 1968-1973. W.M.O Tech. Note. No. 134, World Meterol. Organiz., Geneva.

Oke, T.R. (1978): Boundary-Layer Climates. Methuen & Co., London.

Oke, T.R. (1981): Canyon Geometry and the Nocturnal Heat Island: Comparison of Scale Model and Field Observations, J. of Climatology, 1; 237-254.

Oke, T.R. and R.F. Fuggle (1972): Comparison of Urban Counter and Net Radiation at Night, Boundary-Layer Met., 2; 290-308.

Oke, T.R. and G.B. Maxwell (1975): Urban Heat Island Dynamics in Montreal and Vancouver, Atmos. Environ., 9; 191-200

O'Rourke, P.A. and W.H. Terjung (1981): Urban Parks, Energy Budgets, and Surface Temperatures, Arch. Met. Geoph. Biocl., Ser. B29; 327-344.

Outcalt, S.I. (1972): The Development and Application of a Simple Digital Surface-Climate Simulator, J. of App. Met., 11; 629-636.

Paterson, W.S.B. (1969): The Physics of Glaciers. Pergamon Press, Oxford.

Paulson, C.A., E. Leavitt and R.G. Fleagle (1972): Air-sea transfer of momentum, heat and water determined from profile measurements during BOMEX, J. of Phys. Ocean., 2; 487-497.

Polavarapu, R.J. and R.E. Munn (1967): Direct measurement of vapour pressure fluctuations and gradients, J. of App. Met., 6; 699-706.

Rogers, G.F.C. and Y.R. Mayhew (1980): Engineering Thermodynamics, Work and Heat Transfer. Longman Group, London.

Sellers, W.D. (1965): Physical Climatology. Univ. Chicago Press, Chicago.

Steyn, D.G. (1980): The Calculation for View Factors From Fish-Eye Lens Photography, Atmos.-Ocean, 18; 254-258.

Sutton, O.G. (1953): Micrometeorology. McGraw-Hill, New York.

Szeicz, G., G. Enrodi and S. Tajchman (1969): Aerodynamic and Surface Factors in Evaporation, Water Resources Res., 5; 380-394.

Swinbank, W.C. (1963): Long-wave Radiation from Clear Skies, Quart. J. Royal Meteorol. Soc., 89; 339-348.

Tanner, C.B. and W.L. Pelton (1960): Potential Evapotranspiration Estimates by the Approximate Energy Balance Method of Penman, J. Geophys. Res., 65, 3391-3413.

Terjung, W.H. and S. S-F. Louie (1974): A Climatic Model of Urban Energy Budgets, Geog. Analysis, 6; 341-367.

Terjung, W.H. and P.A. O'Rourke (1978): An Outline of Boundary Layer Climatology : Methods and Analysis. Academic Publishing Service, U.C.L.A., Los Angeles.

Terjung, W.H. and P.A. O'Rourke (1980a): Simulating the Causal Elements of Urban Heat Islands, Boundary-Layer Met., 19; 93-118.

Terjung, W.H. and P.A. O'Rourke (1980b): Energy Input and Resultant Surface Temperatures for Individual Urban Interfaces, Selected Latitudes and Seasons, Arch. Met. Geoph. Biocl., Ser B29; 1-22.

Terjung, W.H. and P.A. O'Rourke (1980c): Influences of Physical Structure on Urban Energy Budgets, Boundary-Layer Met., 19; 421-439.

Terjung, W.H. and P.A. O'Rourke (1980d): An Economical Canopy Model for Use in Urban Climatology, Int. J. Biometeorol., 24; 281-291.

Terjung, W.H. and P.A. O'Rourke (1980e): Energy Exchanges in Urban Landscapes, Publications in Climatology, 33(1).

Terry R.D. and G.V. Chilinger (1955): Summary of "Concerning Some Additional Aids in Studying Sedimentary Formations" by M.S. Shvetsov, J. of Sedimentary Petrology, 25(3); 229-234.

Threlkeld, J.L. (1962): Thermal Environmental Engineering. Prentice-Hall, London.

Tuller, S.E. (1981): Simulating the Effect of Urbanization on the Human Long Wave Radiation Environment, Climatological Bulletin, 29; 1-12.

Unsworth, M.H. (1975): Long-wave Radiation at the Ground (ii), Quart. J. Royal Meteorol. Soc., 101; 25-34.

Unsworth, M.H. and J.L. Monteith (1975): Long-wave Radiation at the Ground (i), Quart. J. Royal Meteorol. Soc., 101; 13-24.

Van Wijk, W.R. and D.A. de Vries (1963): Periodic Temperature Variations, Physics of the Plant Environment. North-Holland Publishing, Amsterdam.

van Straaten, J.F. (1967): Thermal Performance of Buildings. Elsevier, Amsterdam.

Wexler, A. (1970): Measurement of Humidity in the Free Atmosphere Near the Surface of the Earth, Meteorological Monographs, 11, No. 30; 262-282.

Williams, R.B.G. (1984): Introduction to Statistics for Geographers and Earth Scientists. Macmillan Publishers, London.

Zdunkowski, W. and Ch. Brühl (1983): A Fast Approximate Method for the Calculation of the Infrared Radiation Balance within City Street Cavities, Arch. Met. Geoph. Biocl., Ser B33; 237-241.

APPENDIX A

RELEVANT DATA

Data Sheet 1: T_a versus SVF

Date: 3 May 1986
Time: 22:20 to 22:28
Instrument: aspirated mercury thermometer
HI: 1.5 m
Sfc. Type: concrete

T_a(± 0.5 °C)	SVF (approximate)
10.0	0.27
9.5	0.43
8.5	0.75

Notes: apparently an inverse relationship exists between T_a and SVF.

Data Sheet 2: vertical profile of T_a and T_w in an urban canyon over a non-vegetative surface

Date: 18-19 June 1985
Instrument: Assmann psychrometer
Sfc. Type: horizontal concrete
Units: ± 0.5 °C

Time	22:17	23:33	00:42	01:33	02:25	03:08
T_a(2.0m)	20.5	19.5	17.0	16.5	16.0	15.0
T_w(2.0m)	14.0	13.5	12.5	12.5	12.0	12.0
T_a(1.0m)	21.0	19.5	17.0	17.0	16.0	15.0
T_w(1.0m)	14.0	13.0	12.5	12.5	12.5	11.5
T_a(0.1m)	21.5	21.0	17.0	17.0	15.0	15.0
T_w(0.1m)	14.0	13.5	13.0	13.0	12.5	12.0
T_a(0.01m)	22.5	21.0	17.0	17.0	15.0	15.0
T	27.0	27.0	26.0	24.0	24.0	23.0

Notes:
- little vertical variation in T_a and T_w between 2.0 and 0.1 metres later than mid-night
- T decreased by approximately 0.5 °C every 30 minutes throughout the night
- air temperatures tend to be warmer close to the surface (0.01m) than at 2.0 m
- air temperature less than T

Data Sheet 3: vertical profile of T_a and T_w in an urban canyon over a vegetative surface

Date: 18-19 June 1985
Instrument: Assmann psychrometer
Sfc. Type: horizontal grass (≃ 5 cm)
Units: ± 0.5 °C

Time	22:33	23:50	00:50	01:50	02:30	03:33
T_a(2.0m)	20.5	19.0	17.0	15.5	15.0	14.5
T_w(2.0m)	13.5	13.0	12.0	12.5	12.0	11.0
T_a(1.0m)	20.5	19.0	16.5	15.5	15.5	14.5
T_w(1.0m)	13.5	13.0	12.0	12.0	12.0	11.5
T_a(0.1m)	19.5	18.0	15.0	15.0	15.0	14.0
T_w(0.1m)	13.0	12.5	11.0	11.0	11.5	11.0
T_a(0.01m)	18.0	17.5	14.5	14.0	14.5	13.0
T	19.5	18.0	17.5	16.5	16.0	15.0

Notes:
- little vertical variation in T_a and T_w between 2.0 and 0.1 metres throughout the night
- T decreased by approximately 0.5 °C every 30 minutes throughout the night
- air temperatures tend to be cooler close to the surface (0.01m) than at 2.0 m
- average T_a throughout the profile tends to equal T or is slightly cooler

Data Sheet 4: vertical profile of u in an urban canyon over a non-vegetative surface

Date: 18 June 1985
Time: 21:10
Instrument: Alnor Type 8500 Thermo-Anemometer
Sfc. Type: horizontal concrete
Units: $\pm$ 0.05 ms^{-1}
Time Interval: 10 seconds

HI(m)	u high	u low	avg. u
2.0	0.45	0.25	0.35
1.0	0.35	0.20	0.28
0.1	0.35	0.15	0.25
0.01	0.25	0.15	0.20

Notes: wind speed appears to increase with distance from canyon floor

Data Sheet 5: vertical profile of u in an urban canyon over a vegetative surface

Date: 18 June 1985
Time: 21:28
Instrument: Alnor Type 8500 Thermo-Anemometer
Sfc. Type: horizontal grass (≈ 5 cm)
Units: ± 0.05 ms^{-1}
Time Interval: 10 seconds

HI(m)	u high	u low	avg. u
2.0	0.55	0.30	0.43
1.0	0.45	0.35	0.40
0.1	0.50	0.20	0.35
0.01	N.A.*	N.A.	N.A.

Notes: wind speed appears to increase with distance from canyon floor

* N.A. - not available due to interference from surface

Data Sheet 6: T versus aspect for a horizontal non-vegetative surface

Date: 4-5 May 1986
Instrument: Barnes Instatherm (ϕ = 2.8°)
Sfc. Type: concrete
Units: ± 0.5 °C

Time	N	E	S	W	T_3
21:02	15.5	15.0	17.0	16.5	9.5
23:01	13.0	13.5	14.5	14.5	8.5
01:02	11.0	11.0	12.5	13.0	7.5
03:02	10.0	10.0	11.0	11.5	7.0
avg. T	12.4	12.4	13.8	13.9	

Notes: on average and over the course of the night, the S and W facing surfaces appear warmer than the N and E facing surfaces
- stratify these surfaces based on SW,NE strata

Data Sheet 7: T versus aspect for a horizontal vegetative surface

Date: 4-5 May 1986
Instrument: Barnes Instatherm (ϕ = 2.8°)
Sfc. Type: grass (≃ 6 cm)
Sfc. Dimensions: variable
Units: ± 0.5 °C

Time	N	E	S	W	T_a
21:07	11.0	11.0	11.5	11.5	9.5
23:06	9.5	10.0	10.5	10.0	8.5
01:07	8.5	8.5	9.0	9.5	7.0
03:07	8.0	8.0	8.5	8.5	6.5
avg. T	9.3	9.4	9.9	9.9	

Notes: on average and over the course of the night, there is no differnce in T with aspect

Data Sheet 8: T versus aspect for a vertical building shell

Date: 4-5 May 1986
Instrument: Barnes Instatherm (ϕ = 2.8°)
Sfc. Type: plaster and stucco
Sfc. Dimensions: 5 m high
Units: ± 0.5 °C

Time	N	E	S	W	T_a
21:03	15.0	15.0	17.0	16.0	9.5
23:03	12.5	12.5	14.5	14.0	8.5
01:03	11.0	11.0	12.5	12.5	7.5
03:03	10.5	10.5	11.5	11.0	7.0
avg. T	12.1	12.3	13.9	13.4	

Notes: on average and over the course of the night, the S and W facing surfaces appear warmer than the N and E facing surfaces
- stratify these surfaces based on SW, NE strata

Data Sheet 9: T versus aspect for a vertical vegetative surface

Date: 4-5 May 1986
Instrument: Barnes Instatherm (ϕ = 2.8°)
Sfc. Type: Pine Tree
Sfc. Dimensions: 6 m high
Cover: ≃ 75 %
Units: ± 0.5 °C

Time	N	E	S	W	T_a
21:00	15.0	15.0	15.5	15.0	9.0
23:00	12.0	12.0	12.5	12.5	8.0
01:00	10.5	10.0	10.5	10.0	7.0
03:00	8.0	8.5	8.0	8.5	6.5
avg. T	11.4	11.4	11.6	11.5	

Notes: on average and over the course of the night, there is no difference in T with aspect

Data Sheet 10: surface temperature for a horizontal non-vegetative surface

Date: 19 August 1985
Instrument: Barnes Instatherm (ϕ = 2.8°)
Sfc. Type: Concrete
Sfc. Dimensions: 17 x 19 m
Units: ± 0.5 °C
Avg. T_a: 16.0° C

Temperature pattern for evenly spaced intervals in X and Y coordinates over the entire surface area

	Y-Interval	1	2	3	4
	(m)	2.4	7.1	11.9	16.6
X-Interval	(m)				
1	2.1	18.5	18.5	19.5	19.0
2	6.4	19.0	19.0	19.5	19.0
3	10.6	19.0	19.5	19.5	19.5
4	14.9	19.5	19.5	19.0	18.5

Notes: complete coverage: $\bar{T}$ = 19.1 ± 0.5 °C
single random traverse: $\bar{T}$ = 19.4 ± 0.5 °C (3Y)
two random traverses: $\bar{T}$ = 19.0 ± 0.5 °C (4X, 1Y)
centre: $\bar{T}$ = 19.5 ± 0.5 °C
* use centre measurement for T

Summary of Additional Data (T)

Sample	1.	2.	3.
Complete Coverage	12.8	11.5	9.5
Centre	12.5	12.0	9.0
Difference	0.3	0.5	0.5

Average of all differences = 0.43°C

Data Sheet 11: surface temperature for a horizontal vegetative surface

Date: 19 August 1985
Time: 00:15 to 00:40
Instrument: Barnes Instatherm (ϕ = 2.8°)
Sfc. Type: grass (≃ 6 cm)
Sfc. Dimensions: 14 x 17 m
Units: ± 0.5 °C
Avg. T_a: 16.5° C
Cover: 100%

Temperature pattern for evenly spaced intervals in X and Y coordinates over the entire surface

	Y-Interval	1	2	3	4
	(m)	2.1	6.4	10.6	14.9
X-Interval	(m)				
1	1.8	14.0	14.5	14.5	14.0
2	5.3	15.0	15.5	15.0	14.5
3	8.8	15.5	15.0	14.5	14.0
4	12.3	15.0	15.0	15.0	14.5

Notes: complete coverage: $\bar{T}$ = 14.7 ± 0.5 °C
single random traverse: $\bar{T}$ = 14.8 ± 0.5 °C (3X)
two random traverses: $\bar{T}$ = 14.3 ± 0.5 °C (1X, 4Y)
centre: $\bar{T}$ = 15.0 ± 0.5 °C
* use centre measurement for T

Summary of Additional Data (T)

Sample	1.	2.
Complete Coverage	12.9	7.1
Centre	12.5	6.5
Difference	0.4	0.6

Average of all differences = 0.43°C

Data Sheet 12: surface temperature for a vertical non-vegetative surface

Date: 3 May 1986
Time: 22:00 to 22:18
Instrument: Barnes Instatherm (ϕ = 2.8°)
Sfc. Type: concrete block
Sfc. Dimensions: 5 x 6 m
Units: ± 0.5 °C
Spot width: 1.0 metres
Avg. T_a: 9.0° C

Temperature pattern for evenly spaced spots over the entire surface

	Width (m)	0.5	1.5	2.5	3.5	4.5
d(m)	γ (°)					
20.1	10.5	15.0	15.0	15.5	15.5	15.0
20.2	8.5	15.5	15.0	15.5	15.5	15.0
20.4	5.5	15.5	15.5	16.0	16.0	15.0
20.4	3.0	15.5	16.0	16.0	16.0	15.5
20.5	0	15.5	16.0	16.5	16.0	15.5
20.4	-3.0	16.0	15.5	15.5	15.5	15.0

Notes: large spot at centre: T = 16.0 ± 0.5 °C
complete coverage: $\bar{T}$ = 15.6 ± 0.5 °C (3X)
single traverse: $\bar{T}$ = 15.8 ± 0.5 °C (W = 3.5m)
two random traverses: $\bar{T}$ = 14.3 ± 0.5 °C
(W = 1.5m; γ = 5.5)° * use large spot at centre

Summary of Additional Data

Sample	1.	2.	3.	4.
Complete Coverage	12.9	12.4	14.1	19.5
Centre	13.0	12.0	14.0	19.0
Difference	0.1	0.4	0.1	0.5

Average of all differences = 0.28 °C

Data Sheet 13: surface temperature vertical vegetative surfaces

Date: 3 May 1986
Time: 22:00 to 22:15
Instrument: Barnes Instatherm
Units: ± 0.5 °C
Avg. T_a: 9.0° C
HI. 1.5 metres

a) Sfc. Type: cedar hedge
Sfc. Dimensions: 2 x 14 m
Cover: 90%
Spot Diameter: 2.0 m
Canopy Depth: 1.0 m

Horizontal temperature pattern for evenly spaced spots over the entire surface area

	Width (m)	1.4	4.2	7.0	9.8	12.6
d(m)	γ (°)					
40.9	0.5	14.0	14.5	14.5	14.5	14.0

Notes: complete coverage: $\bar{T}$ = 14.3 ± 0.5 °C (3X)
single spot at centre: $\bar{T}$ = 14.5 ± 0.5 °C
difference = 0.2 °C
* use single spot

Data Sheet 13: continued

b) Sfc. Type: plum tree (in full leaf)
Sfc. Dimensions: 3.0 x 3.5 m
Cover: 60%
Spot Diameter: 0.5 m
Canopy Depth: 2.0 m

Cross temperature pattern for spots passing through the centre of the surface area

	Width (m)	0.25	0.75	1.25	1.75	2.25	2.75	3.25
d(m)	γ (°)							
10.1	7.0				12.5			
10.2	4.0				13.0			
10.2	1.5				13.5			
10.2	-1.5	13.0	13.5	14.0	14.0	14.0	13.5	13.0
10.2	-4.0				14.0			
10.1	-7.0				14.5			

Notes: complete coverage: $\bar{T} = 13.5 \pm 0.5$ °C
vertical traverse: $\bar{T} = 13.6 \pm 0.5$ °C
horizontal traverse: $\bar{T} = 13.6 \pm 0.5$ °C
single large spot at centre: $T = 14.0 \pm 0.5$ °C
diff. between complete coverage & large spot = 0.5 °C
* average difference between both samples = 0.35 °C
* use single large spot

* appears to be a direct relationship between cover and surface temperature

Data Sheet 14: radiant sky temperature

Date: 3 May 1986
Time: 21:45 to 21:55
Instrument: Barnes Instatherm (ϕ - 2.8°)
Sfc. Type: asphalt
Units: ± 0.5 °C
Avg. T_a: 8.5° C

a) complete coverage

Aspect	N	E	S	W
Zenith Angle (°)				
75	-5.0	-6.0	-4.0	-4.0
60	-14.0	-15.0	-13.5	-12.5
45	-18.0	-19.0	-18.0	-16.5
30	-21.0	-21.0	-21.0	-20.0
15	-23.0	-24.0	-22.5	-21.0
0	-24.0			

$\bar{T}_0$ = -16.3 ± 0.5 °C

b) quarterly intervals

Aspect	N	E	S	W
Zenith Angle (°)				
76	* N.A.	-8.5	-8.0	-7.5
60	-16.0	-16.5	-16.0	-15.5
41	-21.0	-21.0	-21.0	-20.0
0	-24.0			

$\bar{T}_0 = -15.6 \pm 0.5$ °C

* N.A. - not available due to vertical obstruction

Notes: - quarterly method easier, thus recommended
- L_0^+ based on complete coverage $\bar{T}_0$ and S-B law is:

$L_0^+ = 247.0$ Wm^{-2}

- L_0^+ based on quarterly $\bar{T}_0$ and S-B law is:

$L_0^+ = 249.7$ Wm^{-2}

- L_0^+ using T_a and:

1. Swinbank $L_0^+ = 257.5$ Wm^{-2}
   * overestimates *

1. Monteith $L_0^+ = 259.0$ Wm^{-2}
   * overestimates *

Data Sheet 15: T_a and T_w over a horizontal vegetative surface

Date: 20 August 1985
Time: 22:20 to 22:40
Instrument: Assmann psychrometer
Sfc. Type: grass (≃ 6 cm)
Sfc. Dimensions: 14 x 17 m
Units: ± 0.5 °C
HI: 1.5 m

Dry-bulb and wet-bulb air temperature pattern at evenly spaced intervals over the entire surface area

	Y-Interval	1	2	3	4
	(m)	2.1	6.4	10.6	14.9
X-Interval	(m)				
1	1.8	9.5 * (7.0)	9.5 (6.5)	9.5 (7.0)	9.5 (7.0)
2	5.3	9.5 (7.5)	9.5 (7.0)	9.5 (6.5)	9.0 (7.0)
3	8.8	9.5 (7.0)	9.5 (6.5)	9.0 (6.5)	9.0 (6.5)
4	12.3	9.5 (7.5)	9.0 (7.0)	9.5 (7.0)	9.0 (6.5)

*wet-bulb air temperature in brackets

Notes: complete coverage: $\bar{T}_a = 9.3 \pm 0.5$ °C

$\bar{T}_w = 6.9 \pm 0.5$ °C

reading at centre: $\bar{T}_a = 9.0 \pm 0.5$ °C

$\bar{T}_w = 6.5 \pm 0.5$ °C

* use single reading for each of T_a and T_w taken at centre

Data Sheet 15 (continued)

Summary of Additional Data(T_a)

Sample	1.	2.
Complete Coverage	9.9	5.3
Centre	10.0	4.5
Difference	0.1	0.8

Average of all differences = 0.40 °C

Summary of Additional Data(T_w)

Sample	1.	2.
Complete Coverage	7.4	2.7
Centre	7.5	3.0
Difference	0.1	0.3

Average of all differences = 0.27 °C

Data Sheet 16: T_a and T_w over a horizontal non-vegetative surface

Date: 20 August 1985
Time: 23:05 to 23:25
Instrument: Assmann psychrometer
Sfc. Type: concrete
Sfc. Dimensions: 17 x 19 m
Units: ± 0.5 °C
HI: 1.5 m

Dry-bulb and wet-bulb air temperature pattern for evenly spaced intervals over the entire surface area

	Y-Interval	1	2	3	4
	(m)	2.4	7.1	11.9	16.6
X-Interval	(m)				
1	2.1	15.5 * (11.5)	15.5 (11.0)	15.0 (10.5)	14.5 (10.5)
2	6.4	16.0 (12.0)	16.0 (11.5)	16.0 (11.5)	15.0 (11.5)
3	10.6	16.5 (12.5)	16.0 (11.5)	15.5 (11.0)	15.5 (11.0)
4	14.9	16.0 (12.0)	16.0 (11.5)	16.5 (12.0)	16.0 (11.0)

* wet-bulb air temperature in brackets

Notes: complete coverage: $\bar{T}_a = 15.7 \pm 0.5$ °C

$\bar{T}_w = 11.4 \pm 0.5$ °C

reading at centre: $\bar{T}_a = 16.0 \pm 0.5$ °C

$\bar{T}_w = 11.5 \pm 0.5$ °C

- use single reading for each of T_a and T_w taken at centre

Data Sheet 16 (continued)

Summary of Additional Data(T_s)

Sample	1.	2.
Complete Coverage	12.6	13.2
Centre	12.5	13.5
Difference	0.1	0.3

Average of all differences = 0.23 °C

Summary of Additional Data(T_w)

Sample	1.	2.
Complete Coverage	9.7	9.8
Centre	10.0	9.0
Difference	0.3	0.8

Average of all differences = 0.40 °C

Data Sheet 17: wind speed over a horizontal vegetative surface

Date: 11 September 1985
Time: 23:10 to 23:35
Instrument: Alnor Type 8500 Thermo-Anemometer
Sfc. Type: grass (≈ 5 cm.)
Sfc. Dimensions: 14 x 17 m
Units: ± 0.05 ms^{-1}
HI: 1.5 m
Time Interval: 10 seconds

Wind speed pattern for evenly spaced intervals over the entire surface area

	Y-Interval	1	2	3	4
	(m)	2.1	6.4	10.6	14.9
X-Interval	(m)				
1	1.8	*0 35(0 23)0 10	0 15(0 10)0 05	0 10(0 08)0 05	0 20(0 18)0 15
2	5.3	0 55(0 45)0 35	0 55(0 48)0 40	0 15(0 10)0 05	0 25(0 18)0 10
3	8.8	0 55(0 43)0 30	0 30(0 20)0 10	0 40(0 28)0 15	0 25(0 20)0 15
4	12.3	0 20(0 13)0 05	0 10(0 08)0 05	0 15(0 13)0 10	0 30(0 20)0 10

* high-reading(average-reading)low-reading

Notes: complete coverage: $\bar{u}$ = 0.22 ± 0.05 ms^{-1}
average u at centre: u= 0.14 ± 0.05 ms^{-1}
(based on the average of two high-low readings)
a) high-reading (1) = 0.20 m s^{-1}
b) low-reading (1) = 0.05 m s^{-1}
c) high-reading (2) = 0.25 m s^{-1}
d) low-reading (2) = 0.05 m s^{-1}

Data Sheet 17 (continued)

Summary of Additional Data(u)

Sample	1.	2.
Complete Coverage	0.39	0.45
Centre	0.52	0.40
Difference	0.13	0.05

Average of all differences = 0.09 m s^{-1}

Data Sheet 18: wind speed over a horizontal non-vegetative surface

Date: 12 September 1985
Time: 01:13 to 01:30
Instrument: Alnor Type 8500 Thermo-Anemometer
Sfc. Type: concrete
Sfc. Dimensions: 17 x 19 m
Units: ± 0.05 ms^{-1}
HI: 1.5 m
Time Interval: 10 seconds

Wind speed pattern for evenly spaced intervals over the entire surface area

	Y- Interval	1	2	3	4
	(m)	2.1	6.4	10.6	14.9
X-Interval	(m)				
1	2.1	0.30(0.23)0.15	0.20(0.13)0.05	0.15(0.13)0.10	0.20(0.15)0.10
2	6.4	0.30(0.23)0.15	0.35(0.25)0.15	0.40(0.33)0.25	0.35(0.28)0.20
3	10.6	0.25(0.15)0.05	0.25(0.20)0.15	0.35(0.28)0.20	0.30(0.18)0.05
4	12.3	0.45(0.35)0.25	0.50(0.30)0.10	0.45(0.33)0.20	0.55(0.40)0.25

* high-reading(average-reading)low-reading

Notes: complete coverage: $\bar{u}$ = 0.25 ± 0.05 ms^{-1}

average u at centre: u= 0.19 ± 0.05 ms^{-1}
(based on the average of two high-low readings)

a) high-reading (1) = 0.25 m s^{-1}
b) low-reading (1) = 0.15 m s^{-1}
c) high-reading (2) = 0.20 m s^{-1}
d) low-reading (2) = 0.15 m s^{-1}

Data Sheet 18 (continued)

Summary of Additional Data(u)

Sample	1.	2.
Complete Coverage	0.19	0.33
Centre	0.15	0.40
Difference	0.04	0.07

Average of all differences = 0.06 m s^{-1}

Data Sheet 19: T_a and T_w and u over a horizontal heterogeneous surface configuration

Date: 21 August 1985
Sfc. Type: concrete and grass (≃ 6 cm)
Sfc. Dimensions: 21 x 28 m overall
Sfc. Areas: concrete - 60 m^2
grass - 318 m^2

a) Time: 23:05 to 23:25
Instrument: Assmann psychrometer
Units: ± 0.5 °C
HI: 1.5 m

Dry-bulb and wet-bulb temperature pattern for evenly spaced intervals over both surface areas

	Y-Interval	1	2	3	4
	(m)	2.25	6.75	11.25	15.75
X-Interval	(m)				
1	2.1	17.0 * (12.0)	16.5 (12.5)	16.5 (13.0)	16.0 (13.0)
2	6.3	17.5 (12.0)	16.0 (12.5)	16.0 (13.0)	15.5 (12.5)
3	10.5	17.5 (12.5)	16.5 (13.0)	16.0 (13.5)	15.0 (12.5)
4	14.7	16.5 (12.5)	16.0 (12.0)	15.0 (12.5)	15.0 (12.0)
5	18.9	15.5 (13.0)	15.0 (12.0)	14.5 (11.5)	14.5 (11.5)

* wet-bulb air temperature in brackets

Notes:
concrete centre: T_a = 17.5 ± 0.5 °C; T_w = 12.0 ± 0.5 °C
grass centre: T_a = 16.0 ± 0.5 °C; T_w = 13.0 ± 0.5 °C
complete coverage: $\bar{T}_a$ = 15.9 ± 0.5 °C
complete coverage: $\bar{T}_w$ = 12.5 ± 0.5 °C
weighted coverage: T_a = 16.2 ± 0.5 °C
weighted coverage: T_w = 13.3 ± 0.5 °C
canyon centre: T_a = 16.5 ± 0.5 °C; T_w = 13.0 ± 0.5 °C

Data Sheet 19: continued

b) Time: 22:30 to 22:42
Instrument: Alnor Type 8500 Thermo-Anemometer
Units: ± 0.05 ms^{-1}
HI: 1.25 m
Time Interval: 10 seconds

Wind speed pattern for evenly spaced intervals over both surface areas

	Y-Interval	1	2	3	4
	(m)	2.25	6.75	11.25	15.75
X-Interval	(m)				
1	2.1	0.40(0.30)0.20	0.50(0.35)0.20	0.40(0.30)0.20	0.40(0.35)0.15
2	6.3	0.45(0.28)0.10	0.45(0.28)0.10	0.35(0.25)0.15	0.25(0.23)0.20
3	10.5	0.35(0.30)0.25	0.35(0.23)0.10	0.45(0.28)0.10	0.40(0.30)0.20
4	14.7	0.30(0.25)0.20	0.25(0.20)0.15	0.35(0.25)0.15	0.30(0.23)0.15
5	18.9	0.50(0.33)0.15	0.40(0.30)0.20	0.35(0.33)0.30	0.45(0.33)0.20

* high-reading(average-reading)low-reading

Notes: concrete centre: $u = 0.28 \pm 0.05$ ms^{-1}
grass centre: $u = 0.25 \pm 0.05$ ms^{-1}
complete coverage: $\bar{u} = 0.28 \pm 0.05$ ms^{-1}
weighted average: $u = 0.25 \pm 0.05$ ms^{-1}
canyon centre: $u = 0.23 \pm 0.05$ ms^{-1}

- use weighted averages for each of T_a, T_w and u where weighting is based on surface areas

Data Sheet 20: air temperature and wind speed in a room

Date: 10 September 1985
Room Function: recreation room
Room Dimensions: 4 x 6 m
Special: two exterior walls
heat source under window

a) vertical profile of air temperature at room centre
Time: 22:35
Instrument: Thermistor-Thermometer
Units: ± 0.5 °C

HI(m)	T_{ai}
2.25	22.0
1.50	20.5
0.25	18.5

Notes: average T_{ai} = 20.3 ± 0.5 °C

- use one temperature measurement at 1.5 metres

b) horizontal distribution of air temperature
Time: 22:40 to 22:45
Instrument: Thermistor-Thermometer
Units: ± 0.5 °C
HI: 1.5 m

	Y-Interval	1	2
	(m)	1.5	4.5
X-Interval	(m)		
1	1.0	19.0	19.5
2	3.0	19.5	21.0

Notes: complete coverage

$\bar{T}_{ai}$ = 19.8 ± 0.5 °C

centre T_{ai} = 20.5 ± 0.5 °C

-use one temperature measurement at centre

Data Sheet 20: continued

c) horizontal distribution of wind speed

Time:	22:55 to 23:04
Instrument:	Alnor Type 8500 Thermo-Anemometer
Units:	± 0.05 ms ^{1}
HI:	1.5 m
Time Interval:	10 seconds

	Y-Interval	1	2
	(m)	1.5	4.5
X-Interval	(m)		
1	1.8	0.20(0.13)0.05	0.25(0.15)0.05
2	5.3	0.15(0.13)0.10	0.15(0.10)0.10

* high-reading(average-reading)low-reading

Notes: complete coverage: $\bar{u}_i = 0.13 \pm 0.05$ ms^{-1}
centre: $\bar{u}_i = 0.15 \pm 0.05$ ms^{-1}
* use wind speed measurement at room centre

Summary of Additional Data(T_{ai})

Sample	1.	2.	3.	4.
Complete Coverage	18.4	24.1	8.3	21.6
Centre	19.0	24.0	8.0	21.0
Difference	0.6	0.1	0.3	0.6

Average of all differences = 0.46 °C

Summary of Additional Data(u_i)

Sample	1.	2.	3.	4.
Complete Coverage	0.24	0.32	0.23	0.17
Centre	0.19	0.28	0.17	0.24
Difference	0.05	0.04	0.06	0.07

Average of all differences = 0.052 m s^{-1}

Data Sheet 21: air temperature and wind speed in a vertical vegetative canopy

Date: 3 May 1986
Time: 21:15 to 21:23
Sfc. Type: pine tree
Canopy Depth: 2.0 m
Cover: 70%
HI: 2.25 m (1.0 m within canopy)
Avg. T_a 9.0 °C

a) air temperature in the canopy
Instrument: Thermistor-Thermometer
Units: ± 0.5 °C

T_{ac} at trunk	T_{ac} at centre	T_{ac} at canopy edge
9.5	9.5	9.0

Note: measure T_{ac} halfway between trunk and canopy edge

b) windspeed in the canopy
Instrument: Alnor Type 8500 Thermo-Anemometer
Units: ± 0.05 ms^{-1}
Time Interval: 10 seconds

u_c	u_c trunk	u_c centre	u_c canopy edge	u outside canopy
HIGH u_c	0.15	0.25	0.35	0.50
$\bar{u}_c$	0.10	0.15	0.23	0.28
LOW u_c	0.05	0.05	0.10	0.05

Note: wind speed takes on characteristics of u outside the canopy as readings are taken closer to canopy edge

Data Sheet 21 (continued)

Summary of Addtional Data(T_{ac})

Sample	1.	2.	3.	4.
Linear Axis	4.8	6.0	17.5	11.5
Centre	5.0	6.0	18.0	11.5
Difference	0.2	0.0	0.5	0.0

Average of all differences = 0.18 °C

Summary of Additional Data(u_c)

Sample	1.	2.	3.	4.
Linear Axis	0.23	0.17	0.34	0.23
Centre	0.25	0.15	0.30	0.20
Difference	0.02	0.02	0.04	0.03

Average of all differences = 0.024 m s^{-1}

Data Sheet 22: air temperature and wind speed in a horizontal vegetative canopy

Date: 21 June 1985
Time: 22:20 to 22:25
Sfc. Type: orchard grass
Canopy Depth: 1.25 m
Cover: 65%
Avg. T_a 13.5 °C

a) air temperature in the canopy
Instrument: Thermistor-Thermometer
Units: ± 0.5 °C

T_{ac} at ground	T_{ac} at centre	T_{ac} at canopy edge
14.5	14.5	13.5

Note: measure T_{ac} halfway between ground surface and canopy edge

b) wind speed in the canopy
Instrument: Alnor Type 8500 Thermo-Anemometer
Units: ± 0.05 ms^{-1}
Time Interval: 10 seconds

u_c	u_c ground	u_c centre	u_c canopy edge	u outside canopy
HIGH u_c	0.25	0.35	0.50	0.95
$\bar{u}_c$	0.15	0.20	0.30	0.58
LOW u_c	0.05	0.05	0.10	0.20

Note: wind speed takes on characteristics of u the closer to the canopy edge that it is measured

APPENDIX B

TABLES

TABLE A1
THERMAL CONDUCTIVITIES OF VARIOUS MATERIALS
($Wm^{-1}K^{-1}$)

	Category	Thermal Conductivity
A.	Exterior Materials	
1.	Concrete-areated	0.08-0.11
	Wood-bevel & plywood	"
2.	Asphalt Insulating Siding	0.19-0.22
	Wood-drop siding	"
3.	Gypsum-precast & poured	0.30-0.45
4.	Concrete Blocks -lightweight aggregate	0.64-0.69
	Hollow Clay Tile -2 cells deep (8")	"
5.	Brick-common	0.72-0.80
	Stucco	"
	Flexboard	"
	Hardboard	"
	Concrete Blocks -cinder aggregate	"
	Glass	"
6.	Concrete Blocks -sand & gravel	1.16
7.	Concrete-dense	1.45-1.51
	Brick-face	"
8.	Concrete -sand & gravel or stone	1.93-2.19
	Stone	"
9.	Steel	53.3

TABLE A1
(CONTINUED)

Category	Thermal Conductivity
B. Interior Finishes	
1. Insulating Board	0.06
2. Plywood	0.13-0.18
Gypsum Board	"
3. Gypsum Plaster -lightweight aggregate	0.26
4. Cement Plaster -sand aggregate	0.80-0.90
Gypsum Plaster -sand aggregate	"
C. Natural Materials	
1. Peat Soil-dry	0.06-0.11
Snow-fresh	"
Light Wood-fir, cedar	"
2. Clay Soil-dry	0.19-0.25
Dense Wood-oak, maple	"
3. Sandy Soil-dry	0.30-0.42
Snow-old	"
4. Peat Soil-saturated	0.50-0.57
Water-still	"
5. Clay Soil-saturated	1.58
6. Sandy Soil-saturated	2.20-2.24
Ice-pure	"

Sources: van Wijk & de Vries (1963), List (1966), van Straaten (1967), Johns-Manville (1971), Oke (1978)

TABLE A2
EMISSIVITIES OF VARIOUS SURFACES

Category	Emissivity
A. Water & Soil Surfaces	
Water	0.92-0.97
Snow	0.82-0.99
Ice	0.96
Soils	
Gravel-coarse	0.91-0.92
Ground-moist,bare	0.95-0.98
dry,plowed	0.90
B. Natural Surfaces & Vegetation	
Desert	0.90-0.91
Grasses	0.90-0.95
Fields & shrubs	0.90
Forests	
Deciduous-bare leaved	0.97-0.98
Conifers	0.97-0.99
Oak woodland	0.90
Pine forest	0.90
Agricultural crops	0.90-0.99
C. Man-made Surfaces	
Roads-asphalt	0.95
concrete	0.71-0.88
Walls-brick	0.90-0.92
concrete	0.71-0.90
stone	0.85-0.95
wood	0.90
plaster, white	0.91
Roofs-tar & gravel	0.92
tile	0.90
slate	0.90
corrugated iron	0.13-0.28
Windows-clear glass	0.87-0.94

TABLE A2
(CONTINUED)

Category	Emissivity
Paints-aluminum	0.43-0.55
white,whitewash	0.85-0.95
red,brown,green	0.85-0.95
black	0.90-0.98

Sources: Threlkeld (1962), Sellers (1965), List (1966), van Straaten (1967),Paterson (1969), Monteith (1973), and Oke (1974&1978)

TABLE A3
AERODYNAMIC PROPERTIES OF NATURAL SURFACES

Surface	Remarks	Roughness Length (m)	Zero Plane Displacement (m)
Water*	Still	$0.1\text{-}1.0\times10^{-5}$	-
Ice	Smooth	0.1×10^{-4}	-
Snow		$0.5\text{-}10.0\times10^{-4}$	-
Sand, desert		.0003	-
Soils		0.001-0.01	-
Grass*	0.02-0.1 m.	0.003-0.01	$\leq$ 0.07
	0.25-1.0 m.	0.04-0.10	$\leq$ 0.66
Crops*	Agricultural	0.04-0.20	$\leq$ 3.0
Orchards*		0.5-1.0	$\leq$ 4.0
Forests*	Deciduous	1.0-6.0	$\leq$ 20.0
	Coniferous	1.0-6.0	$\leq$ 30.0

* zero plane displacement depends on wind speed

Sources: Sutton (1953), Szeicz et al. (1969), Kraus (1972), Oke (1978)

TABLE A4
TEMPERATURE DEPENDENT PROPERTIES OF AIR AND WATER VAPOUR

T (°C)	ρ (kg m^{-3})	$e^*_{(T)}$ (Pa)	L_v (J kg^{-1} x 10^6)	K_H (m^2s^{-1} x 10^{-4})	K_w (m^2s^{-1} x 10^{-4})
-5	1.316	421	2.513	0.183	0.205
0	1.292	611	2.501	0.189	0.212
5	1.269	872	2.489	0.195	0.220
10	1.246	1227	2.477	0.202	0.227
15	1.225	1704	2.465	0.208	0.234
20	1.204	2337	2.454	0.215	0.242
25	1.183	3167	2.224	0.222	0.249
30	1.164	4243	2.430	0.228	0.257
35	1.146	5624	2.418	0.235	0.264
40	1.128	7378	2.406	0.242	0.272

Sources: van Wijk & de Vries (1963), Monteith (1973), Oke (1978)

APPENDIX C

VIEWFACTOR MODEL

TERMINOLOGY

S.A.	-	surface area on inaginary hemispherical surface of radius r
V.F.	-	viewfactor where V.F. must be ≤ 1.0
r	-	radius of hemisphere (may be arbritarily set by user)
O	-	origin
OO	-	line from origin to plane of obstruction perpendicular to face of subject surface
A	-	point on face of obstruction closest to OO
OA	-	line from origin to face of obstruction closest to OO

CALCULATION OF VIEWFACTOR

$$V.F. = \frac{S.A.}{2\pi r^2}$$

where S.A. is derived in following sections

APPLICATION

1. seek out appropriate heading in following sections.
2. diagrams and formulae may be applied to any and all obstructions based upon determination of OO

DEGREE & RADIAN FORMULAE

1. degrees to radians $\quad \phi = \frac{\theta^\circ * \pi}{180^\circ}$

2. radians to degrees $\quad \theta^\circ = \frac{180^\circ * \phi}{\pi}$

1. SUBJECT ON VERTICAL SURFACE; VERTICAL OBSTRUCTIONS

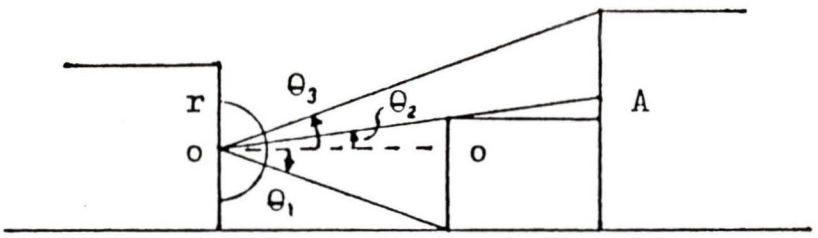

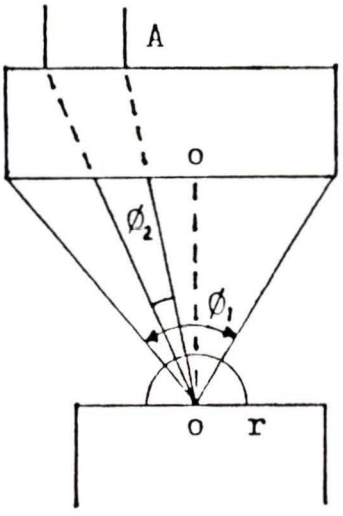

A) Obstruction on both sides of OO in side view;
ϕ_1 on horizontal plane of OO

S.A. = $r^2\phi_1 (\sin\theta_1 + \sin\theta_2)$

B) Obstruction on one side of OO in side view;
ϕ_2 on horizontal plane of OO

S.A. = $r^2\phi_2 (\sin\theta_3 - \sin\theta_2)$

OR ϕ_2' on horizontal plane of OA

S.A. = $\frac{r^2\phi_2'}{\cos\theta_2} (\sin\theta_3 - \sin\theta_2)$

2. SUBJECT ON VERTICAL SURFACE; HORIZONTAL OBSTRUCTIONS

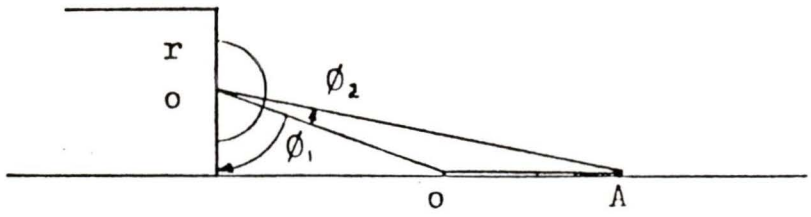

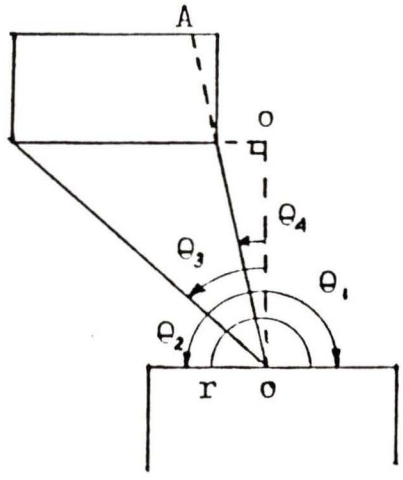

A) Obstruction on both sides of OO in top view:
ϕ_1 on vertical plane of OO

$$S.A. = r^2\phi_1 (\sin\theta_1 + \sin\theta_2)$$

B) Obstruction on one side of OO in top view;
ϕ_2 on vertical plane of OO

$$S.A. = r^2\phi_2 (\sin\theta_3 - \sin\theta_4)$$

OR ϕ_2' on vertical plane of OA

$$S.A. = \frac{r^2\phi_2' (\sin\theta_3 - \sin\theta_4)}{\cos\theta_4}$$

3. SUBJECT ON HORIZONTAL SURFACE; VERTICAL OBSTRUCTIONS

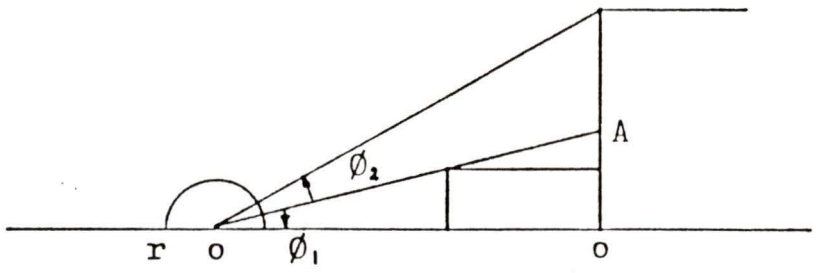

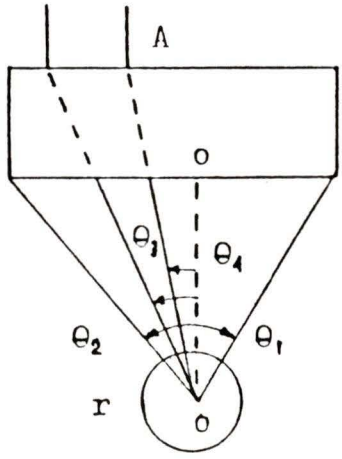

A) Obstruction on both sides of OO in top view;
ϕ_1 on vertical plane of OO

S.A. = $r^2\phi_1 (\sin\theta_1 + \sin\theta_2)$

B) Obstruction on one side of OO in top view;
ϕ_2 on vertical plane of OO

S.A. = $r^2\phi_2 (\sin\theta_3 - \sin\theta_4)$

OR ϕ_2' on vertical plane of OA

S.A. = $\dfrac{r^2\phi_2'}{\cos\theta_4} (\sin\theta_3 - \sin\theta_4)$

APPENDIX D

The Guide to Sampling Radiant Surface Temperatures for Vertical Surfaces Using Spot Data

GUIDE: PART I

Section A.

In this part of the Guide, the width of the element is known to be less than the height of the element. If after a spot or a series of spots have been calculated for a vertical traverse and the residual of the element does not meet the width to height criteria, then proceed to Part II of the Guide if the reseacher feels the residual is worth sampling. All calculations are based upon one of Figures IG1 through IG4.

The researcher should know:

w - width of element (Y-dimension) and/or desired width of the spot,
H - overall height of element of which spot must reach,
r - height from ground level to the base of the element,
HI- height of the instrument, and
ϕ - instrument viewfactor.

All instrument setup and spot dimension calculations begin with:

(a) $f = \dfrac{w}{2\tan \phi/2}$

(b) $c = H + r - HI$
- if c is positive and $\geq w$, proceed to Section B.
- if c is positive and $w > c \geq w/2$, proceed to Section C.
- if c is positive and $w/2 > c > 0$, proceed to Section D.
- if c is negative, proceed to Section E.

where f is the distance from the instrument to the spot centre along the axis through the centre of the instrument viewfactor, and c is the distance from the instrument height, HI, to the top of the spot (see Figure IG1).

FIGURE IG1:vertical orientation, all of spot above HI
(Section B.)

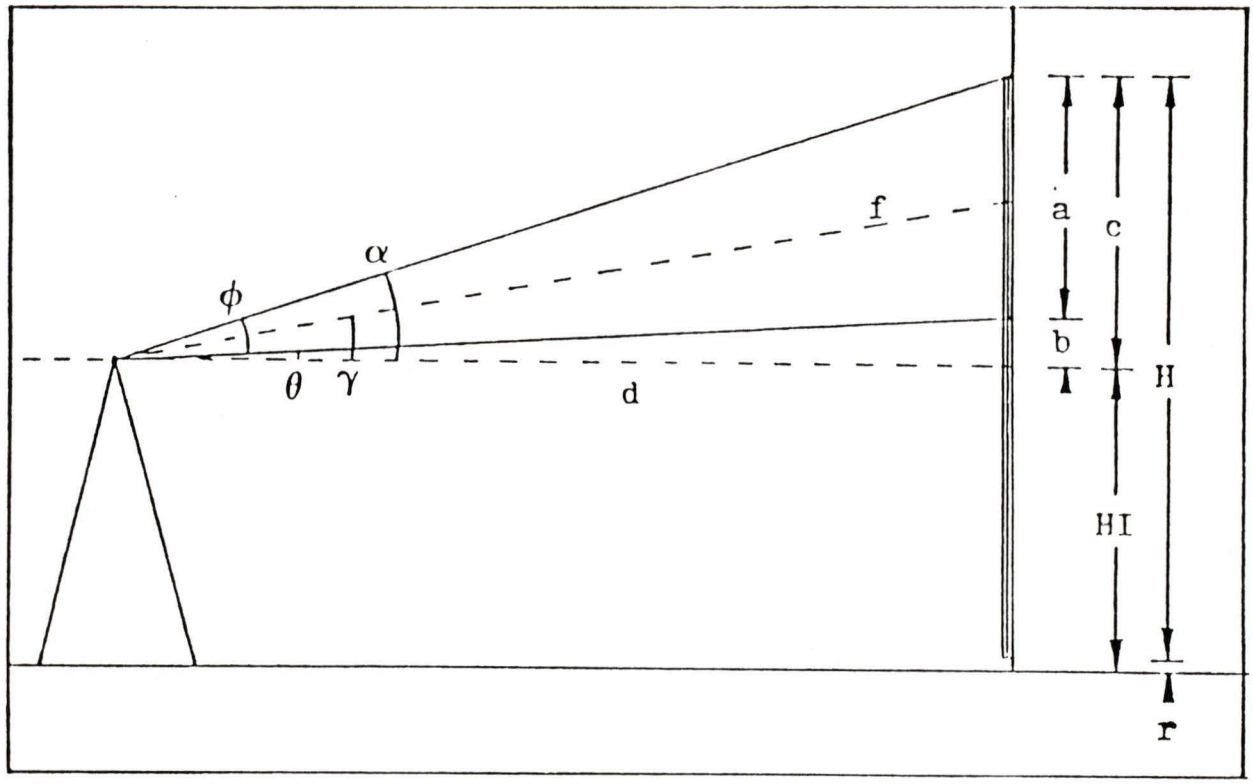

FIGURE IG2:vertical orientation, most of spot above HI
(Section C.)

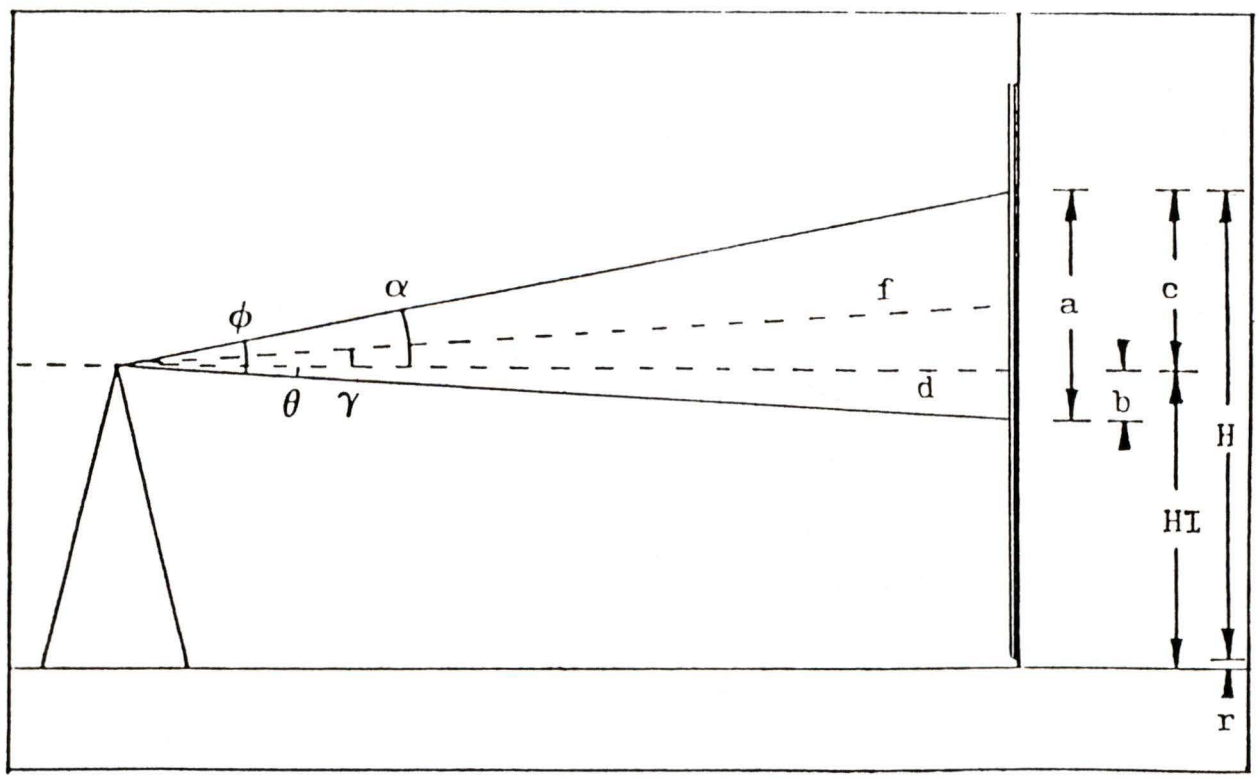

FIGURE IG3:vertical orientation, most of spot below HI
(Section D.)

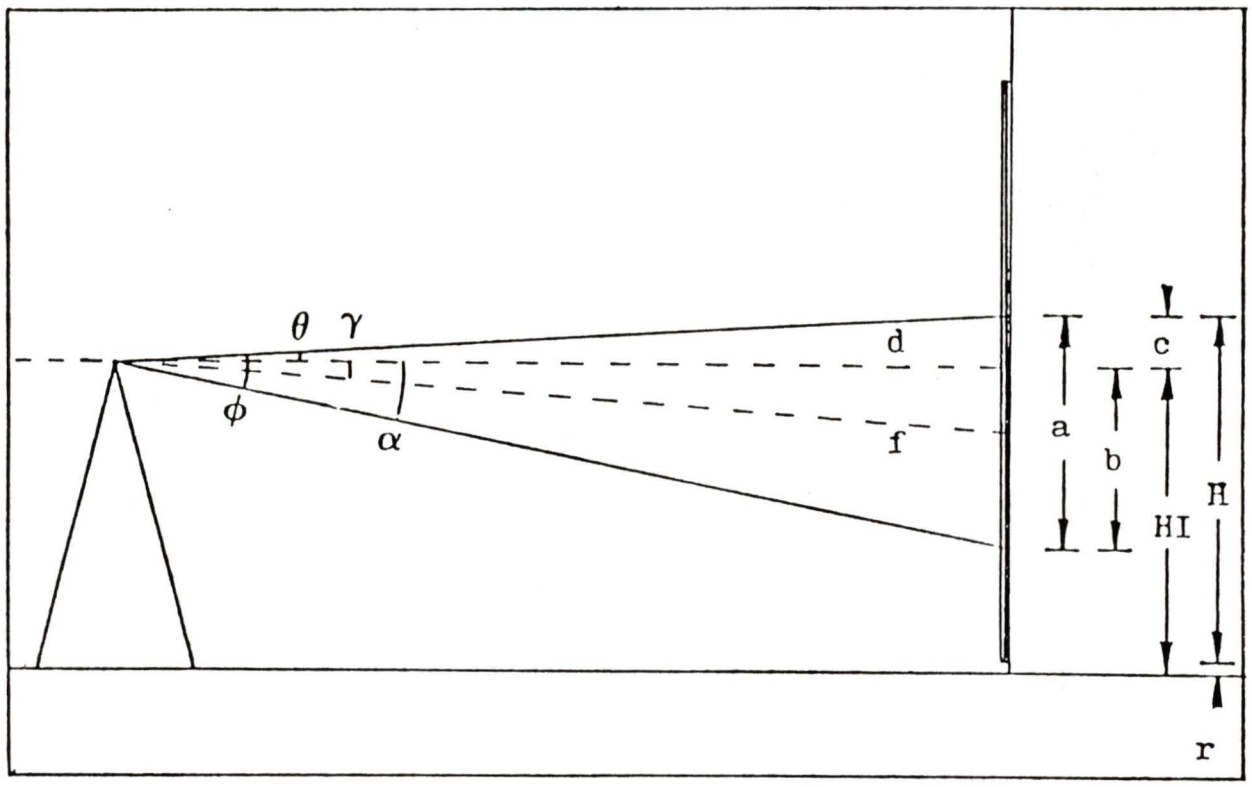

FIGURE IG4: vertical orientation, all of spot below HI
(Section E.)

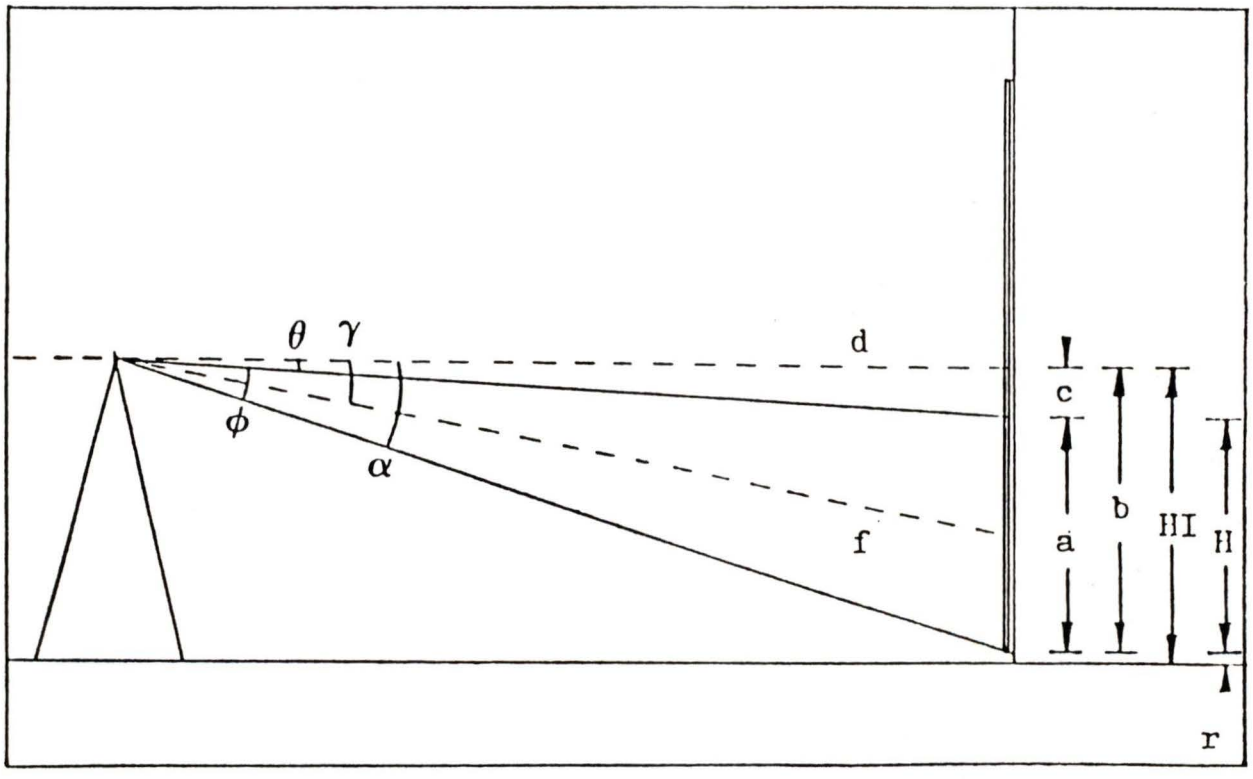

Section B. use Figure IG1

c dimension is positive and greater than or equal to w.

(a) $\cos\gamma \tan(\gamma + \phi/2) = c/f$
- solve for γ and set instrument vertical angle at γ .

(b) $d = f \cos\gamma$
- place instrument at distance d from vertical component.

(c) $\alpha = \gamma + \phi/2$

(d) $\theta = \gamma + \phi/2$

(e) $a = d(\tan\alpha - \tan\theta)$
- if $a > H$, proceed to Part II of the guide and repeat this step maintaining current b.
- if $a = H$, stop.
- if $a < H$, continue to (f)

(f) $b = c - a$

(g) $j = H - a$
- if $j \leq w$, proceed to part II of the Guide
- if $j > w$, b becomes the new c; j becomes the new H; return to Section A (b) to determine the next section.

Section C. use Figure IG2

c dimension is positive and w is greater than c which is greater than or equal to w/2.

(a) $\cos\gamma \tan(\gamma + \phi/2) = c/f$
- solve for γ and set instrument vertical angle at γ .

(b) $d = f \cos\gamma$
- place instrument at distance d from vertical component.

(c) $\alpha = \gamma + \phi/2$

(d) $\theta = \gamma + \phi/2$

(e) $a = d(\tan\alpha - \tan\theta)$
- if $a > H$, proceed to Part II of the guide and repeat this step maintaining current h.
- if $a = H$, stop.
- if $a < H$, continue to (f)

(f) $b = c - a$

(g) $j = H - a$
- if $j \leq w$, proceed to part II of the Guide
- if $j \geq w$, b becomes the new c; j becomes the new H; return to Section A (b) to determine the next section.

Section D. use Figure IG3

c dimension is positive and w is greater than c which is greater than or equal to zero.

(a) $\cos\gamma \tan(\gamma + \phi/2) = c/f$
- solve for γ and set instrument vertical angle at γ.

(b) $d = f \cos\gamma$
- place instrument at distance d from vertical component.

(c) $\alpha = \gamma + \phi/2$

(d) $\theta = \gamma + \phi/2$

(e) $a = d(\tan\alpha - \tan\theta)$
- if $a > H$, proceed to Part II of the guide and repeat this step maintaining current h.
- if $a = H$, stop.
- if $a < H$, continue to (f)

(f) $b = c - a$

(g) $j = H - a$
- if $j \leq w$, proceed to part II of the Guide
- if $j \geq w$, b becomes the new c; j becomes the new H; return to Section A (b) to determine the next section.

Section E. use Figure IG4

c dimension is negative.

(a) $\cos\gamma \tan(\gamma + \phi/2) = |c|/f$
- solve for γ and set instrument vertical angle at γ .

(b) $d = f \cos\gamma$
- place instrument at distance d from vertical component.

(c) $\alpha = \gamma + \phi/2$

(d) $\theta = \gamma + \phi/2$

(e) $a = d(\tan\alpha - \tan\theta)$
- if $a > H$, proceed to Part II of the guide and repeat this step maintaining current h.
- if $a = H$, stop.
- if $a < H$, continue to (f)

(f) $b = c - a$

(g) $j = H - a$
- if $j \leq w$, proceed to part II of the Guide
- if $j \geq w$, b becomes the new c; j becomes the new H; return to Section A (b) to determine the next section.

GUIDE: PART II

Section A.

In this part of the Guide, the width of the element is known to be greater or equal to the height of the element. If after a spot or a series of spots have been calculated for a horizontal traverse and the residual of the element does not meet the width to height criteria, then proceed to Part I of the Guide if the reseacher feels the residual is worth sampling. All calculations are based upon one of Figures IIG1 through IIG4.

The researcher should know:

a - height of the element (Z-dimension) and/or desired height of the spot,
w - overall width of the element (Y-dimension),.
r - height from ground level to the base of the element or spot,
HI- height of the instrument, and
ϕ - instrument viewfactor

All instrument setup and spot dimension calculations begin with:

(a) $b = r - HI$

(b) $c = H + r - HI$
- if c is positive and $\geq a$, proceed to Section B.
- if c is positive and $a > c > a/2$, proceed to Section C.
- if c is positive and $a/2 > c > 0$, proceed to Section D.
- if c is negative, proceed to Section E.

FIGURE IIG1: horizontal orientation, all of spot above HI
(Section B.)

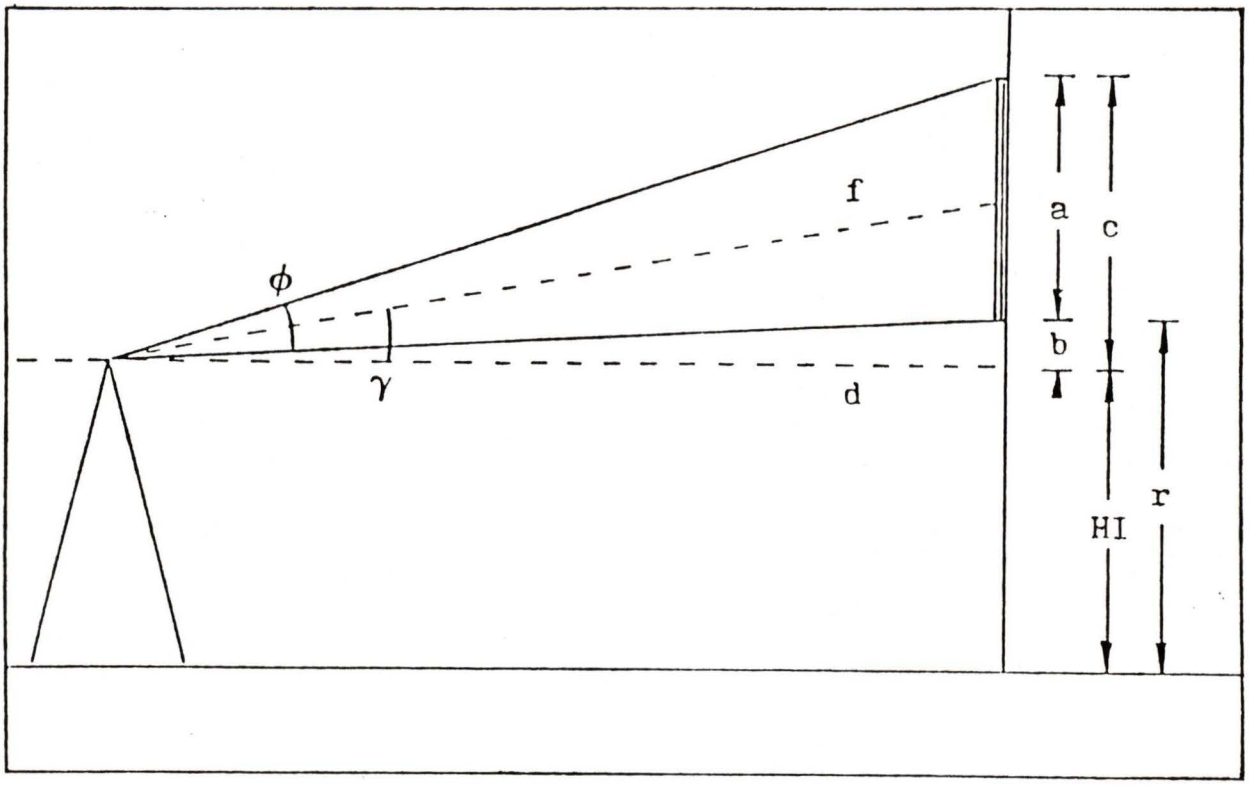

FIGURE IIG2: horizontal orientation, most of spot above HI
(Section C.)

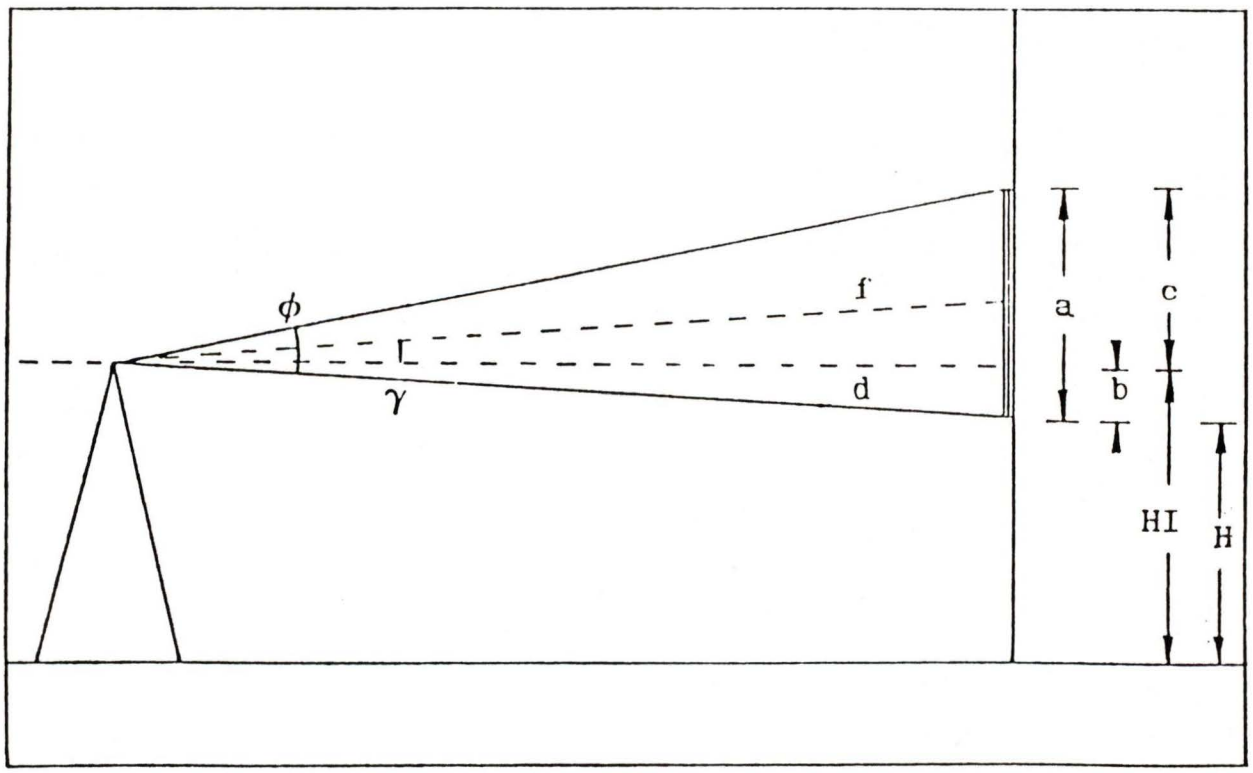

FIGURE IIG3: horizontal orientation, most of spot below HI
(Section D.)

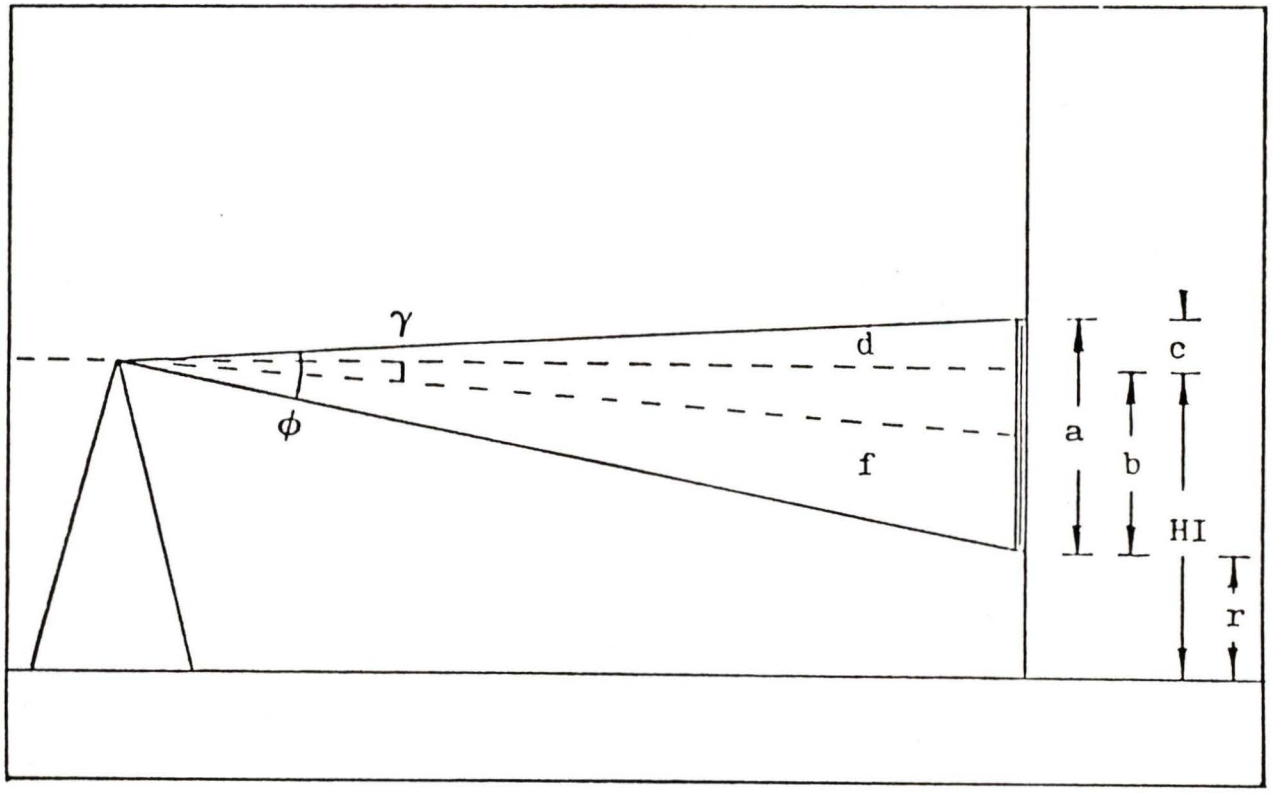

FIGURE IIG4: horizontal orientation, all of spot below HI
(Section E.)

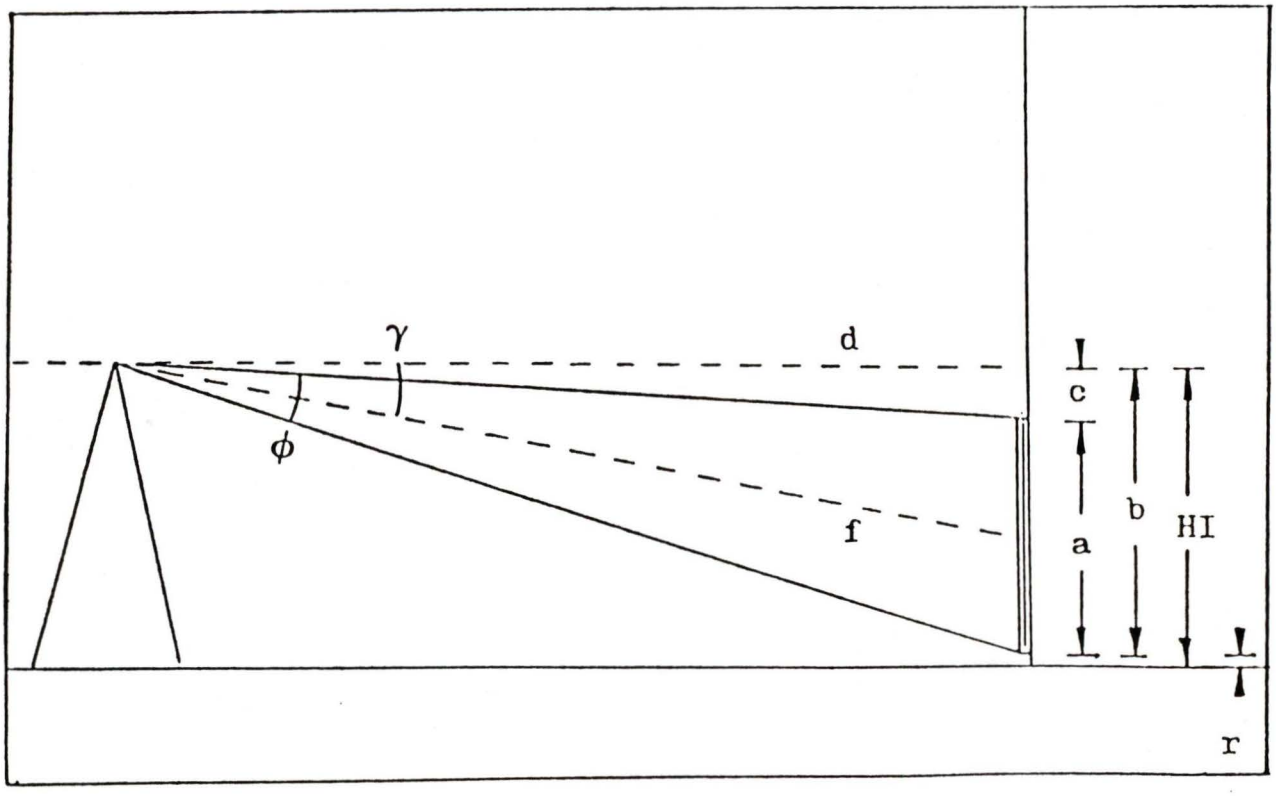

Section B. use Figure IIG1

c dimension is positive and greater than or equal to a.

(a) $\frac{\tan(\gamma - \phi/2)}{\tan(\gamma + \phi/2)} = \frac{b}{c}$

- solve for γ and set instrument vertical angle at γ .

(b) $d = \frac{b}{\tan(\gamma - \phi/2)}$

- place instrument at distance d from vertical component.

(c) $f = \frac{d}{\cos\gamma}$

(d) $w = 2\ f\ \tan\phi/2$

- if one or more spots of width w do not quite cover the overall width W, the researcher may proceed to PART I or split the residual among the spot spacings.

Section C. use Figure IIG2

c dimension is positive and a is greater than c which is greater than or equal to a/2

(a) $\frac{\tan(\gamma - \phi/2)}{\tan(\gamma + \phi/2)} = \left|\frac{b}{c}\right|$

- solve for γ and set instrument vertical angle at γ .

(b) $d = \frac{|b|}{\tan(\gamma - \phi/2)}$

- place instrument at distance d from vertical component.

(c) $f = \frac{d}{\cos\gamma}$

(d) $w = 2\ f\ \tan\phi/2$

- if one or more spots of width w do not quite cover the overall width W, the researcher may proceed to PART I or split the residual among the spot spacings.

Section D. use Figure IIG3

c dimension is positive and a/2 is greater than c which is greater than or equal to zero.

(a) $\frac{\tan(\gamma - \phi/2)}{\tan(\gamma + \phi/2)} = \frac{b}{|c|}$

- solve for γ and set instrument vertical angle at γ .

(b) $d = \frac{c}{\tan(\gamma - \phi/2)}$

- place instrument at distance d from vertical component.

(c) $f = \frac{d}{\cos\gamma}$

(d) $w = 2\ f\ \tan\phi/2$

- if one or more spots of width w do not quite cover the overall width W, the researcher may proceed to PART I or split the residual among the spot spacings.

Section E. use Figure IIG4

c dimension is negative

(a) $\frac{\tan(\gamma - \phi/2)}{\tan(\gamma + \phi/2)} = \left|\frac{b}{c}\right|$

- solve for γ and set instrument vertical angle at γ .

(b) $d = \frac{|c|}{\tan(\gamma - \phi/2)}$

- place instrument at distance d from vertical component.

(c) $f = \frac{d}{\cos\gamma}$

(d) $w = 2\ f\ \tan\phi/2$

- if one or more spots of width w do not quite cover the overall width W, the researcher may proceed to PART I or split the residual among the spot spacings.

VITA

Surname: Wakefield Given Names: Philip Michael

Place of Birth: Victoria, B.C. Date of Birth: 25 June 1954

Educational Institutions Attended, with Dates of Entering and Leaving:

Malaspina College, Nanaimo, B.C.	1972 to 1977
Camosun College, Victoria, B.C.	1980
University of Victoria, B.C.	1980 to 1982
	1983 to 1987

Degrees with Dates and Names of Institutions:

B.Sc. (Major, 1st Class) 1982 University of Victoria, B.C.

Honors and Awards:

N.A.

Publications:

N.A.

PARTIAL COPYRIGHT LICENSE

I hereby grant the right to lend my thesis (the title of which is shown below) to users of the University of Victoria Library, and to make single copies only for such users or in response to a request from the Library of any other university, or similar institution, on its behalf or for one of its users. I further agree that permission for extensive copying of this thesis for scholarly purposes may be granted by me or a member of the University designated by me. It is understood that copying or publication of this thesis for financial gain shall not be allowed without my written permission.

Title of Thesis:

URBMAT: An Urban Canyon Sampling Format for Nocturnal Long Wave Radiation Regime Modelling

Author: [redacted]

PHILIP MICHAEL WAKEFIELD

21 August 1987